Numerical Investigation of the Piston Skirt Lubrication in Heavy Duty Diesel Engines

by

Zhen Meng

B. Eng., Automotive Engineering
Tsinghua University, 2015

Submitted to the Department of Mechanical Engineering in Partial Fulfillment of the Requirements of the Degree of

Master of Science in Mechanical Engineering

at the

MASSACHUSETTS INSTITUTE of TECHNOLOGY

June 2017

Signature of Author: Signature redacted
Department of Mechanical Engineering
May 12, 2017

Certified by: Signature redacted
Dr. Tian Tian
Principal Research Engineer, Department of Mechanical Engineering
Thesis Supervisor

Accepted by: Signature redacted
Professor Rohan Abeyaratne
Quentin Berg Professor, Department of Mechanical Engineering
Chairman, Committee on Graduate Studies

Numerical Investigation of the Piston Skirt Lubrication in Heavy Duty Diesel Engines

by

Zhen Meng

Submitted to the Department of Mechanical Engineering on May 12th, 2017

in Partial Fulfillment of the Requirements of the Degree of

Masters of Science in Mechanical Engineering

Abstract

Friction reduction in the power cylinder system of internal combustion engines has been undergoing broad and intense study in an industry-wide effort to reduce CO_2 from the engines. As a major source of frictional loss in the system, the piston skirt-liner interface, specifically in heavy duty diesel engines, is investigated in this thesis work using a model developed in-house.

Prior to the calculation of various cases for parametric study, improvements were made to the existing model in order to incorporate the characteristics of heavy duty diesel engines, and to enhance the robustness and accuracy of the model in general. These improvements include enabling arbitrary distribution oil supply to the system, more efficient way to incorporate the shear-thinning effect of multigrade lubricants, and new scheme at the start of the simulation to resolve the situation with large overlap between piston skirt and liner.

The first part of the analysis from application focuses on the geometric parameters of the system such as installation clearance, deformation of the components, and surface roughness of piston skirt. The effects of each individual parameter are discussed and summarized.

The second part of the analysis is focused on the sensitivities of the system to the amount and distribution of oil supply. It was found that more lubricant can help reduce friction on thrust side during expansion stroke and on anti-thrust side during compression stroke. However, due to the rapid loss of oil at the piston-liner interface during early compression stroke, there is a limit to the advantage of more oil addition. It has also been suggested that with a certain amount of oil supply, it is more beneficial to add the lubricant higher on the liner.

This thesis work is the first effort with the model to systematically study the piston skirt lubrication in heavy duty diesel engines. It is expected to be facilitated by the measurement and observation from experiments in the future.

Thesis Supervisor: Dr. Tian Tian

Title: Principle Research Engineer, Department of Mechanical Engineering

Acknowledgements

The past two years of graduate study brings me not only academic and personal progress, but also groups of people that I feel lucky and grateful to have in my life.

First of all, I would like to express my sincere gratitude for my advisor, Dr. Tian Tian, for his inspiration and guidance during my time at MIT. I have been brought by him to a higher level of thinking and working in terms of solving real-world problems as an engineer. He has been not only the best source for me to seek advice in research and study, but also a valuable friend as I've learned a lot from his experience and insights of life.

I'd also like to thank Dr. Dongfang Bai and Pasquale Totaro from whom I took over my Master's project. Although there haven't been many chances for me to meet them in person, they still motivated me through the solid foundation they had established for our topic. Their work facilitated my understanding of the problem and smoothed the way towards my further study.

This work is sponsored by the consortium on lubrication in internal combustion engines at MIT with additional support by Argonne national laboratory and US department of energy. The current consortium members are Daimler AG, Mahle GmbH, MTU Friedrichshafen, PSA Peugeot Citroën, Renault S.A., Royal Dutch Shell, Toyota, Volkswagen AG, Volvo Cars, Volvo Truck, and Weichai Power.

Also, I would like to thank the members of the Sloan Automotive Laboratory at MIT for their help and exchange of ideas and knowledge. Especially, I've been really enjoying the time working together with fellow students in my group, Yang Liu, Tianshi Fang, Sebastian Ahling, Chongjie Gu, Vinayak Kalva, Yuwei Li, Sarthak Vaish, Qin Zhang, Aziz Bhouri, Zhe Chen and Xiaofeng Qin. Special thanks to Janet Maslow and Thane DeWitt for assisting our research in the lab.

As always, I appreciate the support and encouragement from my friends and families. Many thanks to my girlfriend, Jingru Cao, for her company and understanding.

Finally, I would like to thank my parents, Xuemin Zhao and Qiang Meng, for everything they've done for me.

Zhen Meng, Cambridge, MA, May 2017

Contents

List of Figures

List of Tables

Chapter 1

Introduction

1.1 Project Motivations

Despite the thriving development and market share of new energy vehicles, internal combustion engine (ICE) is expected to retain its predominance in automotive propulsion systems for decades [1]. In this light, environmental protection and energy consumption have been the main challenges faced by the entire industry.

To address these issues, the first and foremost task is the reduction of energy loss in the power system, to which mechanical friction is a major contributor. It has been estimated that frictional loss accounts for 4-15% of the energy consumed by a fired engine, and around a half of this loss takes place in the power cylinder system, which consists of pistons (25-47%), rings (28-45%), and connecting rods (18-33%) [2].

The friction associated with the piston comes from the contact between piston skirt and cylinder liner. In addition to the waste of energy and possible wear in the surfaces, this contact can bring other problems to the engine components. On the one hand, there might be noise during expansion strokes of the engine, where piston slaps the liner due to the load from combustion chamber. On the other hand, in the cases of wet liner, where its outer surface is direct in contact with the engine coolant, vibration of the liner may cause cavitation inside the coolant, which can in turn erode the liner [3].

These factors have been serving as an incentive for investigating the system in order to improve energy efficiency and engine's durability. These investigations, although to some extent incomprehensive, have led to considerable progresses. Knoll and Peeken [4] described the skirt and liner as a bearing system that was fully flooded with lubricant, and studied the effect of hydrodynamic force on the secondary motion of the skirt. Oh et al. [5] treated the skirt-liner

interface as an elastohydrodynamics lubrication (EHL) regime and took the compliance of the skirt into account. They also designed a new skirt geometry with larger skirt taper, and received less friction than the original skirt. Duyar et al. [6] developed a model with more features including the consideration of liner deformation, the rupture and re-attachment of the oil film, and the oil supply from the liner. These works set a solid foundation for advanced studies, which should deliver more accurate descriptions of the system and more efficient and robust algorithms. In addition, sufficient validation needs to be provided from experimental measurements and observation.

1.2 Introduction to Power Cylinder System

Figure 1-1 shows some of the key components of the power cylinder system in typical four-stroke internal combustion engines. Its major parts include crankshaft, connecting rod, piston pin, piston (skirt and lands), piston ring pack, and cylinder bore.

Inside the power cylinder system, the chemical energy in the fuel is converted to the kinetic energy of the piston in terms of its reciprocating motion. The reciprocation, which is often referred to as the primary motion, is then turned into the rotation of the crankshaft through the connecting rod.

During engine operation, the pressure difference between combustion chamber and crankcase results in an axial (z-direction in figure 1-1) force on the piston. In an ideal situation where there is no contact between piston and cylinder bore, this force is mainly balanced by the axial inertial force of the piston, and the z-component of the force from the piston pin. However, in reality, clearance between piston and cylinder does exist, so the y-component of the latter force will drive the piston to move towards the cylinder liner until it is balanced by the force arisen from the piston-liner interaction. This movement in the y-direction is usually called lateral motion, and is one part of the piston secondary motion which plays a principal role in this project.

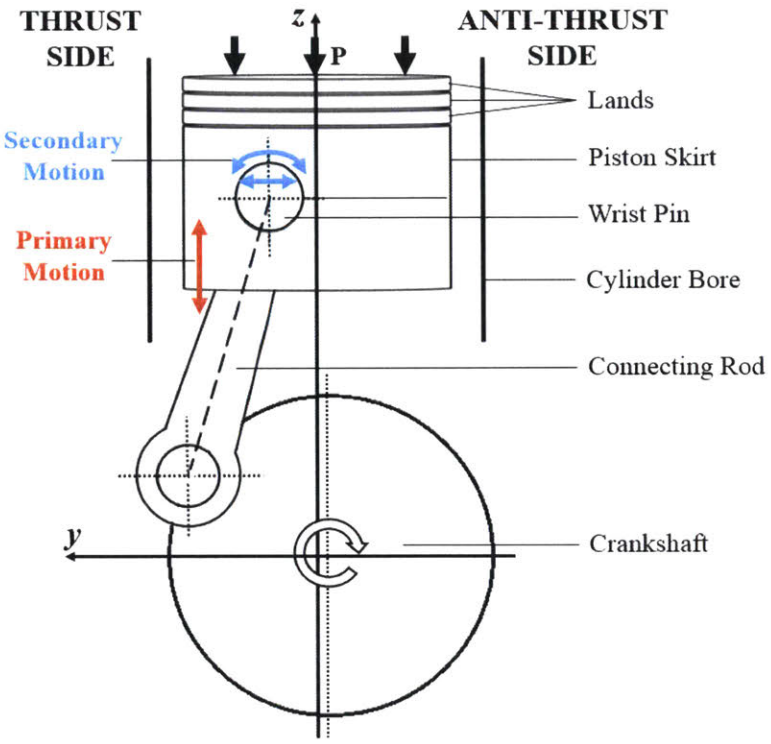

Figure 1-1 Power Cylinder System

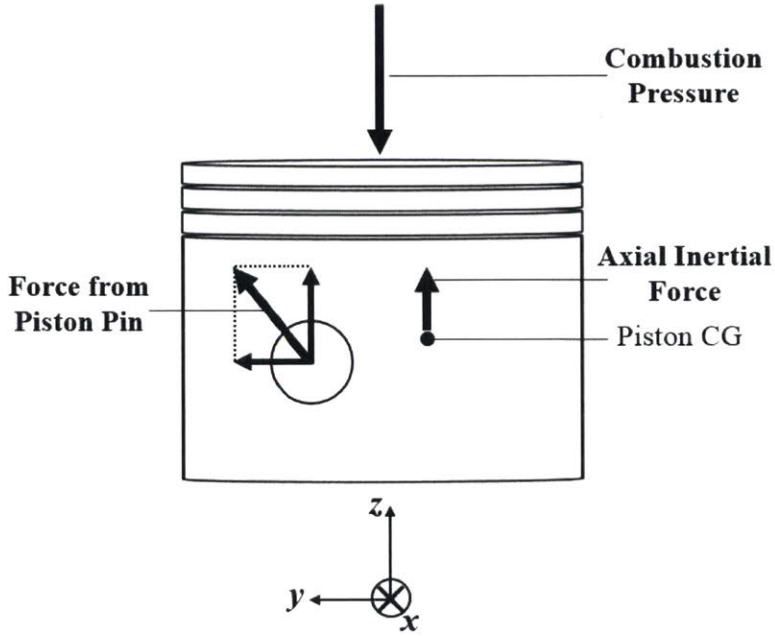

Figure 1-2 Forces on Piston before Contacting Liner

The other part is the piston tilt. Since the center of gravity of the piston is often different from the center of the piston pin, the net force may generate a torque on the piston and make it rotate around the pin. This rotation is called piston tilt. Because the crankshaft rotates in the y-z plane, and all the major forces involved are in either y or z-direction, the other movements of the piston are neglected in this study.

Another important concept in the system is the thrust and anti-thrust side. In figure 1-1, where the crankshaft rotates clockwise, the big end (connecting the crankshaft) of the connecting rod will be to the right of the small end (connecting the piston pin) when piston moves downwards. As a result, the force from piston pin to piston will be in a similar direction as in figure 1-2. During expansion stroke, there will be a dramatic rise in combustion pressure, and the accordingly large lateral force from the pin will push the piston to the left side of the liner. This side is named thrust side and the opposite is anti-thrust side.

Because contact will happen between piston and liner due to secondary motion, proper lubrication needs to be maintained in order to reduce frictional loss. This brings about further complexity for the study. First of all, to predict the lubrication performance of the system, the clearance between piston and liner has to be solved. The clearance can be affected by the installation clearance, the profiles of the two surfaces, secondary motion, dynamic deformation, and the oil film in between. Moreover, some area may still suffer from lack of lubricating oil as a result of oil transport, and other places may experience large gaps between piston and liner due to secondary motion. Therefore, it would be inaccurate to treat the entire surfaces as fully-flooded. Finally, sub-models on asperity contact, oil viscosity, etc. also need to be integrated into the system so that more reliable results can be achieved.

1.3 Scope of the Thesis Work

The project is based on an existing model developed by Bai [7] and then Totaro [8]. The model is an effective tool to study piston secondary motion and skirt lubrication, yet there was still

considerable potential in it to be realized by incorporating a wider range of physical phenomena occurring in the system. Furthermore, some of the assumptions and simplifications in the model turned out to be confining its applications to real cases, especially heavy duty diesel engines. Further improvements needed to be made to address these issues.

The second chapter starts with an introduction of the development of the model and its status before this thesis work. It also includes some supplementary explanation which is crucial for understanding the model, but missing in existing documentation. Then the details of the aforementioned improvements will be discussed.

The third chapter focuses on the major factors contributing to piston skirt friction and mechanisms affecting the performance of lubrication. It firstly goes through some common patterns of secondary motion and oil transport. These patterns come from primary motion and overall force balance, thus hold true for most of the cases. Then the influence of the nominal clearance, the deformation of piston and liner, and the surface description of the skirt are illustrated individually.

The fourth chapter studies the effects of oil supply to the system. In the model, the only source of oil supplies other than the initial condition is the additional oil that is splashed on the liner when piston reaches top dead center. This chapter studies the sensitivity of lubricating performance to the amount and distribution of the oil addition.

The last chapter summarizes the thesis work with conclusions and remarks, and suggests several aspects on this topic to investigate in this future.

Chapter 2

Model Improvement

The piston secondary motion and skirt lubrication model has been established and developed by several fellow researchers [7-10]. It has also been facilitated by the experimental side with floating liner engine (FLE) and High Speed Laser Induced Fluorescence (LIF) systems [11-13]. Bai [7] analyzed the kinematics and dynamics of the system. He also explained the numerical algorithm which uses Universal Reynolds Equation and finite volume method to solve the lubrication problem. Totaro [8] introduced new features such as the shear-thinning and temperature effect on the viscosity of lubricant, and made corresponding updates to the model. Detailed description and explanation of the system can be found in their theses.

In the first section of this chapter, some key components in the model will be illustrated. Then, the modifications made in this thesis work will be introduced in the next sections.

2.1 Existing Work

The most critical elements for the skirt lubrication are the clearance and the oil film distribution. In the following the model consideration for these two elements are discussed together with the numerical scheme on meshing strategy.

2.1.1 Clearance between Piston and Liner

The first variable is the clearance between piston and liner at different places. It consists of five parts.

- The uniform clearance from the difference between the nominal radii. This nominal clearance is usually in the order of 10 microns.
- The cold profiles and thermal expansions of piston and liner.

This part is specified in the model inputs, and is fixed during the simulation. From the base of a cylindrical shape, liner's cold profile has radial distortion due to the constraints on it during the assembly of engine block. For the piston, a barrel-shaped profile is usually adopted to be in favor of retaining the lubricant and generating more hydrodynamic pressure to balance the side force. When an engine is running, especially under fired condition, the temperature of both skirt [14] and liner [15] can easily reach 100°C, leading to thermal expansions in the order of 10 microns. A typical profile of the liner, including both cold and hot profiles, is shown in figure 2-1. A representative of piston profiles is depicted in figure 2-2.

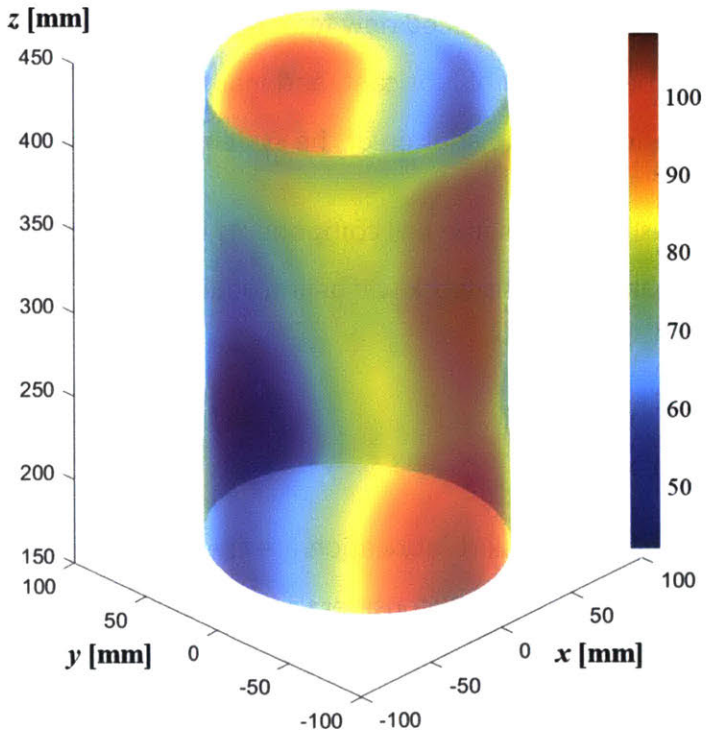

Figure 2-1 Radial Variance of a Liner [μm]

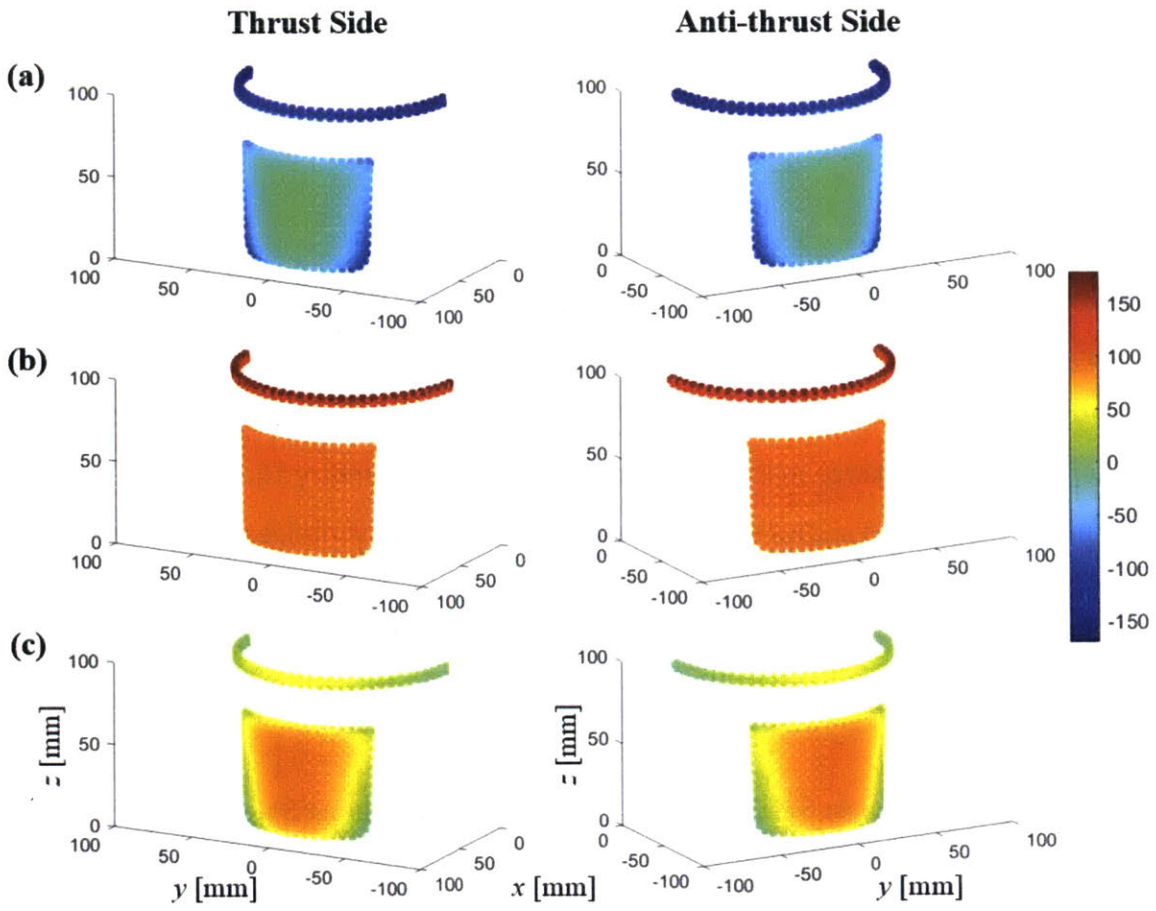

Figure 2-2 (a) Cold Profile, (b) Thermal Expansion, (c) Final Radial Variance of a Piston [μm]

- The dynamic deformation of piston and liner due to the normal forces they exert on each other.

When the piston is pushed or pulled by the lateral force from the pin towards either thrust or anti-thrust side of the liner, hydrodynamic force will be generated in places where there is enough lubricant. For spots with insufficient lubricant, asperity contact may happen and the contact force, although undesirable, also helps balance the lateral force. The model assumes that there are horizontal triangular machine marks on the surface of the skirt and that the liner is flat, thus uses the analytical solution derived by Johnson [16] for a blunt-wedged surface against a plane surface to calculate the magnitude of contact force. The details of the contact sub-model can be found in Bai's and McClure's theses [7, 9].

If the distribution of total normal force ($\vec{F}$) is known, deformation ($\vec{d}$) can be calculated with the compliance (C) of piston and liner.

$$\vec{d} = C \cdot \vec{F} \qquad 2\text{-}1$$

The compliance is often obtained from finite element analysis and is also presented in the input data of the model. For piston, a routine has been developed during the time period of this thesis work by fellow members in the group. The routine uses Abaqus and MATLAB to generate the compliance matrix based on the meshed geometry and material properties of the piston. Figure 2-3 shows a typical distribution of radial variance on a piston caused by a one-Newton force on a certain point. The left part is when the point is around the center of skirt on thrust side and the right part is on anti-thrust side. Sometimes the thrust side is designed to be stiffer to withstand larger forces.

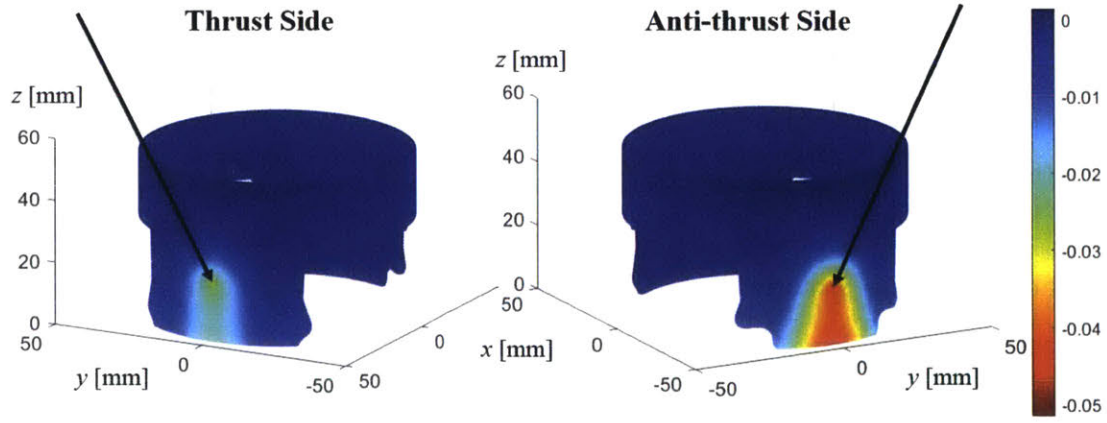

Figure 2-3 Deformation Distribution of a Piston with Unit Force [μm]

Note that there should be reasonable boundary conditions when calculating the compliance matrix. For example, it is often assumed that the points on the pin bore are fixed in the radial direction of the pin.

Figure 2-4 illustrates the radial deformation of the cylinder liner in a heavy duty diesel engine. In the figure, six points at different heights on thrust side are chosen to receive

respectively a force of one Newton and the deformation is calculated according to its compliance matrix. As can be seen from the two plots on the right of figure 2-4, the liner has constraints at the top and lower part, around which the area does not deform as much. Under the lower constraint, the liner is easier to deform especially at the bottom.

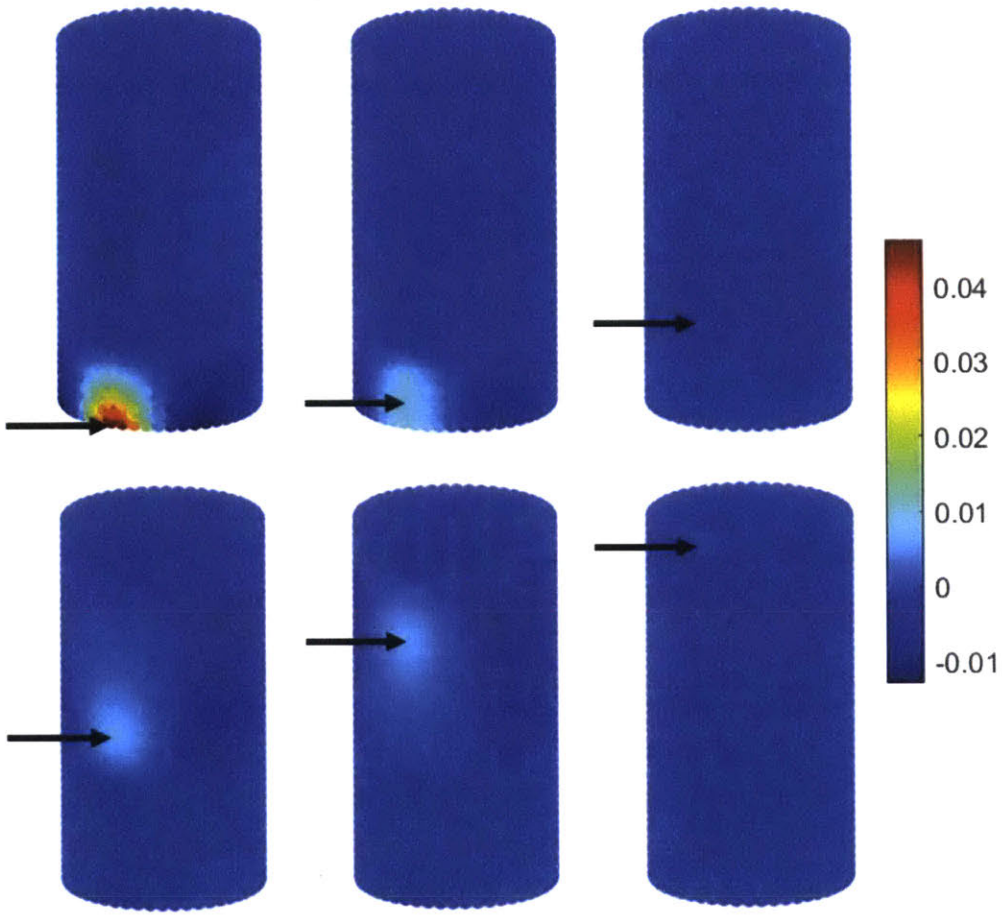

Figure 2-4 Deformation Distribution of a Liner with Unit Force [μm]

- The secondary motion of the piston.
- Deformation of the piston induced by combustion pressure and inertia force.

As a result, at a certain place on the piston, the local clearance can be expressed by the following equation.

$$h = h_N + (\Delta R_{\mathrm{L}} - \Delta R_{\mathrm{P}}) + (d_{\mathrm{P}} + d_{\mathrm{L}}) + \sin\theta \cdot [(z - z_{\mathrm{Pin}}) \cdot \alpha_{\mathrm{tilt}} - s_{\mathrm{lat}}] + d_{\mathrm{ip}} \qquad 2\text{-}2$$

Here h_N is the nominal clearance, ΔR_{L} and ΔR_{P} are radial variances of the liner and the piston, d_{P} and d_{L} are deformation from hydrodynamic and asperity contact forces, d_{ip} is the deformation of piston due to combustion pressure and inertia force.

Secondary motion is described by tilt angle (α_{tilt}) and lateral movement (s_{lat}). A positive tilt angle and positive lateral movement is illustrated on the right part of figure 2-5. The location of the place is defined by θ and z as shown in figure 2-5. z_{Pin} is the z-coordinate of the center of piston pin.

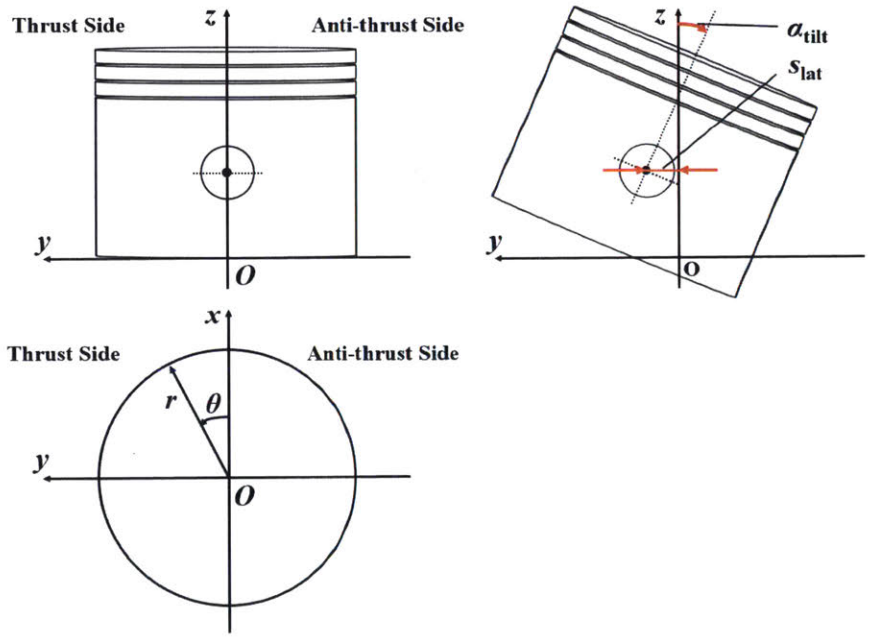

Figure 2-5 Coordinate System for Piston in the Model

2.1.2 Oil Film Thickness

The second important variable is the oil film thickness between piston and liner. The model has a distinguishable capability of considering cavitation and partial film using the Jakobson-Floberg-Olsson (JFO) theory described by Elrod [17].

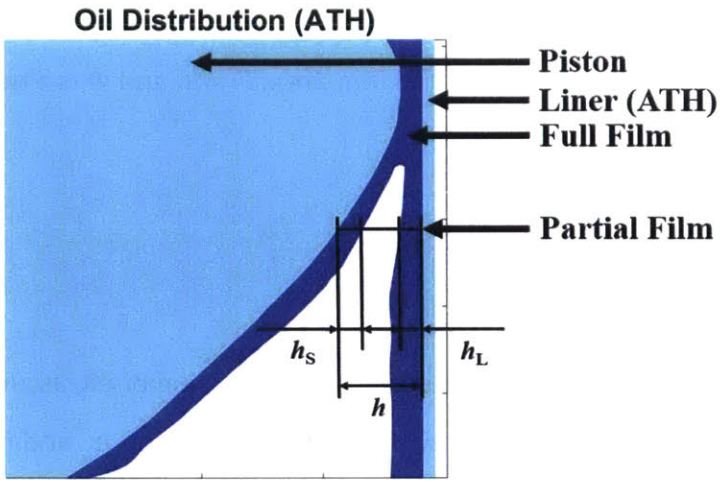

Figure 2-6 Full Film and Partial Film Areas

Figure 2-6 shows a part of an axial cross section in the y-z plane. The piston (left) and liner (right) are depicted in cyan and the oil film is in blue. Inside the full film area, where oil film touches both piston and liner, the governing equation used in the model is the Reynolds Equation according to lubrication theory.

$$\frac{\partial}{\partial s}\left(\frac{h^3}{12\mu}\frac{\partial p}{\partial s}\right)+\frac{\partial}{\partial z}\left(\frac{h^3}{12\mu}\frac{\partial p}{\partial z}\right)=\frac{U}{2}\frac{\partial h}{\partial z}+\frac{\partial h}{\partial t} \qquad 2\text{-}3$$

In equation 2-3, s is the distance along the circumferential direction, and both the clearance and oil film thickness can be represented by h. In order to incorporate the partial film area where there is no pressure gradient and the oil fil thickness is less than the clearance, two global variables, F and Φ, are introduced. The pressure p and oil film thickness h_o are expressed as in the following equation.

$$p = F\Phi p_0 \qquad 2\text{-}4$$

$$h_o = [1 + (1 - F)\Phi]h \qquad 2\text{-}5$$

Here p_0 is a reference relative pressure. In full film area, $F = 1$ and Φ is a positive value standing for the pressure in the film. In partial film area, $F = 0$ and Φ is a negative value representing the oil occupancy.

$$1 + \Phi = \frac{h_S}{h} + \frac{h_L}{h} \tag{2-6}$$

The existing model, which does not consider the surface tension of oil, assumes that the oil film will separate once the pressure drops below the ambient pressure. h_S and h_L are the thicknesses of oil film that stay on piston and liner, respectively, after separation. Then, the part of oil that is attached to the liner and represented by h_L moves with the liner at a velocity of U when the piston is taken as the reference. The other part that is attached on the skirt is only driven by the inertia [7]. In the end, the governing equation for partial film is

$$0 = U\frac{\partial h_L}{\partial z} + \frac{\partial}{\partial t}[(1+\Phi)h] + \frac{\partial}{\partial z}\left(\frac{a_p \cdot h_S^3}{3v}\right) \tag{2-7}$$

As a result, Reynolds Equation will be modified and become the Universal Reynolds Equation that incorporates both kinds of film.

$$\begin{aligned}\frac{\partial}{\partial s}\left(\frac{h^3}{12\mu}\frac{\partial(F\Phi p_0)}{\partial s}\right) + \frac{\partial}{\partial z}\left(\frac{h^3}{12\mu}\frac{\partial(F\Phi p_0)}{\partial z}\right) &= \frac{U}{2}\frac{\partial}{\partial z}\{[1+(1-F)\Phi]\cdot[Fh_S + (2-F)h_L]\} \\ &+ \frac{\partial}{\partial t}\{[1+(1-F)\Phi]h\} + (1-F)\frac{\partial}{\partial z}\left(\frac{a_p \cdot h_S^3}{3v}\right)\end{aligned} \tag{2-8}$$

2.1.3 Meshed Geometry

In the model, the piston-liner system is divided into three regions. The first and foremost one is the skirt region. It is where all the hydrodynamic and most of the contact forces occur, and where the lubrication algorithm from equation 2-8 is applied. A typical skirt in passenger cars has an axial height of 20-80 millimeters. The second region is the chamfer, which is between the skirt region and the oil control ring. The height of chamfer region is usually one order of

magnitude smaller than the skirt region, but the clearance is much larger, usually reaching several hundred microns. The third region is the open liner, which is the part of the liner that is below the bottom of the skirt. Figure 2-7 is a sketch of those regions on the thrust side when piston is at top dead center. Note that at this point, the height of the open liner is usually from twice to three times as large as the skirt region.

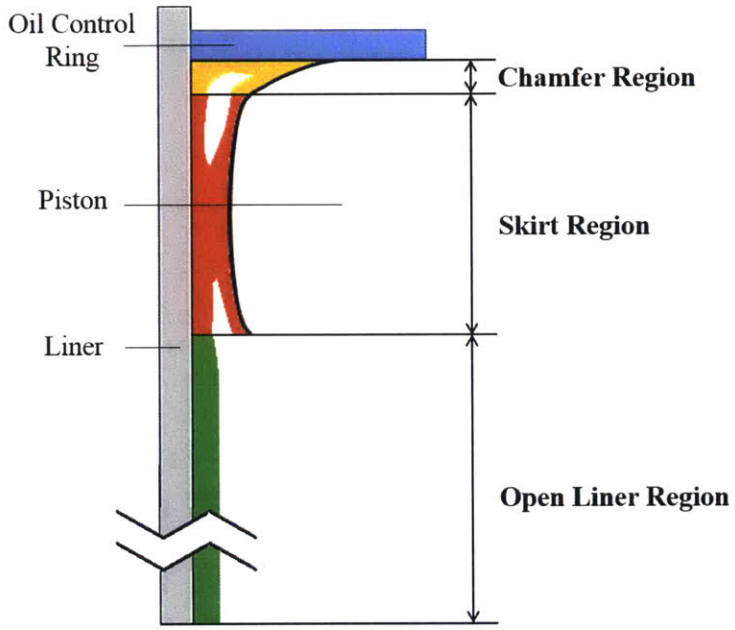

Figure 2-7 Three Regions in the System

When using the finite volume method to linearize the equations, several sets of grid are defined in these regions. For the skirt region, one grid with moderate amount of cells is used for the calculation of dynamic deformation as in equation 2-1. As for other parameters, especially the hydrodynamic pressure, a much finer grid is required in order to capture the characteristics of the skirt's surface profile. When calculating the clearance, deformation will be mapped from the coarse grid to the fined grid.

Figure 2-8 and figure 2-9 show the definition of skirt grids and their connection.

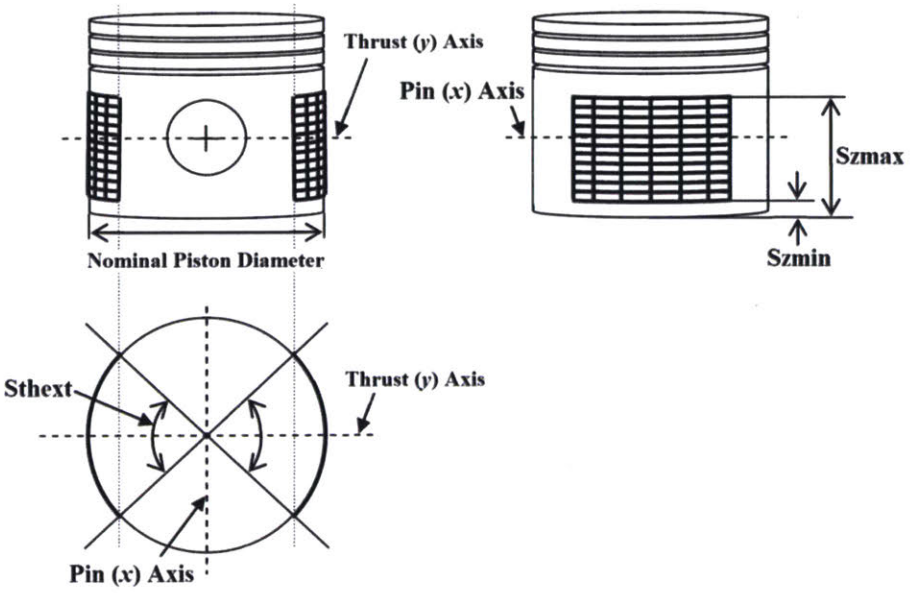

Figure 2-8 Rectangular Grid on the Skirt

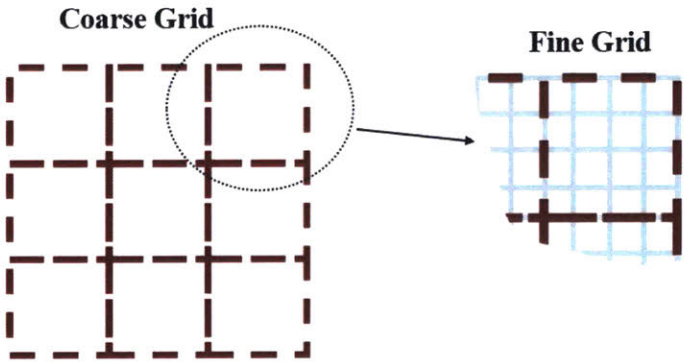

Figure 2-9 Two Sets of Skirt Grid

The input data usually comes from finite element method, which is prior to the calculation of the model and not in the scope of this work. It does not have to contain the same cells as the grids in the model, since the data will be interpolated during the preprocessing part of the model.

For the chamfer region, only one set of grid is defined because of its small axial height as well as the unlikelihood of deformation. In the model, the only interaction between these two regions

is the oil transport between the bottom row of cells on the chamfer and the top row of cells on the skirt. Therefore, the number of cells in each row, as well as the circumferential range of calculation domain, should be the same for the grid on the chamfer and the fine grid on the skirt.

The open liner region has two sets of grid as well, and the sizes of their cells are respectively the same as those on the skirt region. The circumferential range also equals to that of the skirt.

2.2 Arbitrary Oil Supply to Cylinder Liner

When piston travels upwards, some oil between the skirt and liner will stay with the liner. This oil film on the liner will be available to the skirt when it comes back. Additionally, oil droplets from different sources may also be added on the liner and become available to the skirt during the ensuing down stroke. The sources of the oil droplets depend on the exact engine design on oil cooling jet and oil sump.

In the model, because the area of each cell in the grids is fixed during the calculation, the volume of oil in an individual cell can be represented by the thickness. The model used to assume that the oil jet brings an additional oil film with a uniform thickness to the entire open liner, as shown in figure 2-10.

Although this might be a reasonable simplification as the distribution of this splashed oil is almost unpredictable, it prevents people from looking into the effects of oil addition, therefore confines the versatility of the model. In this thesis work, such simplification is cancelled and modification to the model is made so that the users can define arbitrary oil supply to the open liner.

In the current model, users can provide extra input files specifying the distribution of additional oil film thickness. The input files contain a matrix with the same size as the fine grid on open liner. This thickness will be added every time the piston is at top dead center.

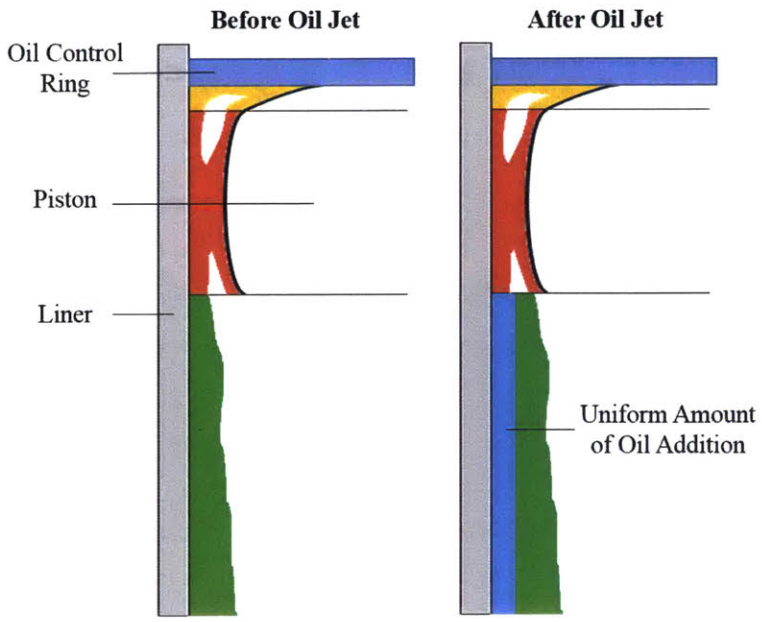

Figure 2-10 Uniform Oil Addition to Open Liner

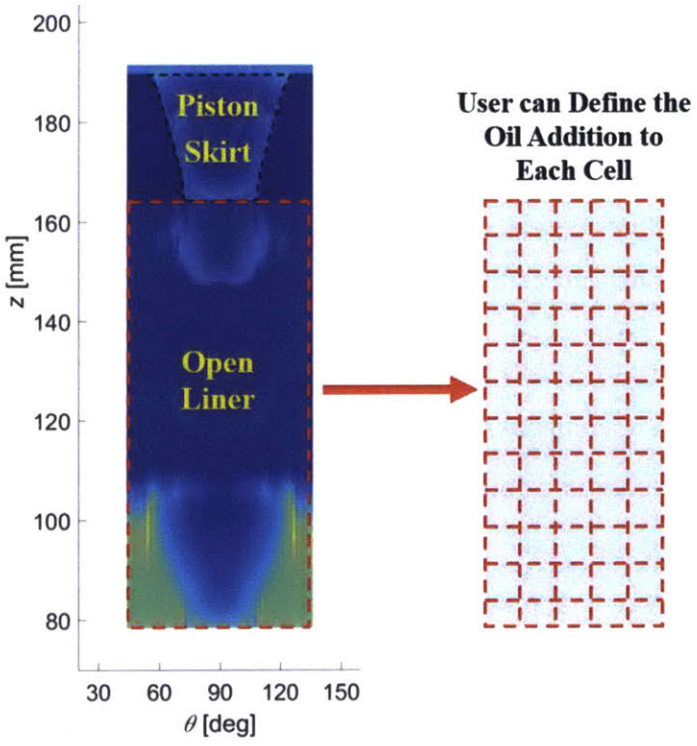

Figure 2-11 Arbitrary Oil Addition to Open Liner

Figure 2-11 shows the 2D view of thrust side. On the left part, z and θ denote the axial and circumferential direction. The upper and lower dashed lines enclose the skirt region and open liner region respectively.

With the consideration of arbitrary oil supply, it is now possible to study the system's sensitivity to the location and amount of oil addition. There are some interesting findings in this part and they will be introduced in Chapter 3.

2.3 Description of Shear Rate

Viscosity of the oil is one of the major parameters that can influence lubrication and friction, therefore a more comprehensive calculation of viscosity can improve the accuracy of the model. Totaro [8] included the effects of temperature and shear-thinning behavior on the viscosity of the lubricant. He used an expression proposed by Taylor [19], which combines the Vogel equation and Cross equation.

$$\mu(\gamma, T) = \kappa \cdot \exp\left(\frac{\theta_1}{\theta_1 + T}\right) \cdot \left(\frac{\mu_\infty}{\mu_0} + \frac{1 - \frac{\mu_\infty}{\mu_0}}{1 + \left|\frac{\gamma}{10^{A+BT}}\right|}\right) \qquad 2\text{-}9$$

In equation 2-8, κ, θ_1, θ_2 , A, and B are fitting parameters from experimental measurements, T is the temperature in degree Celsius, γ is the shear rate, μ_0 and μ_∞ are the viscosities in two extreme cases where the shear has no and maximum effects.

For oil flow in the system, the model considers Couette flow in the axial direction and Poiseuille flow in both axial and circumferential direction, and both of these kinds of flow can contribute to the shear rate. However, the shear rate γ used in the previous model did not include the Poiseuille part, which can be fairly comparable to the Couette part or even dominant. Therefore, a more accurate description of shear rate is needed.

Figure 2-12 shows an interior cell P and its four neighbors in the fine grid of the skirt. Cell N is above P in the axial direction. For simplicity, choose P on the centerline of the skirt ($x = 0$) so that the circumferential direction is the same as the x direction since the radius of piston is much larger than the width and height of a cell.

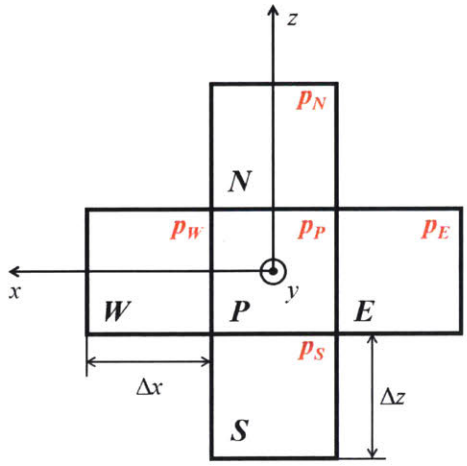

Figure 2-12 An Interior Cell on the Skirt

If the piston is taken as the reference, and is moving up with a velocity of v_{ps}, the axial velocity profile of the oil film in cell P will have two components if the cells are fully flooded. The first component is the wall-driven (Couette) flow and the second is the pressure-driven (Poiseuille) flow. They result in the following velocity fields.

$$w_1 = -v_{\mathrm{ps}} \cdot \frac{y}{h_P} \tag{2-10}$$

$$w_2 = \frac{1}{2\mu_P} \cdot \frac{p_S - p_N}{2\Delta z} \cdot (h_P y - y^2) \tag{2-11}$$

In equation 2-9 and 2-10, h_P is the clearance at cell P, $y \in [0, h_P]$ is the radial coordinate from skirt to liner, μ_P is the local viscosity, p_S and p_N are the pressure at cell S and N.

Therefore, the total velocity profile and its derivative with respect to y are

$$w = w_1 + w_2 = -\frac{1}{2\mu_P} \cdot \frac{p_S - p_N}{2\Delta z} \cdot y^2 + \left(\frac{h_P}{2\mu_P} \cdot \frac{p_S - p_N}{2\Delta z} - \frac{v_{\mathrm{ps}}}{h_P}\right) y \qquad 2\text{-}12$$

$$\frac{\partial w}{\partial y} = \frac{1}{4\mu_P \Delta z}(p_S - p_N)(h_P - 2y) - \frac{v_{\mathrm{ps}}}{h_P} \qquad 2\text{-}13$$

In the x direction, where there is only Poiseuille flow considered, the velocity profile and its derivative are

$$u = \frac{1}{2\mu_P} \cdot \frac{p_W - p_E}{2\Delta x} \cdot (h_P y - y^2) \qquad 2\text{-}14$$

$$\frac{\partial u}{\partial y} = \frac{1}{4\mu_P \Delta x}(p_W - p_E)(h_P - 2y) \qquad 2\text{-}15$$

The rate-of-strain tensor and its magnitude are

$$\dot{\vec{\gamma}} = \begin{bmatrix} 2\frac{\partial u}{\partial x} & \frac{\partial u}{\partial y} + \frac{\partial v}{\partial x} & \frac{\partial u}{\partial z} + \frac{\partial w}{\partial x} \\ \frac{\partial u}{\partial y} + \frac{\partial v}{\partial x} & 2\frac{\partial v}{\partial y} & \frac{\partial v}{\partial z} + \frac{\partial w}{\partial y} \\ \frac{\partial u}{\partial z} + \frac{\partial w}{\partial x} & \frac{\partial v}{\partial z} + \frac{\partial w}{\partial y} & 2\frac{\partial w}{\partial z} \end{bmatrix} \qquad 2\text{-}16$$

$$\left\|\dot{\vec{\gamma}}\right\| = \sqrt{\frac{1}{2}\sum\sum \dot{\gamma}_{ij}\dot{\gamma}_{ji}} = \sqrt{\left(\frac{\partial u}{\partial y}\right)^2 + \left(\frac{\partial w}{\partial y}\right)^2} \qquad 2\text{-}17$$

After inserting the expressions of the derivatives, the magnitude becomes

$$\left\|\dot{\vec{\gamma}}\right\| = \sqrt{a(2y - h_P)^2 + b(2y - h_P) + c} \qquad 2\text{-}18$$

$$a = \frac{1}{16}\left[\left(\frac{p_S - p_N}{\Delta z}\right)^2 + \left(\frac{p_E - p_W}{\Delta x}\right)^2\right], b = \frac{v_{\mathrm{ps}}}{2\mu_P h_P}\frac{p_S - p_N}{\Delta z}, c = \left(\frac{v_{\mathrm{ps}}}{h_P}\right)^2$$

Because the variables do not change within a cell, the model needs to use an averaged value of shear rate. The first candidate is the mean value of $\|\vec{\dot{\gamma}}\|$ along y direction.

$$\overline{\|\vec{\dot{\gamma}}\|} = \frac{1}{h_P}\int_0^{h_P}\|\vec{\dot{\gamma}}\|dy = \frac{b + 2ah_P}{8h_P}\sqrt{ah_P{}^2 + bh_P + c} - \frac{b - 2ah_P}{8h_P}\sqrt{ah_P{}^2 - bh_P + c} + \frac{4ac - b^2}{16h_P a^{\frac{3}{2}}} ln\left|\frac{2ah_P + b + 2\sqrt{a(ah_P{}^2 + bh_P + c)}}{-2ah_P + b + 2\sqrt{a(ah_P{}^2 + bh_P + c)}}\right| \quad 2\text{-}19$$

The expression in equation 2-18 is obviously too complicated to be implemented. On the other hand, the root mean square is

$$\|\vec{\dot{\gamma}}\|_{RMS} = \sqrt{\frac{1}{h_P}\int_0^{h_P}\|\vec{\dot{\gamma}}\|^2 dy} = \sqrt{\frac{1}{3}ah_P^2 + c} \quad 2\text{-}20$$

This expression is much simpler than equation 2-18. Meanwhile, it includes the contribution of both Couette flow and Poiseuille flow to the shear rate of the oil film. So in the current model, the shear rate term γ is expressed as

$$\gamma = \sqrt{\frac{h_P^2}{12\mu_P^2}\left[\left(\frac{p_S - p_N}{\Delta z}\right)^2 + \left(\frac{p_W - p_E}{\Delta x}\right)^2\right] + \left(\frac{v_{\mathrm{ps}}}{h_P}\right)^2} \quad 2\text{-}21$$

2.4 Overlap Between Piston and Cylinder Liner

Before this thesis work, the starting point of a calculation used to be the top dead center of the intake stroke when the cylinder pressure is limited to a few bars at most.

On the other hand, the model uses zero deformation for the initial condition. In other words, d_{P} and d_{L} in equation 2-2 is zero for every cell at the beginning of the calculation. In situations where the thermal expansion of piston skirt is much larger than that of liner, the clearance h can be negative at some points on both thrust and anti-thrust sides, as shown in the left part of figure 2-13. This is called an overlap between piston and liner, and it could result in large contact force, thus some considerable amount of deformation. As a result of this contradiction, calculation could easily fail at its beginning.

To address this issue, the most straightforward solution would be an initial condition that can have appropriate none-zero deformation. However, according to equation 2-1, such condition will introduce an initial side force as well as its distribution on the entire piston. As has been discussed, side force can contain both hydrodynamic and asperity parts, and the proportions of these two parts will also need an initial guess. In addition, the initial oil film thickness in the skirt region will have to be adjusted according to whether there is contact. This solution, although achievable, is not worth the cost of the modification to the model.

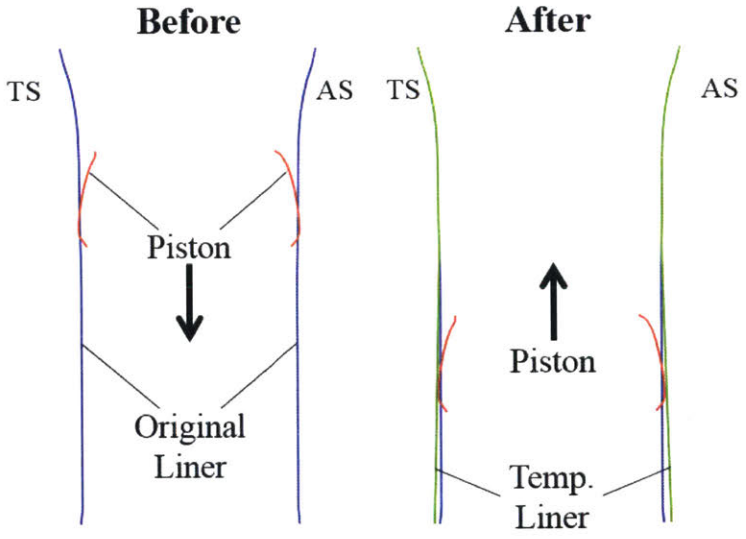

Figure 2-13 Temporary Liner and New Starting Point

An alternative method is used to deal with the overlap. On the left part of figure 2-13, the extra lines represent the liner at thrust and anti-thrust sides. They are expanded from the original

liner in order to not in contact with the piston. The piston is now at its new starting point, which is now the mid-stroke of exhaust stroke. This liner is temporarily used from the new starting point to the forthcoming top dead center, after which the original liner will be used with the same deformation as the temporary one.

To prevent the variables in the model from sudden changes, the upper parts of the two liners are identical in terms of radial variation. The compliance matrices are also the same. Since the temporary liner is generated in the preprocessing part of the model, this solution does not bring any cost to the main calculation except for the extra 90 degree of crank angle.

2.5 Summary

This chapter focused on further developing the existing model. On one hand, the robustness and efficiency used to be an issue when applying the model, especially to cases with higher loads. On the other hand, the lack of consideration of some features in real engines had restricted the application of the model. The overlap problem discussed in section 2.4 serves as a typical illustration of these limitations. Another example would be the situation where the piston exceeds the bottom of the liner around bottom dead center. In this thesis work, several issues are addressed so that the model has become more versatile and adaptable.

Another major improvement to the model is the consideration of non-uniform distribution of oil addition to the liner. The addition of the oil droplets to the liner below the skirt depends on the design of oil cooling jet and interaction between the moving parts and the oil in the sump. Additionally, there could be intentional oil jet shooting to the liner for cooling. Thus, in general the distribution of the oil addition on the liner is not readily known and it is convenient to give freedom to this input.

Chapter 3

Major Geometric Factors and Their Influence

As introduced in the previous chapter, a comprehensive description of the system's geometry is included in the model. This chapter discusses the effects of some major geometric factors on the lubrication performance in a heavy duty diesel engine with a steel piston. The radial variances of the liner and piston for this engine are shown in figure 2-1 and figure 2-2.

The first section illustrates some generic trends in piston secondary motion and oil transport during an engine cycle. A baseline case is calculated and analyzed in this section. In the following sections, cases with different values of each individual factor are calculated in order to study the corresponding influence.

3.1 General Pattern of Piston Secondary Motion and Oil Transport

Table 3-1 gives some key parameters of the baseline case.

Table 3-1 Model Parameters of the Baseline Case

Parameter	Value	Unit
Nominal Clearance	60	μm
Stroke	0.158	m
Axial length of Skirt	0.0654	m
Axial length of Chamfer	0.0075	m
Engine Speed	1200	rpm
Peak Cylinder Pressure	20.22	MPa
Wave Height of Machine Marks	11	μm
Wavelength of Machine Marks	270	μm
Effective Young's Modulus	3.308	GPa
Boundary Friction Coefficient	0.03	-
Thickness of Oil Addition (Uniform)	15	μm

Figure 3-1 shows the pressure trace used in the case, which is given as an input for the model. In the x-axis, -360° crank angle stands for the top dead center of the intake stroke, while 0° is when the piston is at top dead center before the expansion stroke.

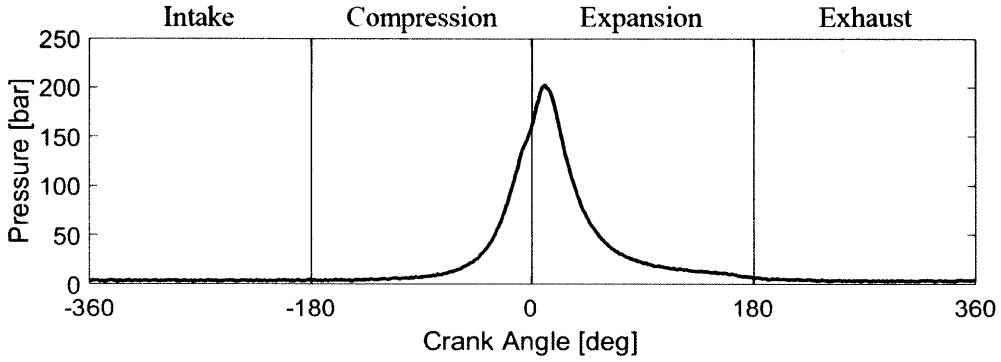

Figure 3-1 Pressure in the Combustion Chamber

3.1.1 Overall Results for Entire Engine Cycle

The case is calculated for six engine cycles to reach certain convergence, where the difference in the values of major output variables between current and previous cycles is less than 0.5%. Figure 3-2 and 3-3 show the axial velocity and acceleration of the piston. In the model, the angular velocity of the crankshaft is assumed to be constant, thus it is straightforward to calculate the primary motion of the piston. The primary motion remains the same for all the cases discussed in this chapter.

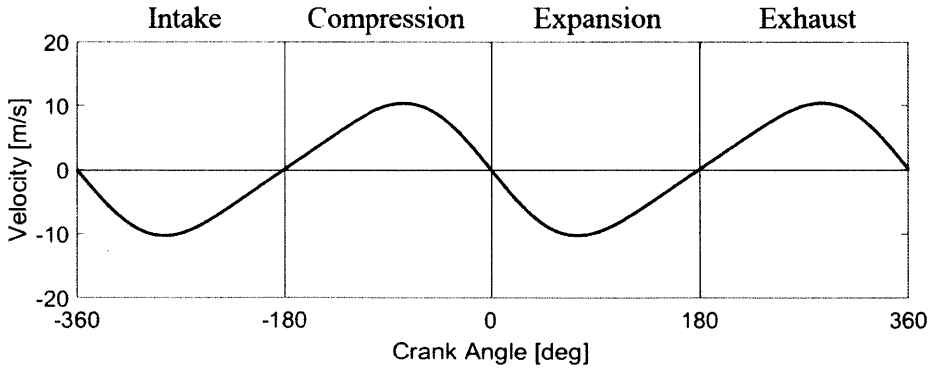

Figure 3-2 Axial Velocity of Piston

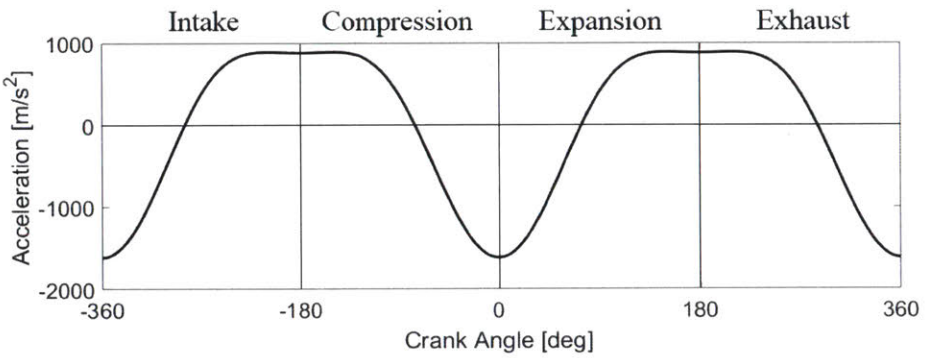

Figure 3-3 Axial Acceleration of Piston

The baseline case (as well as the other cases discussed in this thesis) was calculated for six engine cycles until the cycle-converged results are obtained. Figure 3-4 and 3-5 show the secondary motion of the sixth cycle. Figure 3-6 explains how secondary motion is defined in the model. Taking the center of the cylinder bore, based on which bore distortion is measured, as the reference, the original lateral position of the center of piston pin would equal to the pin offset, and lateral motion would be the distance of pin center from this original place. A positive value of lateral movement means the piston is closer to the thrust side. For tilt angle, positive values are used when piston is tilting clockwise (the bottom of the piston is closer to the thrust side).

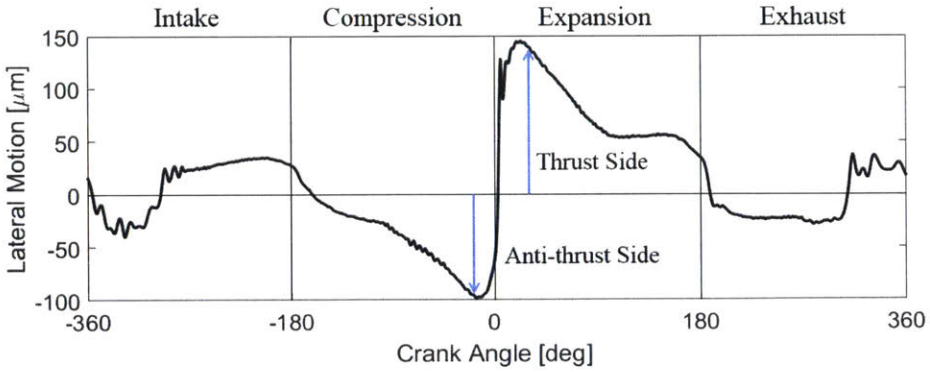

Figure 3-4 Lateral Motion of Baseline Case

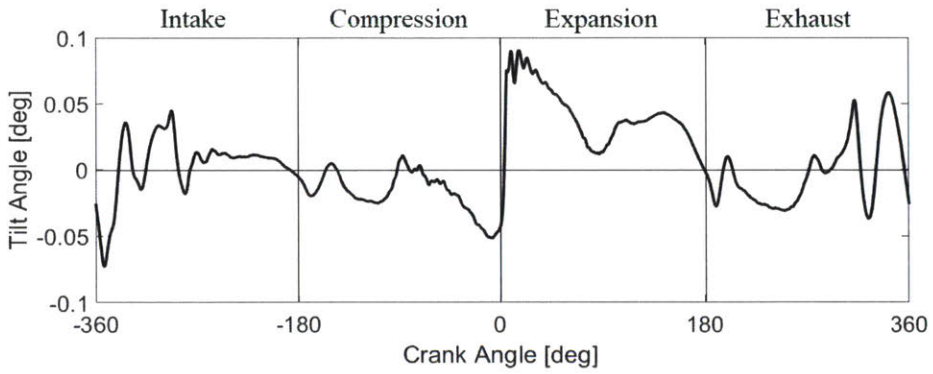

Figure 3-5 Tilt Angle of Baseline Case

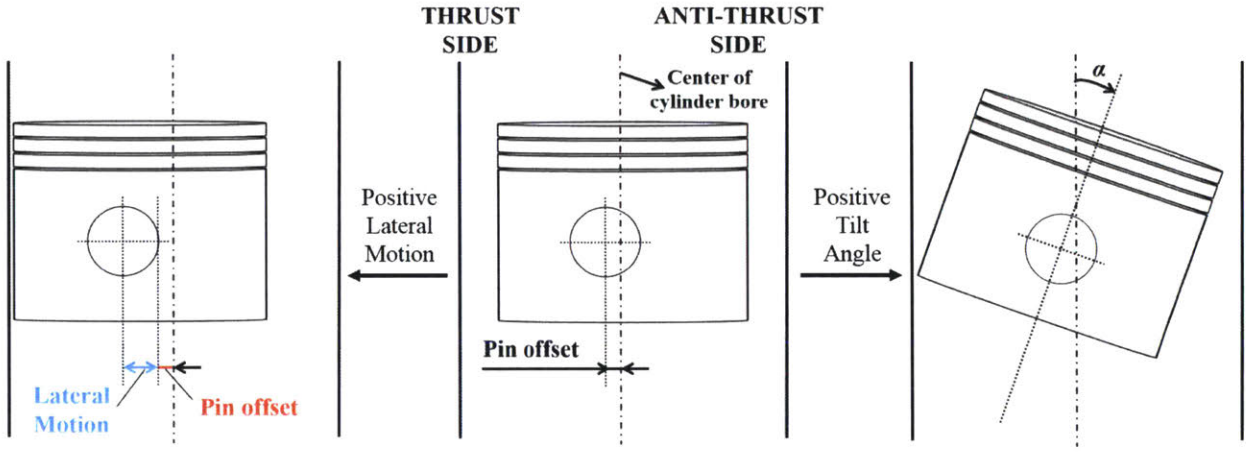

Figure 3-6 Definition of Secondary Motion

As discussed in section 1.2, the lateral motion is controlled by force balance. Since the primary motion is fixed, the motion of the connecting rod before any lateral motion is also straightforward. If there were no secondary motion at all, it would also be easy to determine the lateral force between piston and connecting rod, and this lateral force would give piston a lateral motion with the same direction. Even when some secondary motion exists, and force starts to develop between skirt and liner, lateral motion will still be guided by the positions of piston and rod. As a result, many features of the curve in figure 3-4, such the direction of lateral motion, can be directly related to the primary motion of piston regardless of the specific engine parameters.

The direction of the tilt angle is less straightforward. This is because the tilt angle determines the location of the contact area along the skirt to provide both force and moment balance. For instance, if the piston skirt is only in contact with one side, the total force from the skirt is meant to balance the force from the pin. Moment balance determines the center of the force on the skirt, which may be not easy to be attained with any tilt angle. Therefore, tilt angle is more likely to have fluctuation and depends more on the running conditions.

As discussed in the first chapter, secondary motion results from the lateral force from the pin, which is shown in figure 3-7. Apart from the inertia of piston in the same direction, this lateral force is balanced by contacting the liner through asperity contact and hydrodynamic pressure. The forces along the y-direction in figure 1-1 are plotted in figure 3-8 and 3-9.

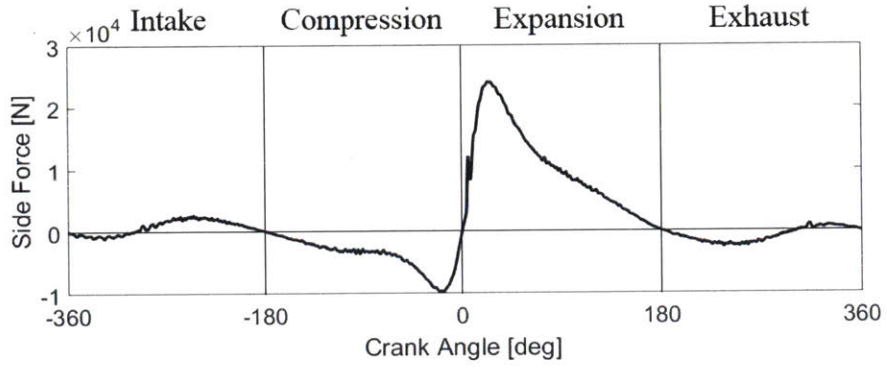

Figure 3-7 Lateral Force from Pin to Piston of Baseline Case

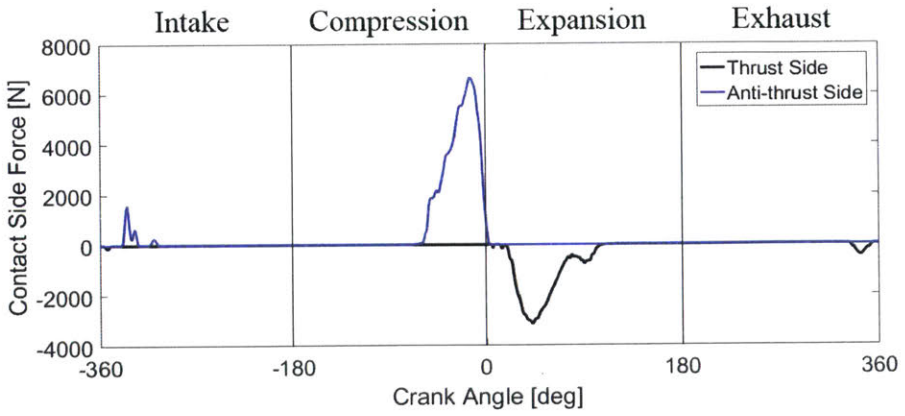

Figure 3-8 Side Force from Asperity Contact of Baseline Case

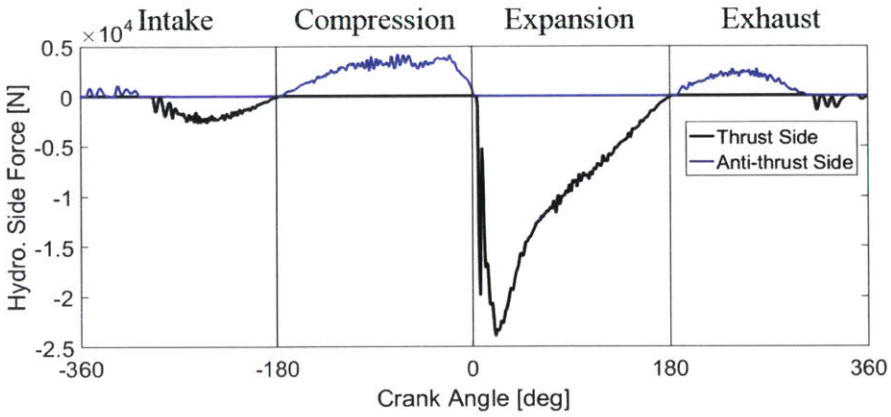

Figure 3-9 Side Force from Hydro. Pressure of Baseline Case

Both contact and hydrodynamic pressure can lead to friction between piston and liner. In figure 3-10, the friction force in z-direction is plotted separately for thrust and anti-thrust sides. Most of the friction force in the figure happens around 0° crank angle, where the pressure in the combustion chamber is much larger than other places. Also, the lateral motion during this period of time is in consistence with which side does the friction exist.

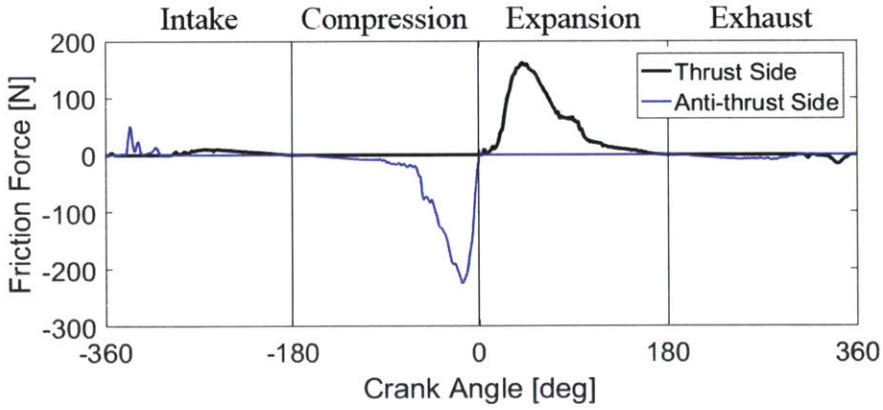

Figure 3-10 Friction Force of Baseline Case

As mentioned before, forces between skirt and liner, secondary motion, and oil transport are interacting with each other in the system. So to investigate the cause of friction, it is important to look at the oil distribution in the skirt region. The following subsections analyze the details during different strokes.

3.1.2 Intake Stroke

The intake stroke has the least cylinder pressure in the entire cycle and thus inertia plays a critical role in determining the piston secondary motion. In the following, the piston secondary motion will be discussed first, followed by the oil transport.

Figure 3-11 shows the direction of the axial acceleration of the piston and the side force from the pin during an intake stroke. The piston accelerates downward at first, as is shown in figure 3-3 and the left part of figure 3-8. Because the piston does not experience substantial pressure difference between its top and bottom surfaces, it will be pulled by the connecting rod towards anti-thrust side, as shown in figure 3-4. After mid-stroke, where the piston reaches its maximum velocity and acceleration becomes zero (around 75° CA after TDC in this case), the piston will decelerate and be pushed by the rod to thrust side.

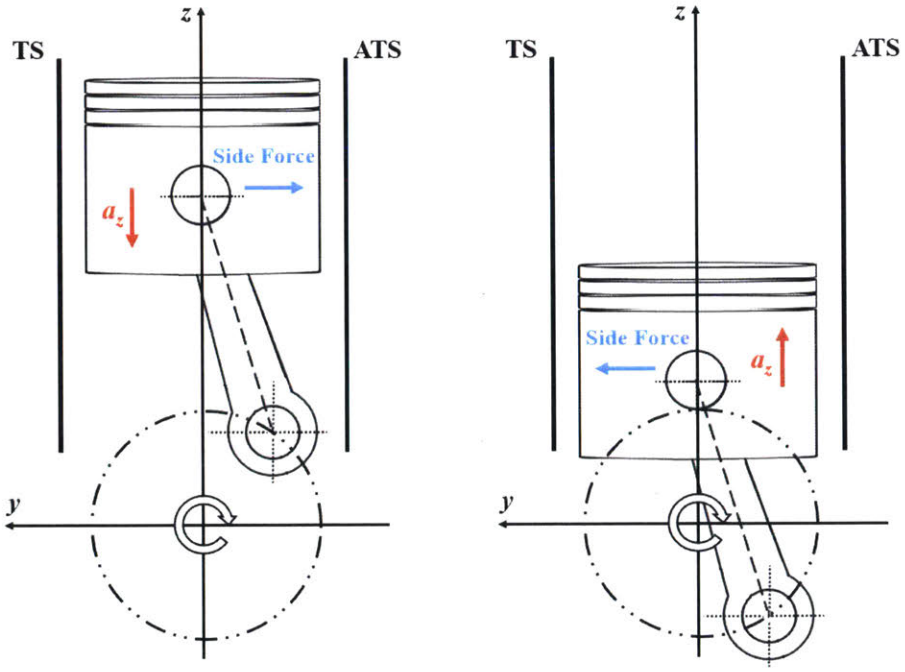

Figure 3-11 Direction of Side Force in Intake Stroke

The oil on the open liner will firstly enter the skirt region and then the chamfer region. In order to study the change in the total oil volume in these two regions, an average oil film thickness is defined. It is the average oil height in the radial direction of all the cells in the meshes. In partial

film region, the oil films that attached to both liner and piston are included. From the calculation result, the average oil film thickness in these two regions are plotted in figure 3-12 and 3-13.

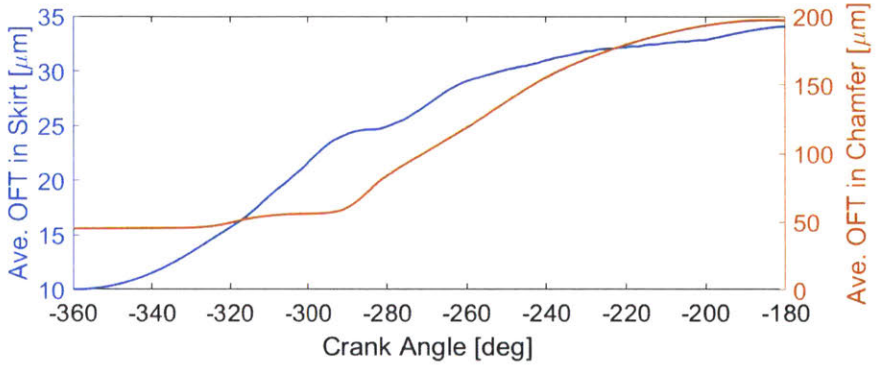

Figure 3-12 Average OFT on TS in Intake Stroke

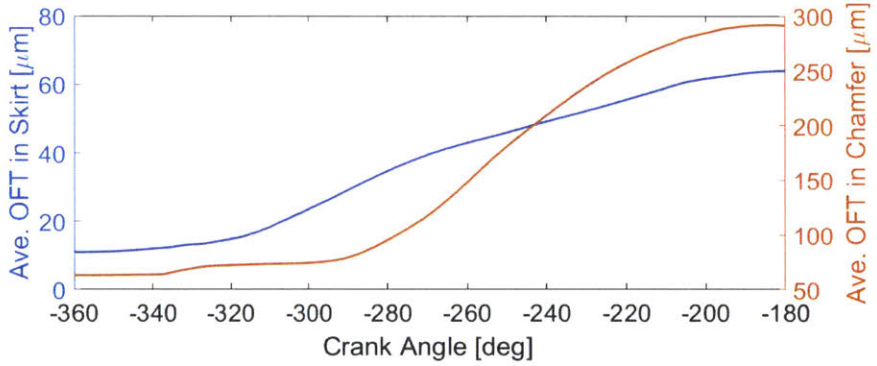

Figure 3-13 Average OFT on ATS in Intake Stroke

On both thrust and anti-thrust side, the growth in the average oil film thickness in the chamfer region occurs later than that in the skirt region. This is because the axial size of piston skirt is comparable to the open liner. The oil that enters the skirt region will not reach the chamfer until after a certain amount of time. In this case, the amounts of oil in the chamfer on both sides start a sharp increase at around -290° CA, where the distance that the piston has traveled from top dead center is 0.063 meter, which is close to the axial length of the skirt.

Before starting to accumulate the lubricant that is originated from the open liner, the chamfer can also receive oil from other approaches. For example, there is a slight rise in the chamfer oil accumulation on anti-thrust side between -340° and -320° CA, which is the contribution from lateral forces and secondary motion.

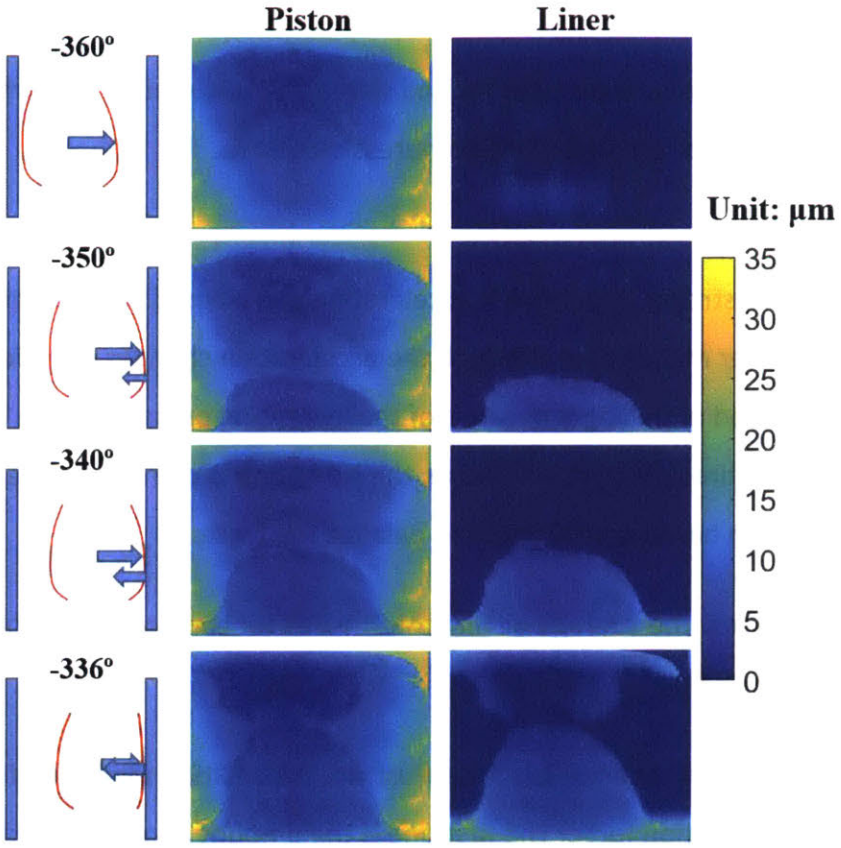

Figure 3-14 Distribution of Oil Film Thickness in Skirt Region during Intake Stroke

The left part of figure 3-14 contains some schematic diagrams of the lateral forces and piston secondary motion at different crank angles. The vertical bars and curves represent the contours of liner and skirt, and the arrows represent the forces on the piston from pin and liner. The middle and right parts of figure 3-14 show the distributions of oil film thicknesses on liner and piston in the skirt region at corresponding crank angles. In partial film, the thicknesses are respectively h_{L} and h_{S} in figure 2-6; in full film region, they are defined here as half of the local clearance h.

After top dead center, piston moves towards anti-thrust side driven by the force from piston pin. The lower part of the skirt touches the liner first, forming full film region and generating a force against the pin. The two forces lead to a torque that rotates the piston clockwise. As a result, the lubricant on the upper part of the skirt also touches the liner, and is dragged into the chamfer region.

At the end of the intake stroke, both chamfer and skirt accumulate oil, and chamfer will serve as the source of lubricant for the upcoming compression stroke.

3.1.3 Compression Stroke

At the beginning of this stroke, the piston is accelerating and pushed back to anti-thrust side by the connecting rod. After mid-stroke, although the acceleration changes direction, the rod still pushes the piston instead of pulling it because of the increasing pressure in the combustion chamber. During the entire compression stroke, the side force is pointing to the anti-thrust side, at which the piston has to stay in order to balance the force.

Figure 3-15 and 3-16 show the average oil film thicknesses for compression stroke, which drop rapidly with piston moving up.

There are several interesting phenomena that illustrate the relation among oil film thickness, secondary motion, and friction force. The first one is the amount of oil in the skirt region for thrust and anti-thrust sides. Although both sides suffer from rapid loss of lubricant, the total oil volume, which is proportional to the average oil film thickness, stops decreasing on thrust side at around -85° CA. This is because there is a large clearance between skirt and liner on this side due to lateral motion. As the piston leaves the liner on thrust side, the oil film in between will detach and part of the oil will stay on the skirt. However, on anti-thrust side, skirt and liner are close to each other, and the liner will keep dragging oil out of the skirt.

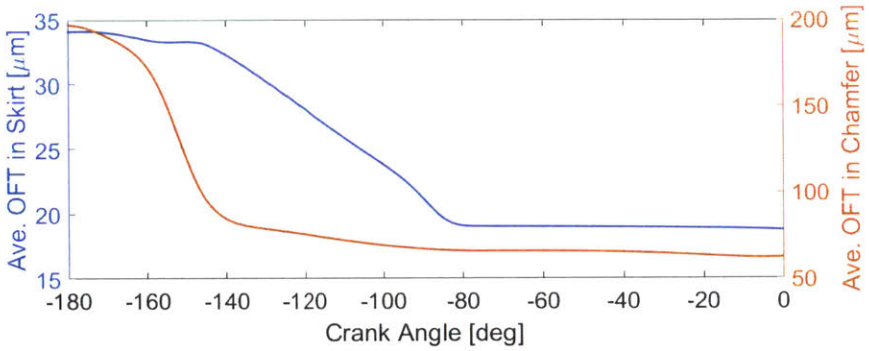

Figure 3-15 Average OFT on TS in Compression Stroke

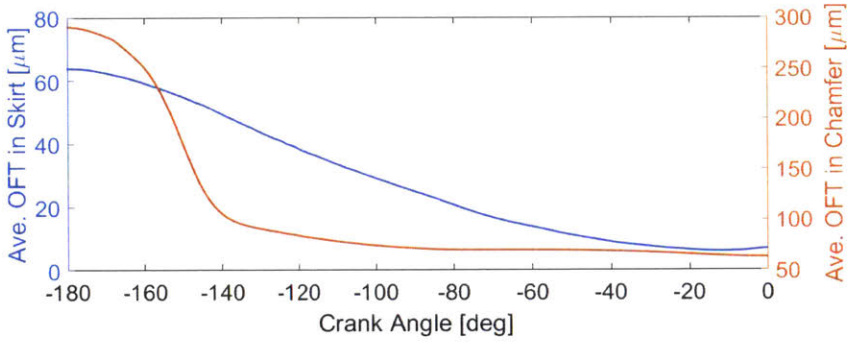

Figure 3-16 Average OFT on ATS in Compression Stroke

Figure 3-17 shows the secondary motion of the piston as well as the deformation of piston and liner at four different crank angles. In each part of the plot, the two long black lines represent the original liner at thrust and anti-thrust sides without factoring the deformation, and the two outer blue lines depict the liner with deformation. The blue and black lines are identical at -180° CA where the liner does not deform. For the skirt, the green lines depict its original shape and the red lines include the deformation. The dashed green line in the center of each part stands for the centerline of the piston. The secondary motion is magnified so that it can be manifested by the centerline.

When the piston gets close to the top dead center, there is insufficient oil in both skirt and chamfer while the side force becomes very large. Therefore, asperity contact occurs between skirt and liner on anti-thrust side, which brings a large friction force as shown in figure 3-10.

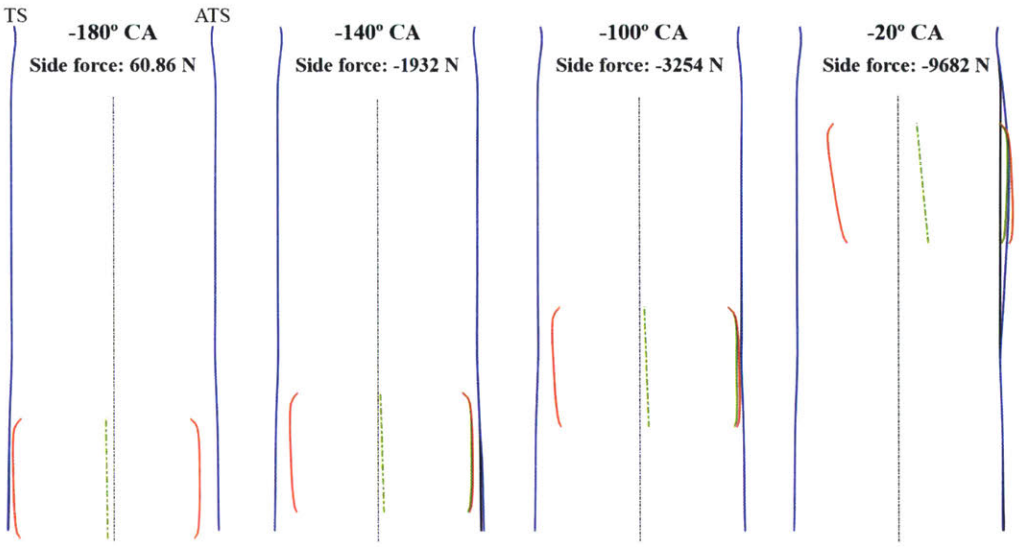

Figure 3-17 Secondary Motion in Compression Stroke

3.1.4 Expansion Stroke

The lateral motion during expansion stroke is similar to that of compression stroke. Because of the combustion pressure, the connecting rod keeps pushing the piston and the piston stays to the thrust side. This is different from the other down stroke, so the oil accumulation is also different.

As discussed in 3.1.3, there is some lubricant left on the skirt on thrust side at the beginning of expansion stroke. However, at early expansion stroke, the combustion pressure will dramatically increase and result in severe side force, as shown in figure 3-7 and 3-18. The piston skirt will slap to the thrust side and hence squeeze the oil out of the skirt region. In figure 3-19, the average oil film thickness in skirt region on the thrust side reduces from its starting point instead of growing like the other side. This lack of oil leads to elevated direct asperity contact and friction on the thrust side.

As seen in figure 3-19, after piston slap the average oil film thickness of the skirt/liner maintains a relatively constant value until around 75° CA due to high side force and flexibility of the skirt

and liner that conforms them. Afterwards, the skirt reaches the end of the wet part of the liner where liner becomes much stiffer. The constraint can be seen in the third part of figure 3-18, where the clearance is limited at the bottom of the skirt on thrust side since its counterpart on the liner does not deform. The oil on the open liner is consequently difficult to enter the skirt region until the piston passes the constraint and the clearance starts to increase.

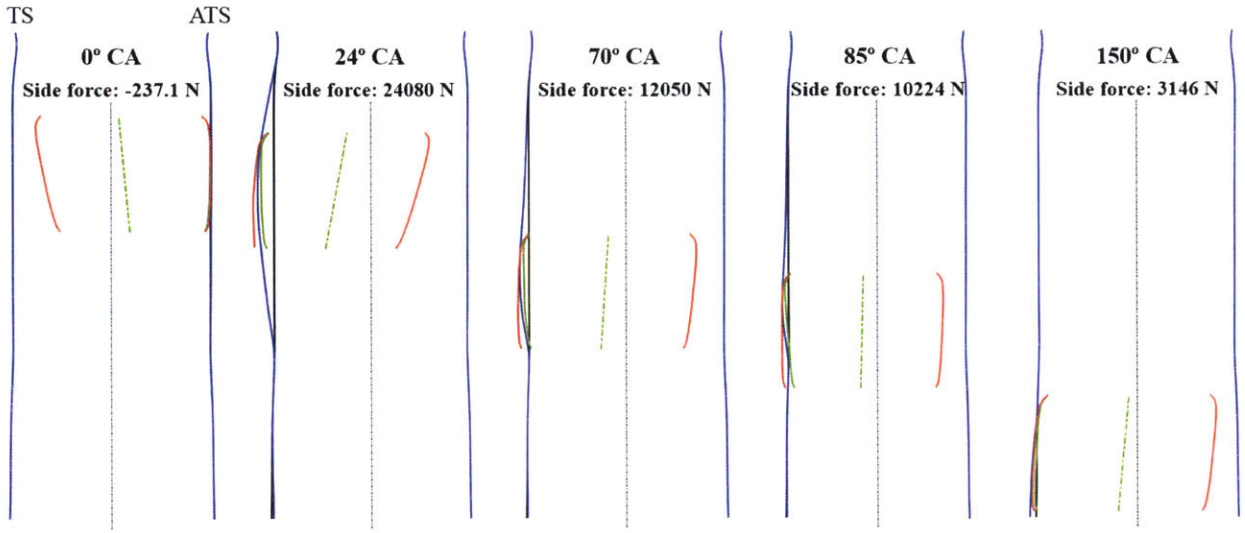

Figure 3-18 Secondary Motion in Expansion Stroke

As for anti-thrust side, things are not as interesting as the piston is far from the liner during the entire stroke. At the end, both skirt and chamfer collect much more lubricant than the other side.

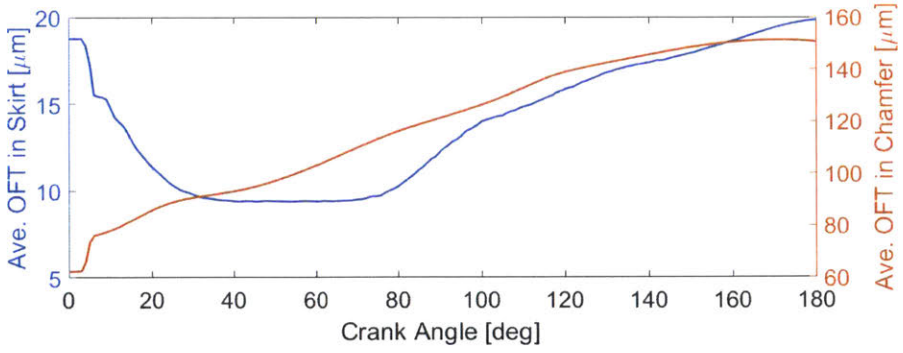

Figure 3-19 Average OFT on TS in Expansion Stroke

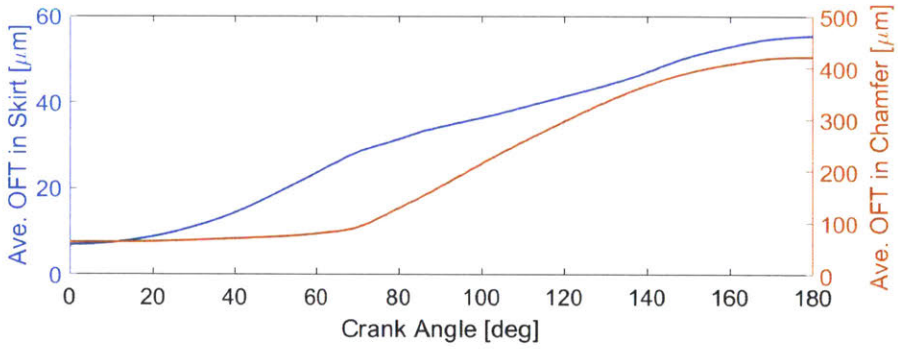

Figure 3-20 Average OFT on ATS in Expansion Stroke

3.1.5 Exhaust Stroke

Similar to the intake stroke, the exhaust stroke is quiet in terms of side force and friction. The axial acceleration of the piston will change sign at some point. Most of the oil in skirt and chamfer will be spread on the liner along the way.

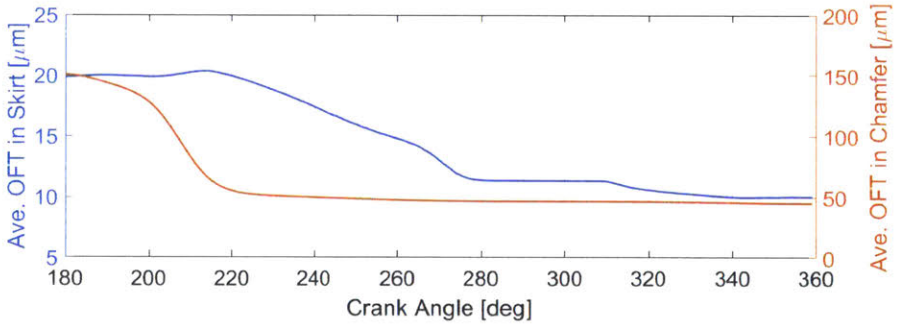

Figure 3-21 Average OFT on TS in Exhaust Stroke

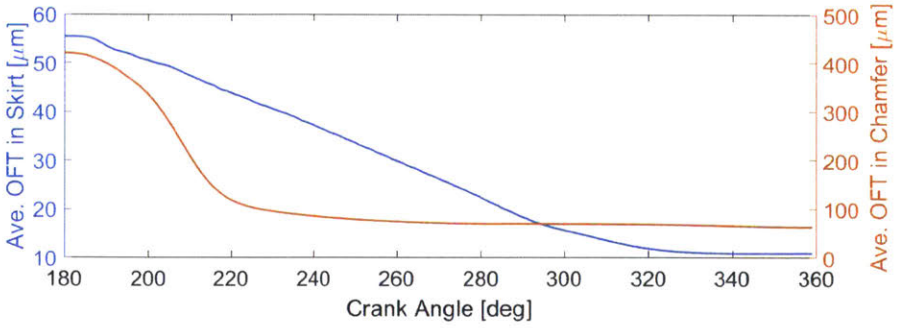

Figure 3-22 Average OFT on ATS in Exhaust Stroke

3.1.6 Summary

Since the model assumes that no oil can pass the oil control ring, lubricant that is attached to the open liner enters the skirt and then the chamfer region during intake stroke. At bottom dead center, the chamfer oil can reach several hundred microns in average film thickness, and will provide lubrication for the upcoming compression and expansion strokes. Unfortunately, most of this part of oil will be left back on the liner long before the piston reaches top dead center. At late compression stroke and early expansion stroke, the combination of high side force and lack of oil results in severe lubrication condition for piston skirt.

Figure 3-23 shows the distribution of the averaged product of asperity contact pressure and sliding speed of the piston over the entire cycle. This parameter has a positive correlation with the wear rate on the skirt. As can be seen in the figure, the side of the skirt on thrust side and the upper part of the skirt on anti-thrust side are likely to experience wear, based on the results of the model.

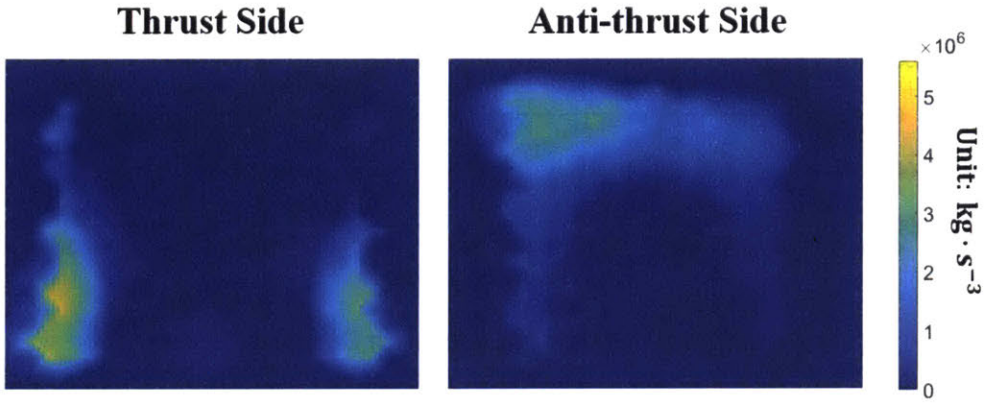

Figure 3-23 Distribution of a Pressure-Velocity Factor on the Skirt of Baseline Case

3.2 The Effects of Installation Clearance

Among all the factors that play a part in the clearance, installation clearance, which is the difference between the nominal diameters of piston and cylinder liner, has the most direct impact. In this section, cases with different nominal diameters for the liner are calculated and compared with the baseline case discussed in 3.1. All the other inputs and engine parameters stay unchanged.

3.2.1 Secondary Motion and Friction

Figure 3-24 and 3-25 contain the secondary motion for different cases. The magnitude of lateral motion increases with the clearance, and fluctuation happens when clearance gets to 200 microns. As for tilt angle, the change is not as significant because the tilting can be subject to the lateral movement.

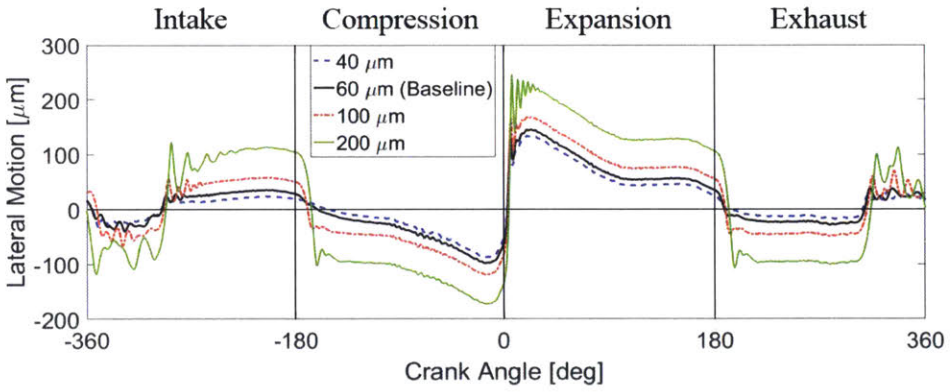

Figure 3-24 Lateral Motion of Cases with Different Clearances

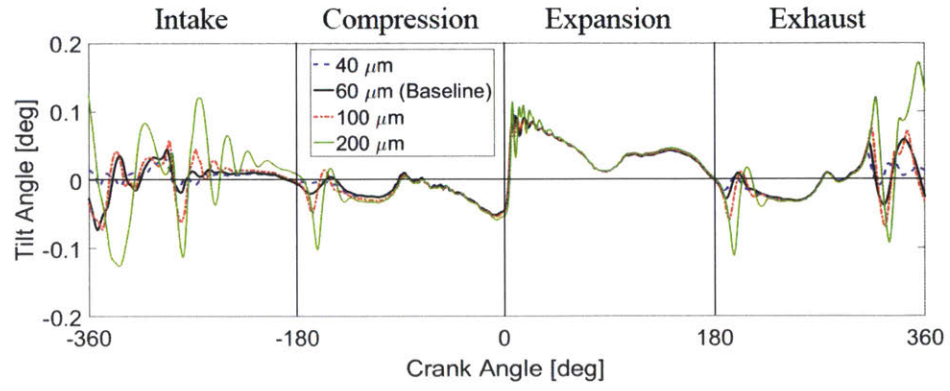

Figure 3-25 Tilt Angle of Cases with Different Clearances

The traces of friction force for these cases are plotted in figure 3-26, and the friction mean effective pressures (FMEP) and their components from the skirt are listed in table 3-2.

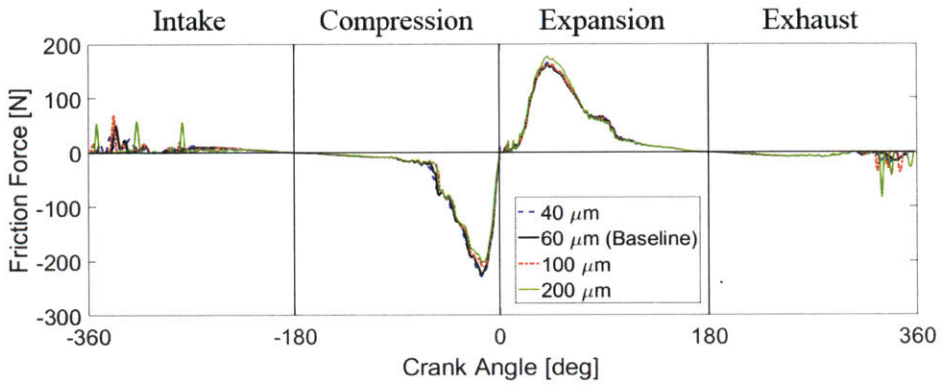

Figure 3-26 Friction Force of Cases with Different Clearances

The curves in figure 3-25 show that during late compression stroke, friction force decreases with larger clearance. Because this period is the major contributor to the FMEP on anti-thrust side, it is agreed with the third and fifth rows of table 3-2.

Table 3-2 FMEP [bar] of Cases with Different Clearances

	40 μm	**60 μm**	**100 μm**	**200 μm**
Total FMEP	0.117	0.112	0.107	0.109
From Hydrodynamic Lubrication on TS	0.0454	0.0438	0.0415	0.0413
From Hydrodynamic Lubrication on ATS	0.0185	0.0175	0.0170	0.0160
From Boundary Lubrication on TS	0.0308	0.0296	0.0294	0.0307
From Boundary Lubrication on ATS	0.0224	0.0211	0.0182	0.0175

On the thrust side, friction during expansion stroke also decreases except for the 200-micron case. On the one hand, this comes from the contact between the liner and the piston second land, which contributes 0.003 bar to the total FMEP. The model can include the lands in the calculation. Because the radius of the lands is in general smaller than the skirt, contact will not happen on the land until the secondary motion is sizable enough, which is the case for an installation clearance of 200 microns in figure 3-24 and 3-25. On the other hand, FMEP from the skirt is also larger due to the fluctuation in secondary motion and side force.

In order to avoid the influence of such fluctuation and look at the most distinctive effects of the clearance, only the cases with clearances of 40 microns ('Case I') and 100 microns ('Case II') will be studied in the next part of this section.

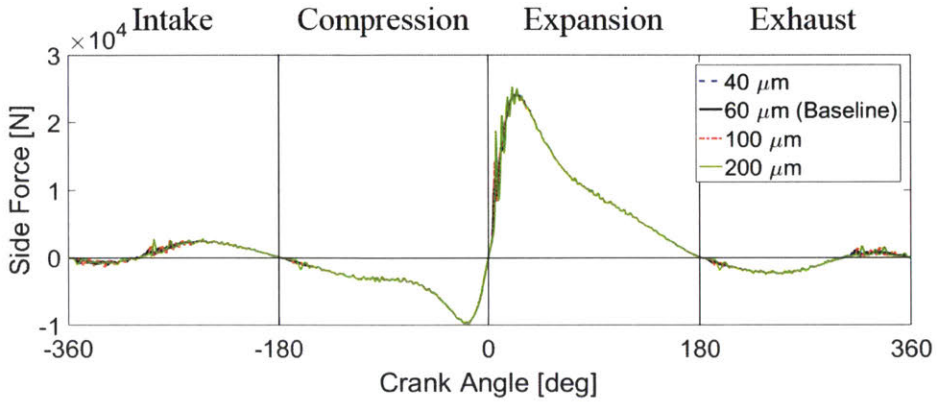

Figure 3-27 Side Force of Cases with Different Clearances

3.2.2 Oil Transport

As discussed before, when the piston moves to or stays at one side of the liner, the average oil film thickness in the skirt area on that side has a negative correlation with the friction force. Therefore, it is necessary to look at it in order to determine how clearance plays its role.

From a comparison between the numbers in the second and fourth columns in table 3-2, the part of friction that has the most significant drop is the boundary friction on anti-thrust side. This is very different from the results of gasoline engines. Still, this part of decrease can be attributed to oil transport and availability.

Figure 3-28 shows the average clearance between skirt and liner on anti-thrust side, while figure 3-29 and 3-30 give the overall development of the oil film thickness in skirt and chamfer region. At the beginning of the intake stroke, because the piston stays on anti-thrust side, the average clearance is limited for both cases, so the oil amount is also similar.

However, after around -270° CA, the oil volume in the skirt region for Case II does not rise as much as Case I, whereas its chamfer region accumulates significantly more lubricant. This can be explained by looking at the oil film distributions for these cases.

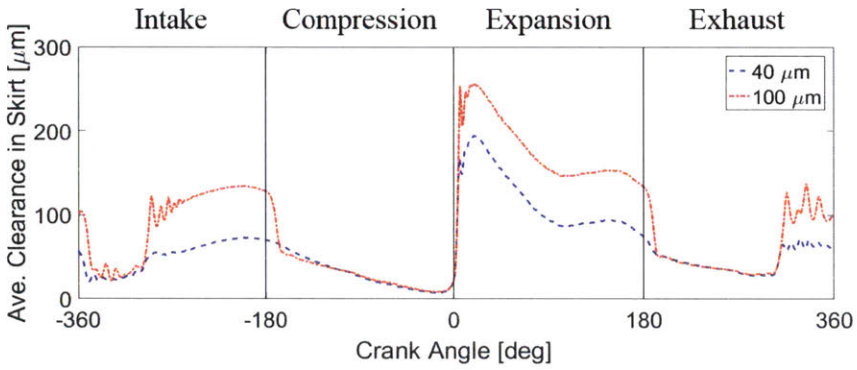

Figure 3-28 Average Clearance on ATS for Different Clearances

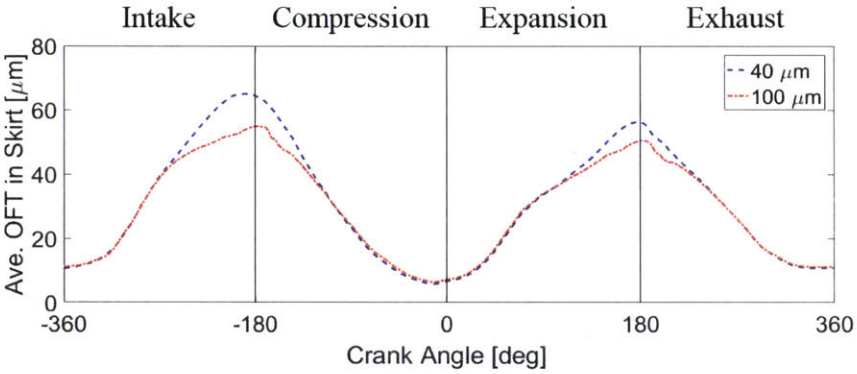

Figure 3-29 Average OFT in Skirt on ATS for Different Clearances

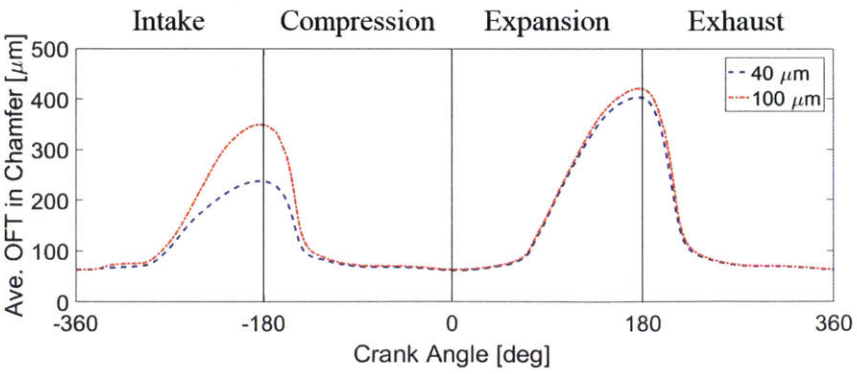

Figure 3-30 Average OFT in Chamfer on ATS for Different Clearances

Figure 3-31 and 3-32 give the reason behind the divergence of the curves. After mid-stroke, the piston moves away from the anti-thrust side. Since there is a lot of lubricant on the open liner, in Case I, where lateral motion is limited by the clearance, a considerably large area of full film is maintained and even developed from -285° to -235° CA. The consequent viscous drag slows the oil flow towards the chamfer. On the other hand, during the same period of time, the piston in Case II is so far from the liner that the lubricant on the open liner is barely in touch with the oil on the piston. So the lubricant on the liner on the anti-thrust side can move as fast as the liner itself (if the piston is taken as the reference).

In figure 3-31, the oil spreads as full film between piston and liner, both of which experience accumulation. In figure 3-32, the oil film distribution on the piston is only slightly affected by the inertia, while the oil on the liner moves through the skirt region to the chamfer region much faster.

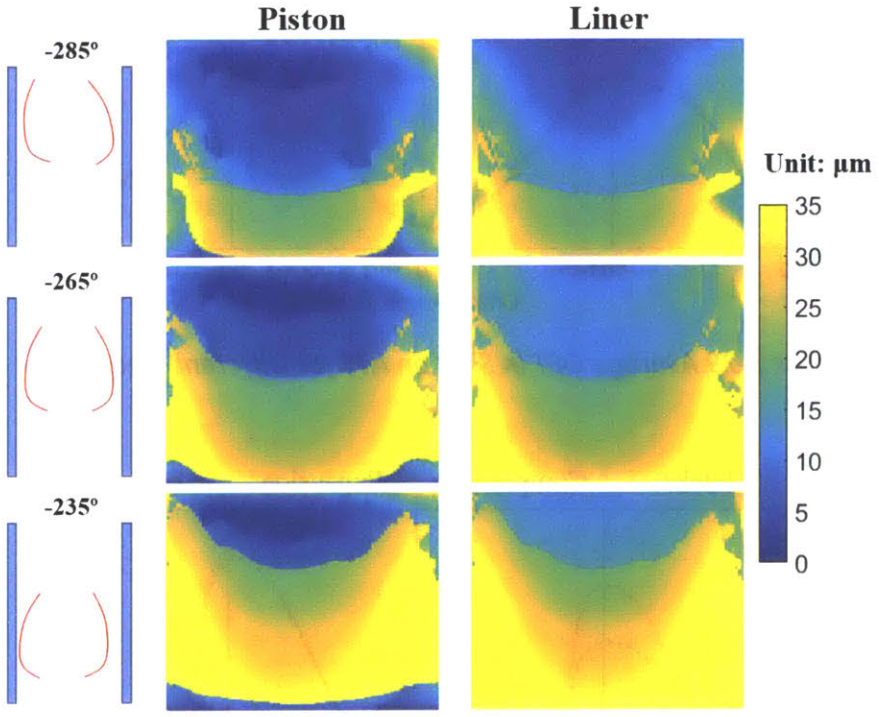

Figure 3-31 Distribution of Oil Film Thickness in Skirt Region on ATS in Case I

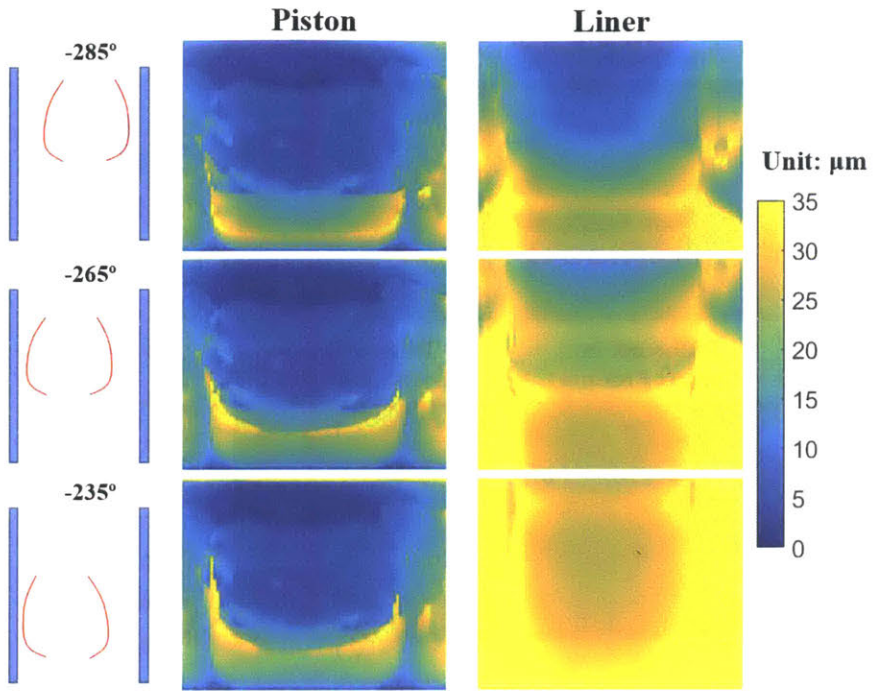

Figure 3-32 Distribution of Oil Film Thickness in Skirt Region on ATS in Case II

When piston arrives at the bottom dead center, although Case II has less oil in skirt area, it stores much more in the chamfer. During upstroke, the lubricant in the skirt leaves the piston earlier than chamfer oil, so the curve for Case I in figure 3-29 drops faster than the other curve between -180° and 0° CA. In late compression stroke, Case II has a higher average skirt oil film thickness, thus experiences less friction. Figure 3-33 shows the distributions of contact pressure and hydrodynamic pressure on anti-thrust side at -15° CA in Case I, and the differences between Case II and Case I. It can be seen that Case two has less contact and more hydrodynamic pressure, although the relative differences are not very substantial.

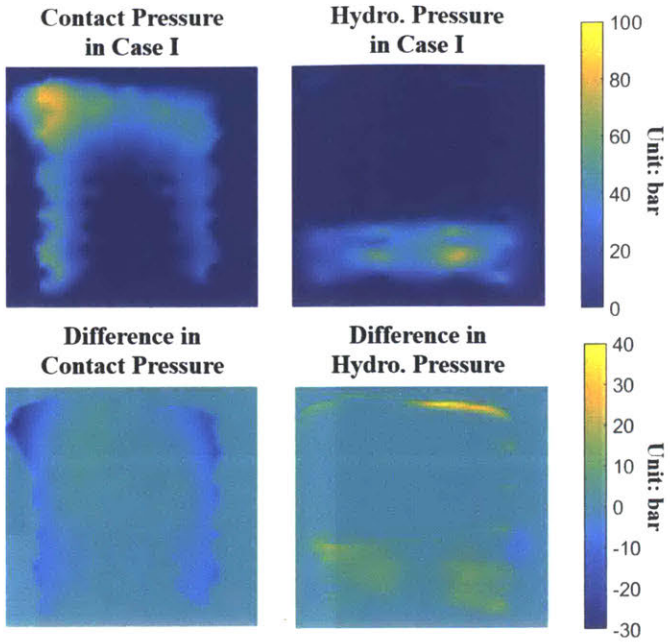

Figure 3-33 Difference in Pressure Distributions on ATS at -15° CA between Cases

3.2.3 Summary

The distributions of the pressure-velocity factor for Case I and Case II are shown in figure 3-34. Similar to figure 3-33, the difference between these cases is also limited.

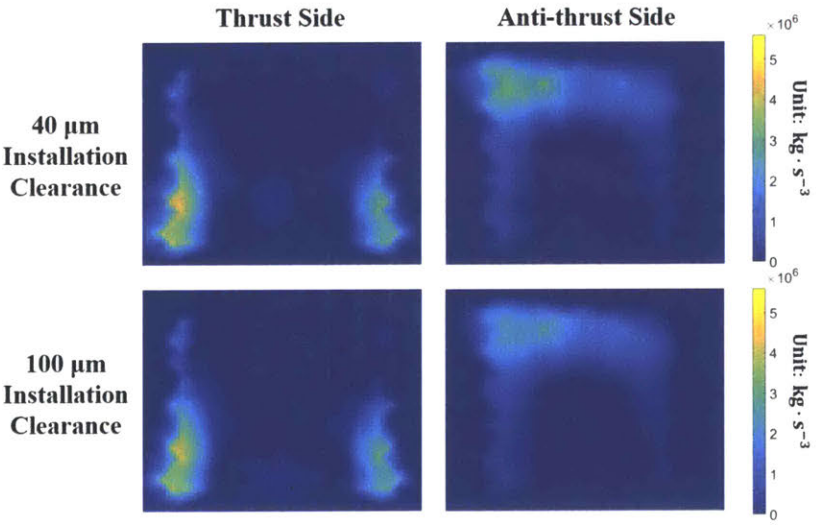

Figure 3-34 Distribution of Pressure-Velocity Factor of Cases with Different Clearance

For the heavy duty diesel engine studied in this section, some reduction in frictional loss can be achieved by increasing the installation clearance between piston and liner. However, the improvement is not as promising considering the side effect of larger clearances, including noise, vibration and harshness (NVH), and excessive piston slap.

The friction reduction associated with larger clearance used to be attributed to the release of overlap, since more friction force will occur when piston touches the liner on both sides at the same time. The results of this study, however, do not agree with such reason. Figure 3-35 and 3-36 show the side force from liner to piston at each side. It is clear that only one side is in contact during compression stroke and expansion stroke, where most of the friction takes place. Therefore, less available oil stored in the chamfer and skirt after down strokes, instead of more overlap, is not responsible for the larger frictional loss in Case I.

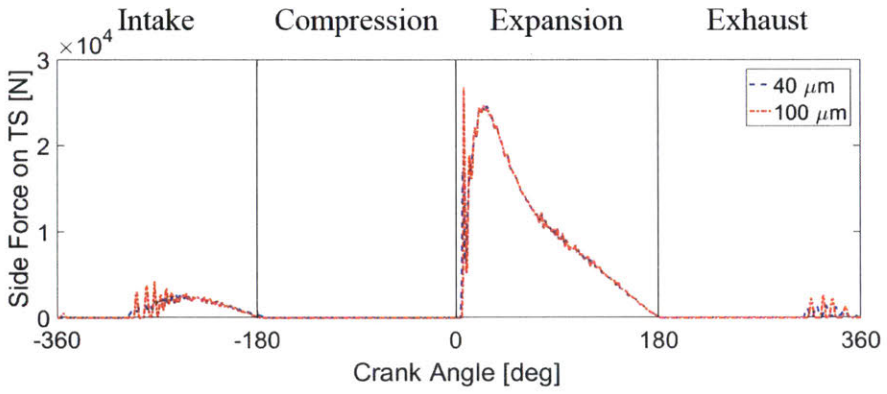

Figure 3-35 Side Force on TS of Cases with Different Clearances

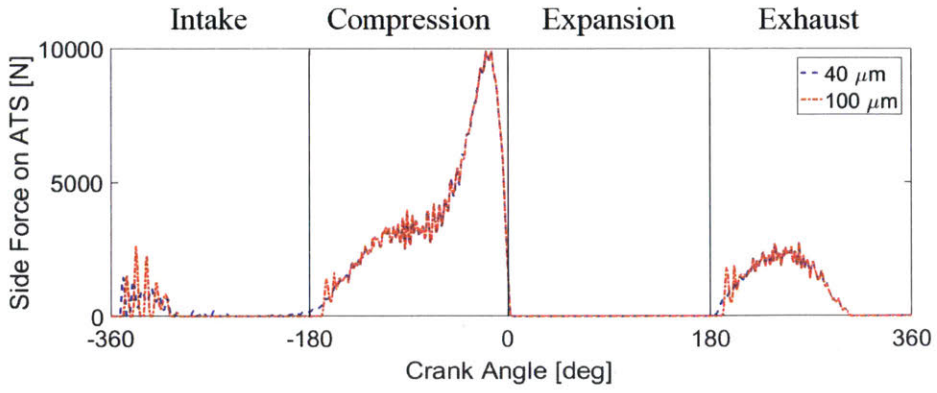

Figure 3-36 Side Force on ATS of Cases with Different Clearances

3.3 The Effects of Dynamic Deformation of Cylinder Liner

The side force between piston and liner induces deformation for both of these components. According to equation 2-2, deformation of the liner d_{L} contributes to the gap between the two surfaces, and is calculated from the compliance matrix.

$$\overrightarrow{d_L} = C_L \cdot \vec{F} \qquad 3\text{-}1$$

This section studies the effects of the stiffness of liner by comparing the results of cases with different compliance matrices C_{L}.

First of all, secondary motion can be affected by the stiffness. Figure 3-37 shows the lateral movement and tilt angle of three cases. In addition to the baseline case, 'Case III' uses a C_{L} with half of the values in the original compliance matrix, and 'Case IV' assumes the liner does not deform at all. It is evidently that with softer liner, the piston will have more space to move in the lateral direction. The tilt angle of piston is also changed for different stiffness.

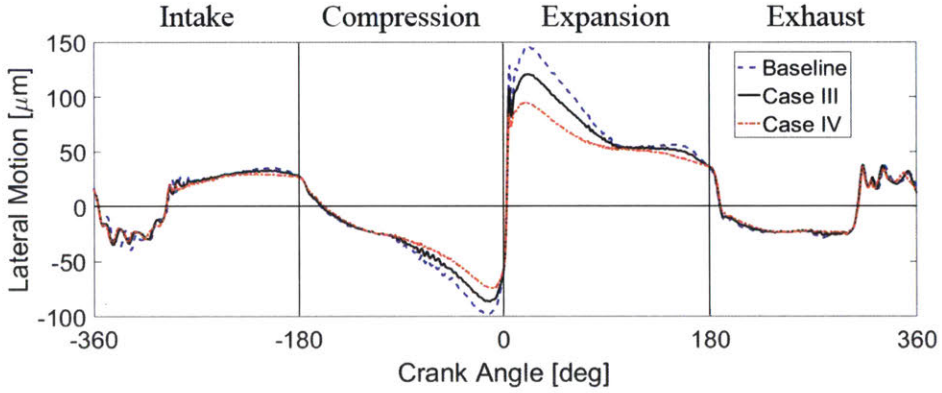

Figure 3-37 Lateral Motion of Cases with Different Liner Compliances

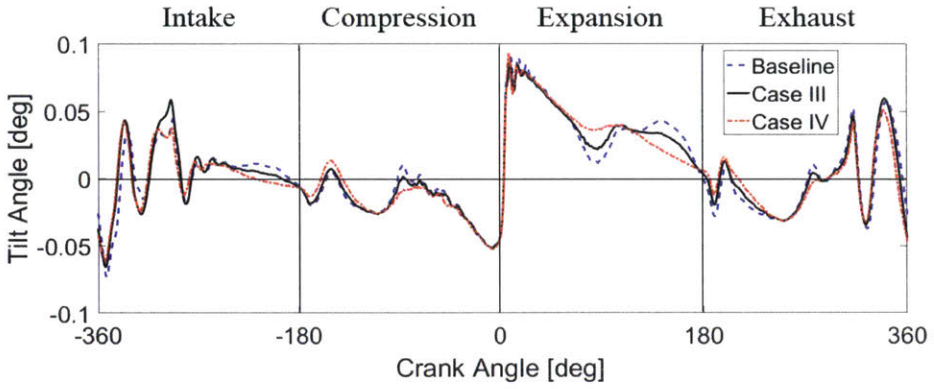

Figure 3-38 Tilt Angle of Cases with Different Liner Compliances

From figure 3-39 and table 3-3, which contain the friction force and the components of FMEP, stiffer liner tends to reduce frictional loss on thrust side during expansion stroke. This can again be attributed to the difference in oil transport.

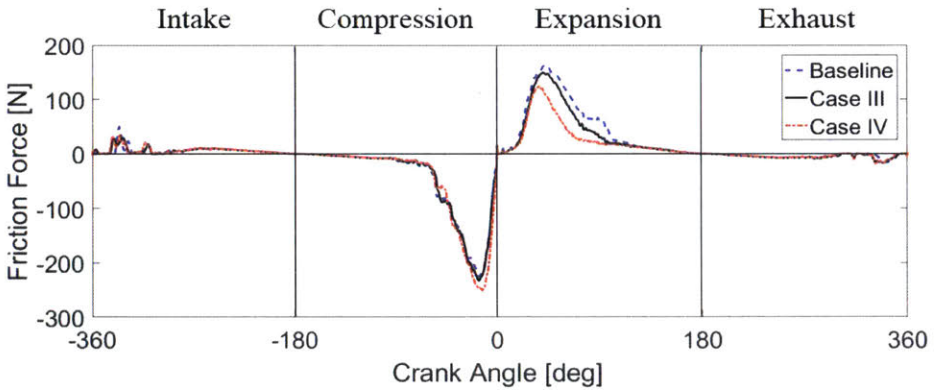

Figure 3-39 Friction Force of Cases with Different Liner Compliances

Table 3-3 FMEP [bar] of Cases with Different Liner Compliances

	Baseline	**Case III**	**Case IV**
Total FMEP	0.112	0.0969	0.0767
From Hydrodynamic Lubrication on TS	0.0438	0.0384	0.0287
From Hydrodynamic Lubrication on ATS	0.0175	0.0175	0.0178
From Boundary Lubrication on TS	0.0296	0.0211	0.0104
From Boundary Lubrication on ATS	0.0211	0.0199	0.0198

The average oil film thicknesses in the skirt and chamfer regions on thrust side are plotted in figure 3-40 and 3-41, while the average clearance in skirt area is in figure 3-42. Case IV enjoys more lubricant in the skirt region during the entire engine operation, which shows that the stiffness of the liner can affect oil accumulation. As shown in figure 3-38, Case IV has less tilt angle during late intake stroke, which means that the clearance at the bottom of the skirt on thrust side is larger than the baseline case. This allows more oil to be able to enter the skirt region.

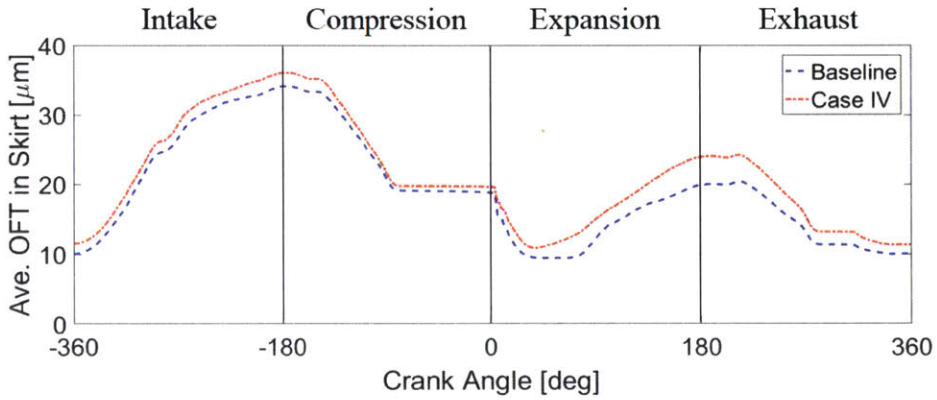

Figure 3-40 Average OFT in Skirt on TS for Different Liner Compliances

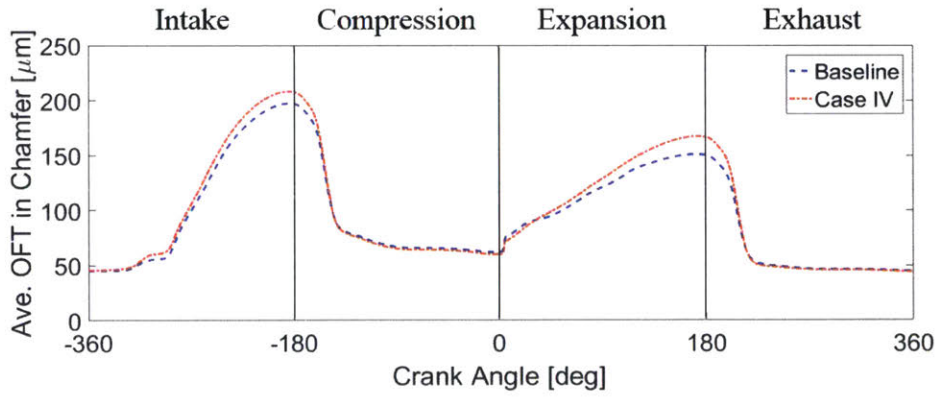

Figure 3-41 Average OFT in Chamfer on TS for Different Liner Compliances

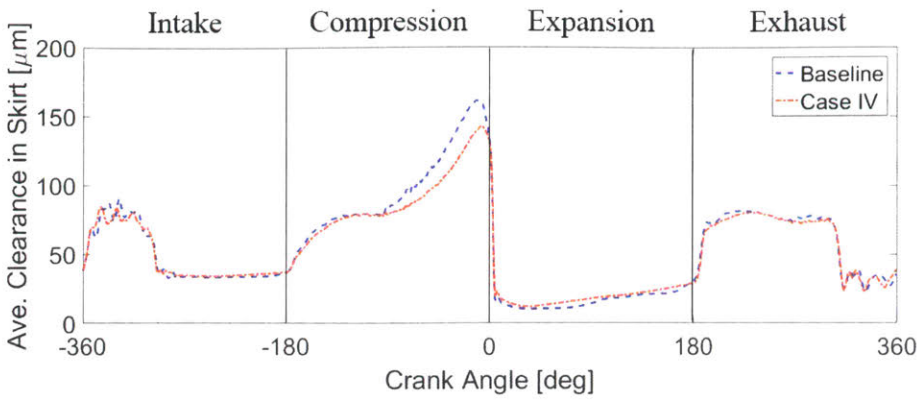

Figure 3-42 Average Clearance on TS for Different Liner Compliances

Figure 3-43 indicates the wear rate on the skirt for the three cases discussed in the section. On the thrust side, stiffer liner leads to less contact; while on the anti-thrust side, contact is more concentrated in the middle of the skirt when the liner is stiffer.

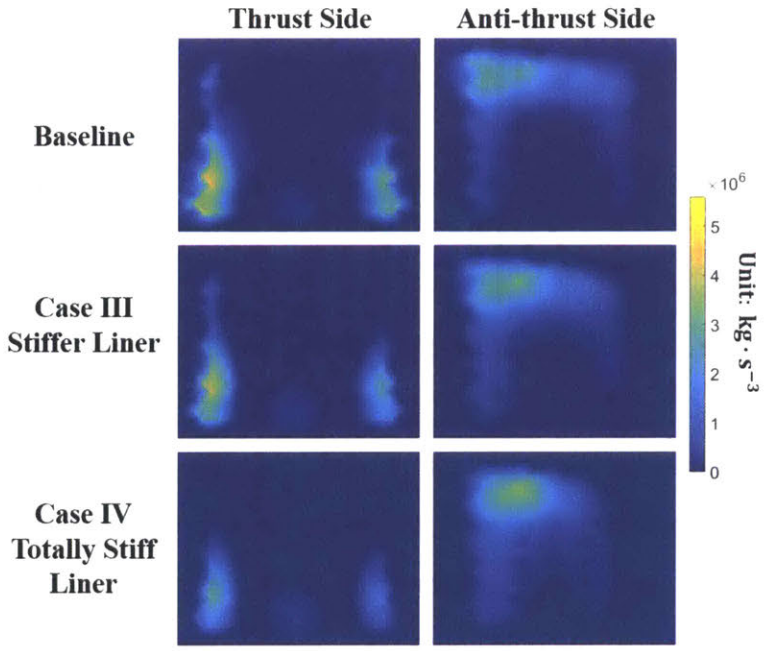

Figure 3-43 Distribution of P-V Factor of Cases with Different Liner Compliance

3.4 The Effects of Waviness on the Surface of Skirt

In the current model, the surface of piston skirt is assumed to have triangular machine marks with constant wavelength λ and wave height Ω along the axial direction, as is shown in figure 3-44.

The waviness of the machine marks affects the results in three different ways. Firstly, the wave height determines the criteria for asperity contact to happen. The radius of the piston is defined by the centerline of machine marks, which is the solid line in the right hand side of figure 3-44. When a local clearance h between skirt and liner drops below half of the wave height $\Omega/2$, contact will occur at this point.

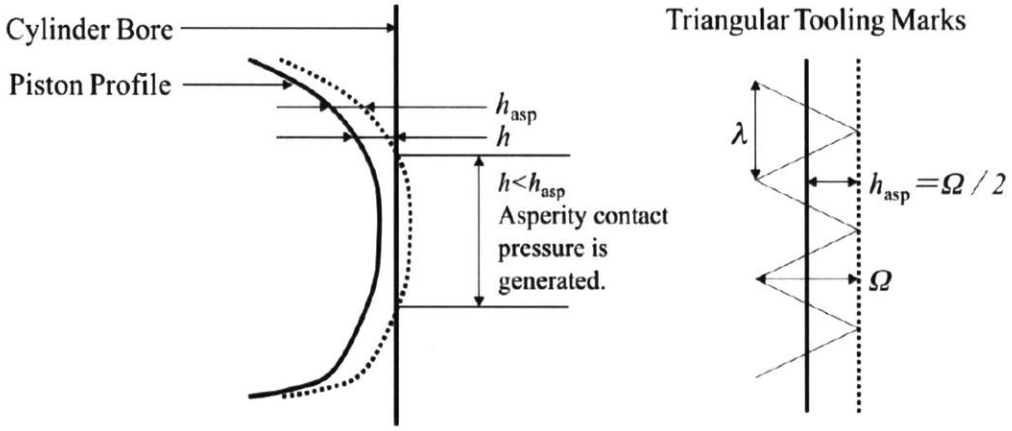

Figure 3-44 Triangular Machine Marks on the Surface of Skirt

The second way through which the waviness plays its role is the average flow model [18] applied by the model. The model uses volume average method to consider the surface of the skirt, and both λ and Ω is used in the corresponding coefficients which modifies the original Reynolds Equation to Average Reynolds Equation.

Finally, together with the Young's moduli of the material at the surface of liner and skirt, λ and Ω determine the coefficients in the contact model mentioned in the previous chapter [16].

Between the two parameters, the wave height has more significant influence since it to some extent stands for the roughness and hardness of the surface. To briefly illustrate its effects, cases with different Ω are calculated for this section. The wavelength for all these cases is 270 microns.

Figure 3-45 and 3-46 show the secondary motion for different cases. The first effect of waviness discussed above can be seen from the lateral motion as the curves for larger wave heights experience larger magnitude of movement.

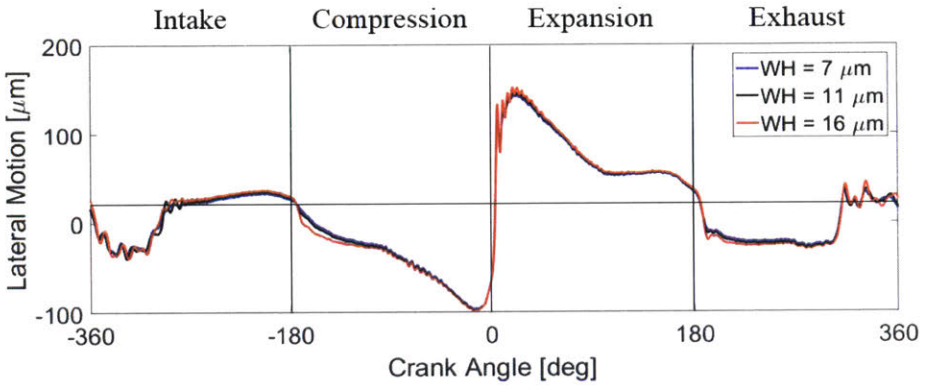

Figure 3-45 Lateral Motion of Cases with Different Skirt Waviness

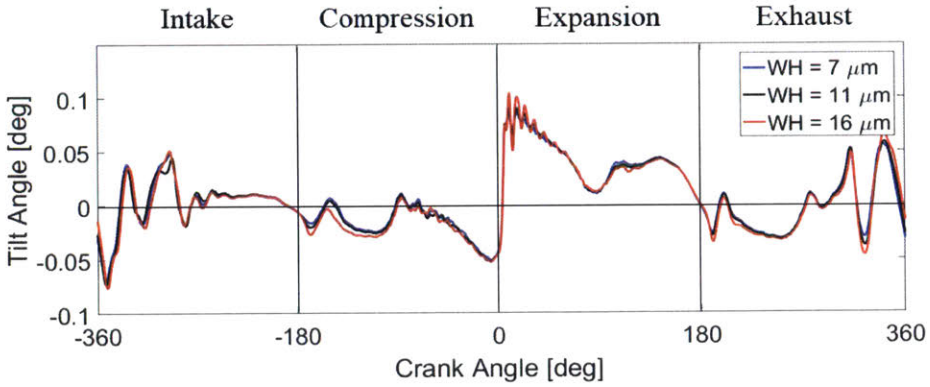

Figure 3-46 Tilt Angle of Cases with Different Skirt Waviness

Figure 3-47 gives the friction trace, which shows that smoother surface has overall less frictional loss. Figure 3-48 shows the indicated wear rate.

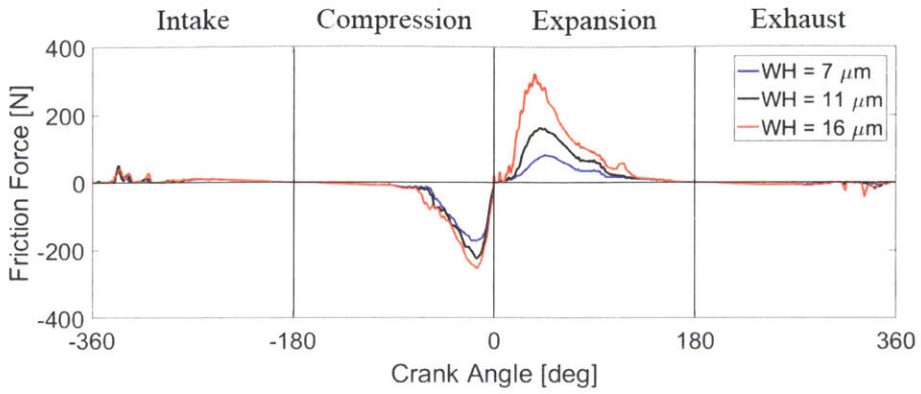

Figure 3-47 Friction Force of Cases with Different Skirt Waviness

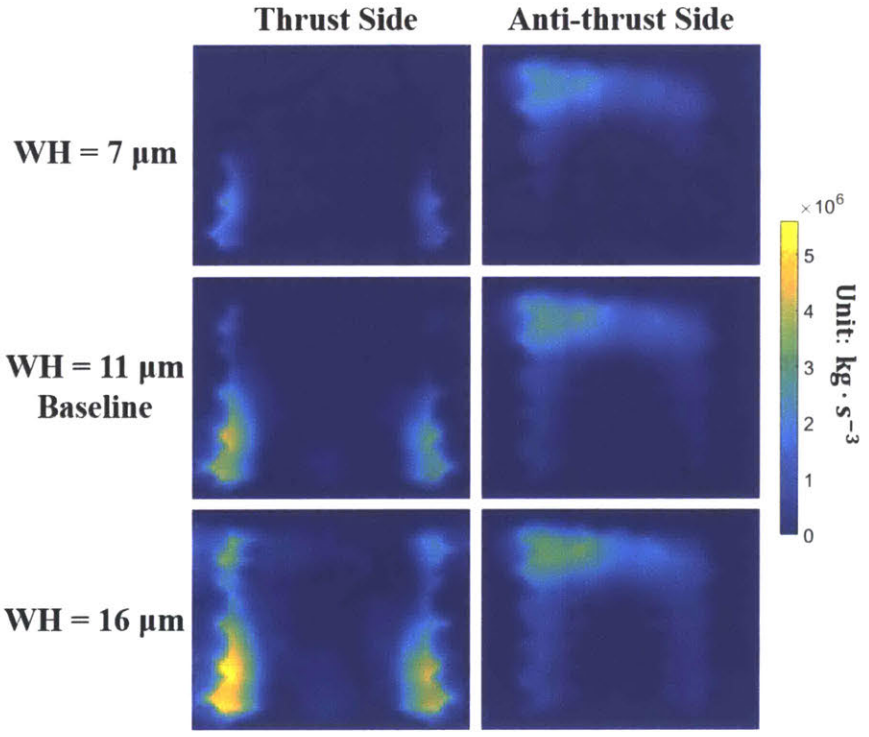

Figure 3-48 Distribution of P-V Factor of Cases with Different Skirt Waviness

3.5 Summary

The upgraded model was applied to the simulation of a heavy duty diesel engine. This chapter started by summarizing some general patterns of the interaction among secondary motion, axial and lateral forces, and oil transport. Then, parametric study was carried out to look into the effects of clearance, deformation, waviness on the skirt surface, and oil supply to the open liner.

It was found that secondary motion, especially the lateral movement, is mainly determined by the position of the connecting rod, the inertia of the piston, and the pressure from combustion chamber. During the periods of time when high pressure is built above the piston, large lateral force will be generated between the piston and the liner on either thrust (expansion stroke) or anti-thrust (compression stroke) side, which can cause severe friction if the skirt-liner interface is not effectively lubricated.

In the parametric study, several changes to the system were discovered to be able to reduce friction by keeping more lubricant in the skirt region during those critical times. The first important finding is that a properly larger installation clearance is favorable for lubrication, particularly on the anti-thrust side during compression stroke. This is because larger clearance allows the oil film on that side to separate earlier in late intake stroke, facilitating the lubricant on the open liner to go through the skirt region and accumulates in the chamfer. During compression stroke, the chamfer oil stays longer than the skirt oil before being left on the open liner, therefore more oil is available after mid-stroke.

However, after the clearance is large enough for the oil film to separate during intake stroke, there is no use to further increase it because the advantage of larger clearance in this case is confined by the quick release of lubricant to the open liner during early compression stroke. Also, side effects such as NVH is another challenge for real engines with excessively big clearance. Therefore, there are limitations to the benefit of larger clearance.

Higher stiffness of the liner and smoother surface of the skirt were also found to be associated with less frictional loss. The stiffer liner, which confines the extent of secondary motion, leads to slightly larger gap at the bottom of skirt on the thrust side during intake stroke to collect the lubricant. The smaller waviness slows down the formation of contact pressure, therefore reduce the magnitude of friction force in the situation of boundary lubrication.

In addition to what has been discussed in this chapter, there are other factors that influence the secondary motion, forces, and oil transport, including the profile of the skirt, which is studied by Totaro [8].

Chapter 4

Effects of Oil Supply in Heavy Duty Diesel Engines

This chapter studies the sensitivity to the oil addition to the cylinder liner. In reality, it is basically an unknown for the engines, varying from cycle to cycle with unpredictable patterns. Nevertheless, it is crucial to the system as the only source of lubricant and thus worth of being investigated.

The first section starts the investigation by looking at the simplest cases where a uniform thickness of oil is added to the entire open liner when piston is at top dead center, as is shown in figure 2-10. Then in the second section, cases with oil addition to different axial locations on the liner are compared.

4.1 Amount of Uniformly Distributed Oil Addition

4.1.1 Secondary Motion and Friction

The baseline case in chapter 3 has a uniform oil splash to the open liner with a thickness of 15 microns. To look into the effects of the thickness, other cases are calculated, and some of their FMEP values are listed in table 4-1. Figure 4-1 shows the changing pattern of the total FMEP and the part of FMEP from boundary lubrication with the thickness of oil addition

Table 4-1 FMEP [bar] of Cases with Different Oil Addition

Uniform Oil Addition [μm]	3	4	8	15	30
Total FMEP	0.171	0.154	0.125	0.112	0.111
From Hydro. Lubrication on TS	0.0557	0.0512	0.0472	0.0438	0.0418
From Hydro. Lubrication on ATS	0.0192	0.0189	0.0205	0.0175	0.0175
From Boundary Lubrication on TS	0.0568	0.0437	0.0316	0.0296	0.0296
From Boundary Lubrication on ATS	0.0395	0.0387	0.0253	0.0211	0.0212

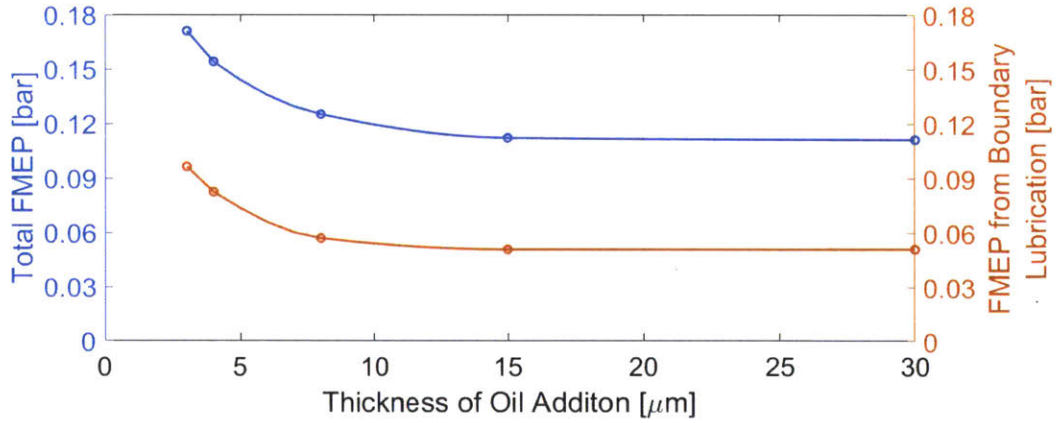

Figure 4-1 FMEP of Cases with Different Oil Addition

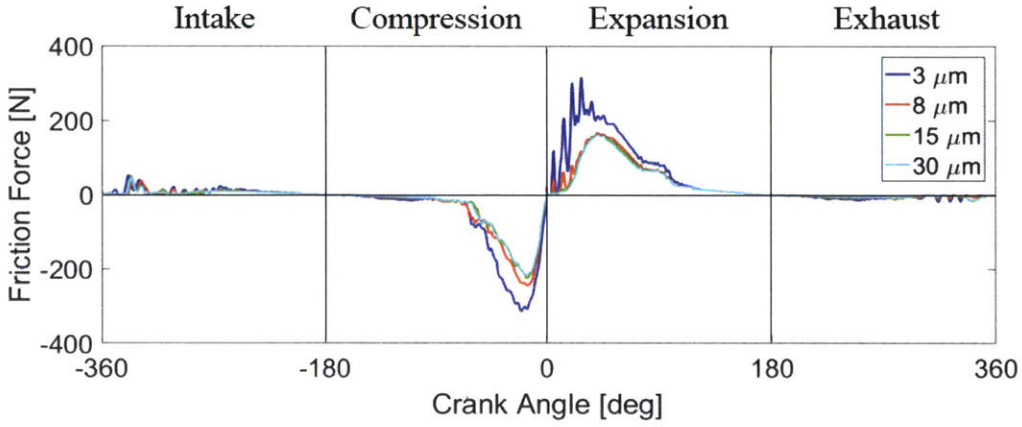

Figure 4-2 Friction Force of Cases with Different Oil Addition

From table 4-1 and figure 4-2, a significant drop in friction is achieved by increasing oil addition from 3 microns to 8 microns. Then, the 15-micron case receives some further benefit, while extra oil addition beyond it does not result in additional improvement.

Figure 4-3 shows the distributions of contact pressure and hydrodynamic pressure on anti-thrust side at -15° CA in three cases, and Figure 4-4 shows the situations on thrust side at 35° CA.

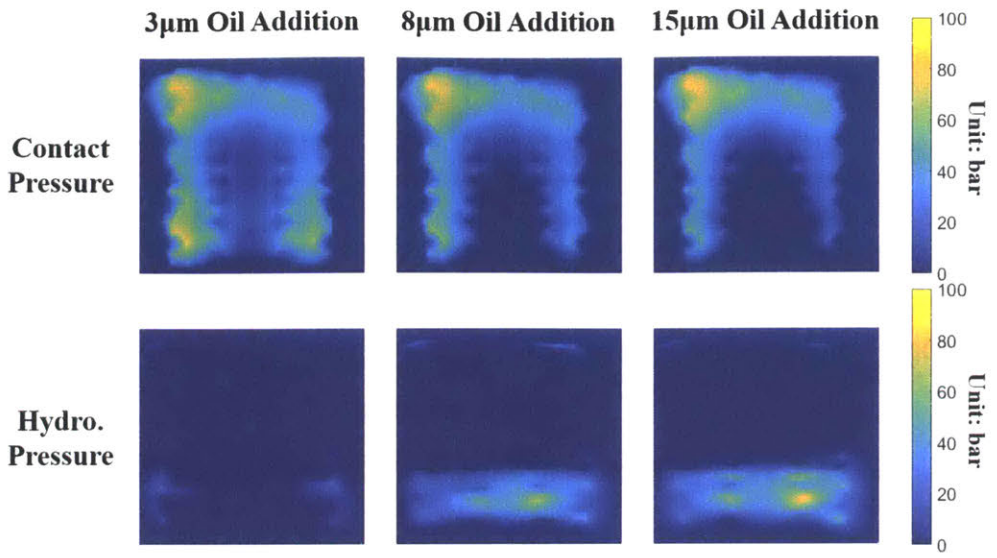

Figure 4-3 Pressure Distributions on ATS at -15° CA for Different Oil Addition

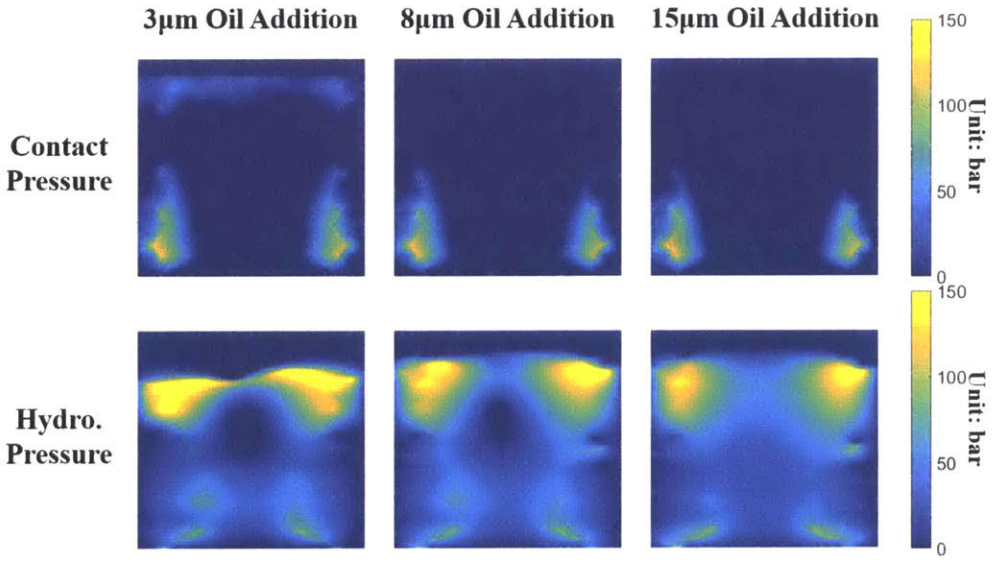

Figure 4-4 Pressure Distributions on TS at 35° CA for Different Oil Addition

In figure 4-5, which shows the lateral motion of different cases, higher amounts of addition usually have less movement. This is simply because more oil between skirt and liner prevents these surfaces from getting closer to each other. This also benefits the system during down strokes in terms of letting more oil enter the skirt and chamfer regions, which will be discussed in the next subsection.

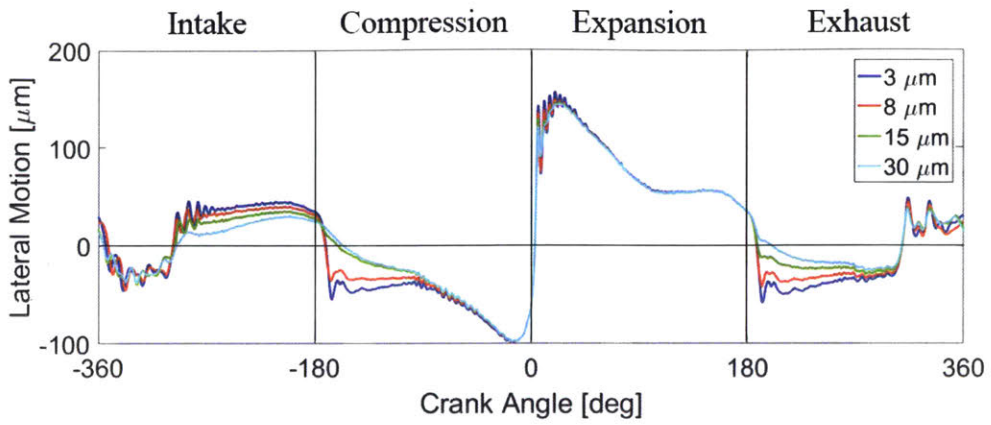

Figure 4-5 Lateral Motion of Cases with Different Oil Addition

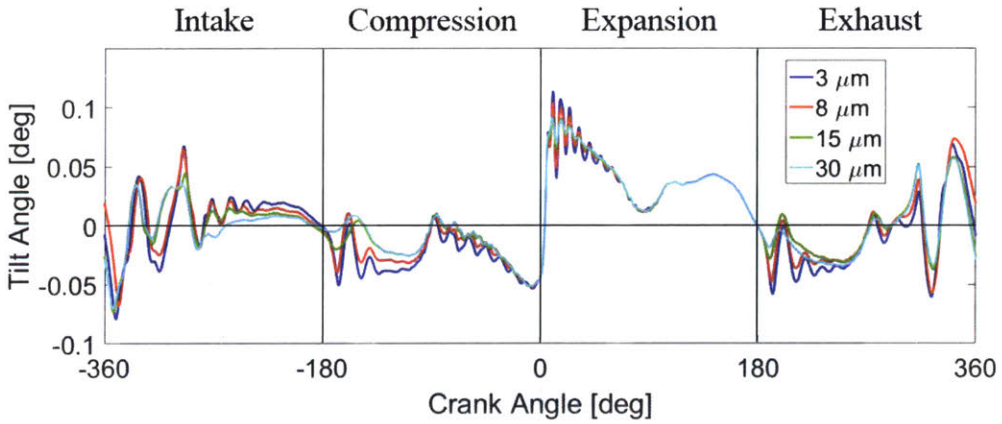

Figure 4-6 Tilt Angle of Cases with Different Oil Addition

4.1.2 Oil Transport

The first major component of frictional loss happens on thrust side during expansion stroke. Figure 4-7 and 4-8 show the changing patterns of total FMEP, as well as the average oil film thickness on thrust side when piston is at bottom dead center of intake stroke, when the amount of oil addition is increased. According to the curves of average oil film thicknesses, when the amount of lubricant splashed to the open liner increase, more oil can enter the skirt-liner interface, and accumulate in the chamfer region.

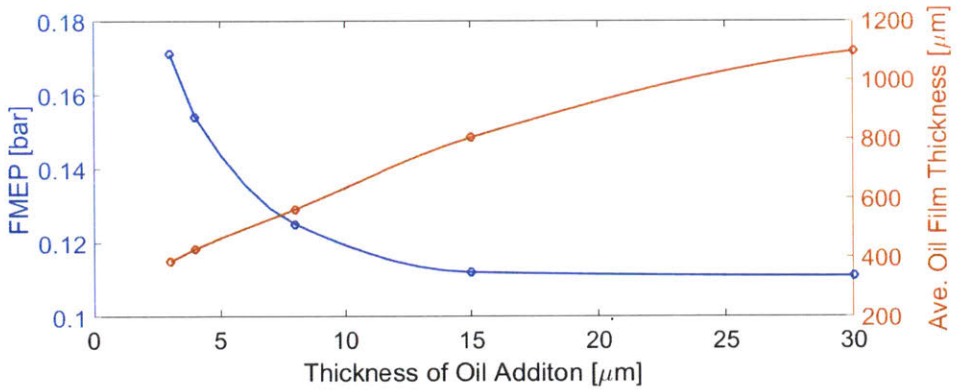

Figure 4-7 FMEP and Average OFT in Chamfer on TS at Intake BDC

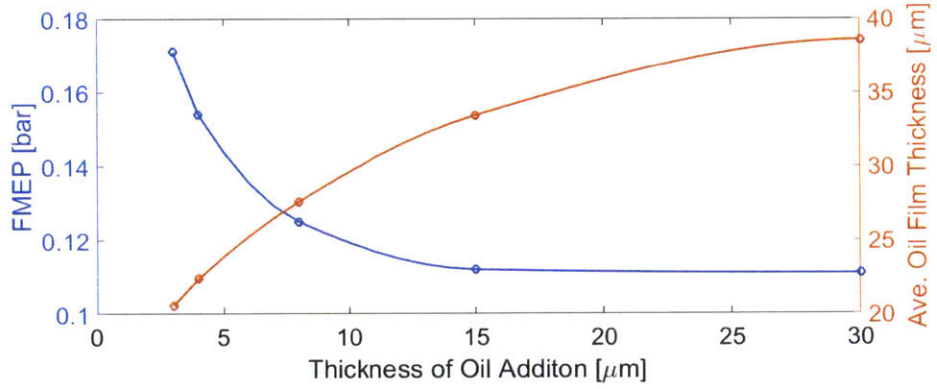

Figure 4-8 FMEP and Average OFT in Skirt on TS at Intake BDC

Ideally, this storage of oil will be released on the liner in compression stroke, and provide lubrication when piston slaps on the liner during expansion stroke. This is true for smaller thicknesses of oil addition (from 3 to 15 microns) as shown in 4.1.1. However, lack of better lubricating performance afterwards requires further explanation.

Figure 4-9 and 4-10 give the average oil film thicknesses at the end of compression stroke. At this point, both skirt and chamfer in the 30-micron case have only slightly more lubricant than the 15-micron case. Figure 4-11 provides an overall picture of how the oil amount in the chamfer develops. It shows the rapid loss of lubricant during early compression stroke, which then leads to the similar amount of oil for 30 and 15-micron cases at 0° crank angle.

Figure 4-12 shows the average oil film thickness in the skirt region on the thrust side. During intake stroke, the skirt of the 30-micron case experience a decrease in oil volume because some of the lubricant is squeezed out by the piston then it moves to the thrust side after mid-stroke. Same thing happens at the very beginning of the expansion stroke, where the skirt oil has a sudden drop and the chamfer has a rise. The flat part of the curves before 0° CA is because of the separation of oil film and one part of the lubricant stays on the piston, while the other part leaves the skirt region with the liner. At top dead center of the expansion stroke, the 30-micron case actually keeps more oil on the skirt than the 15-micron case. But they become closer to each other during piston slap when the oil is squeezed out.

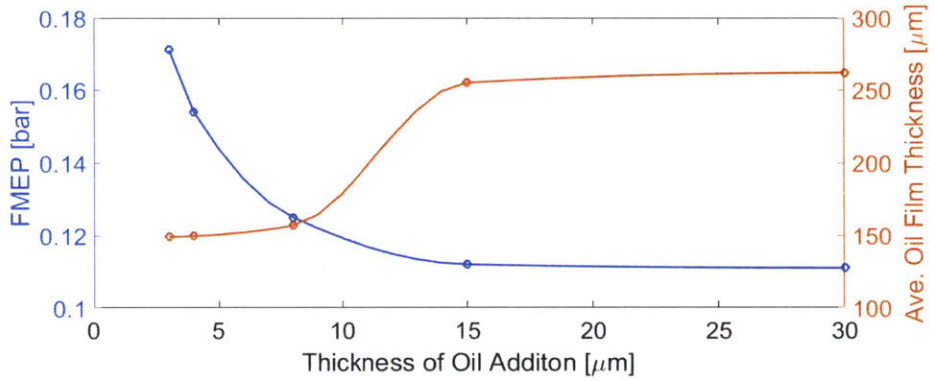

Figure 4-9 FMEP and Average OFT in Chamfer on TS at Compression TDC

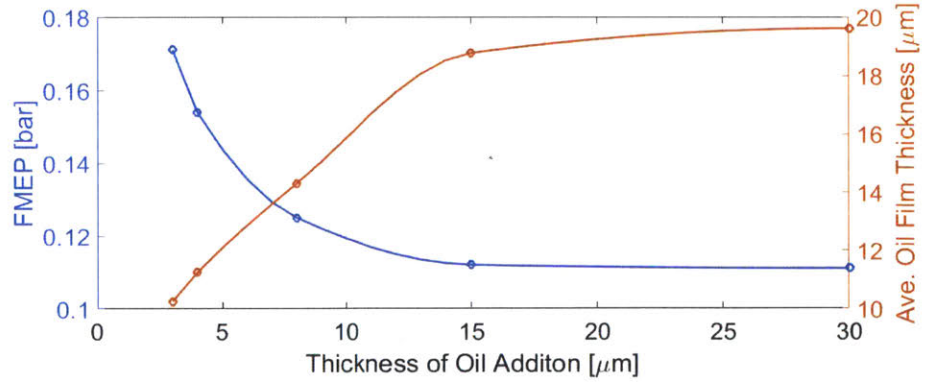

Figure 4-10 FMEP and Average OFT in Skirt on TS at Compression TDC

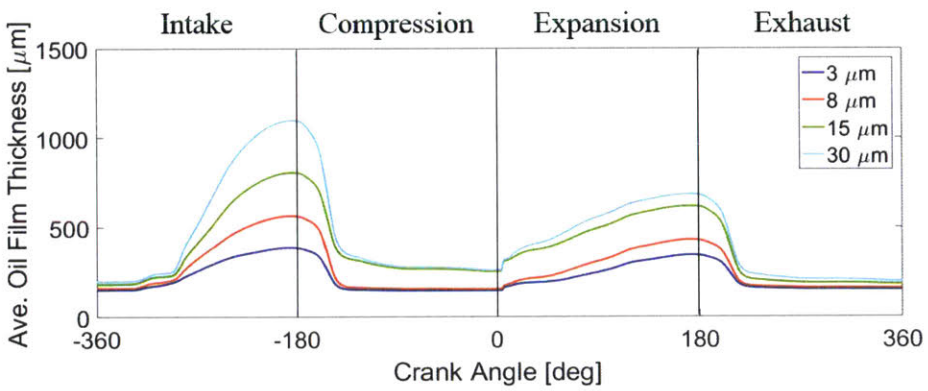

Figure 4-11 Average OFT in Chamfer on TS of Cases with Different Oil Addition

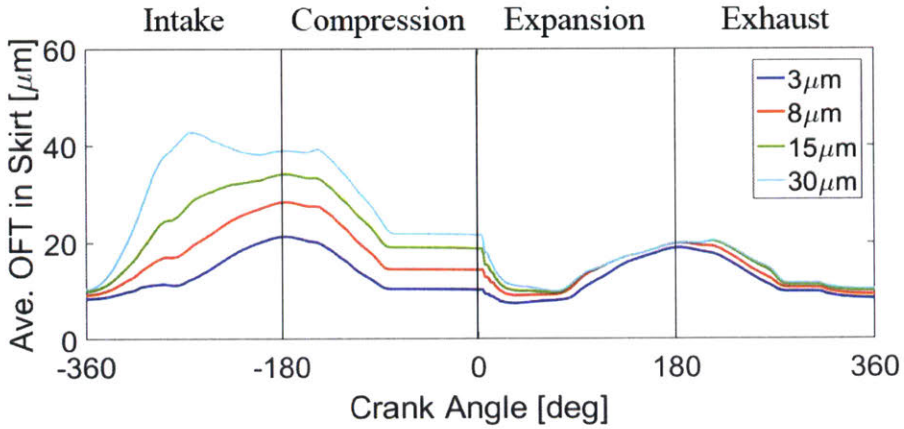

Figure 4-12 Average OFT in Skirt on TS of Cases with Different Oil Addition

On anti-thrust side, the mechanism behind the amount of reduction of friction is a little different. As seen in 4-13, around -180° CA, 30-micron case actually has less oil than 15-micron case. This is because after mid-stroke when piston decelerates and moves to the thrust side, the oil film on anti-thrust side will separate, and the inertia force will drive the oil that stays with the piston out of the skirt region. Also, the oil volume accumulated in the chamfer leaves rapidly when piston starts to move upwards. Therefore, at late expansion stroke when side force is high, the lubricant in the skirt is limited (figure 4-14), and a certain amount of friction still happens on anti-thrust side even the oil addition is further increased.

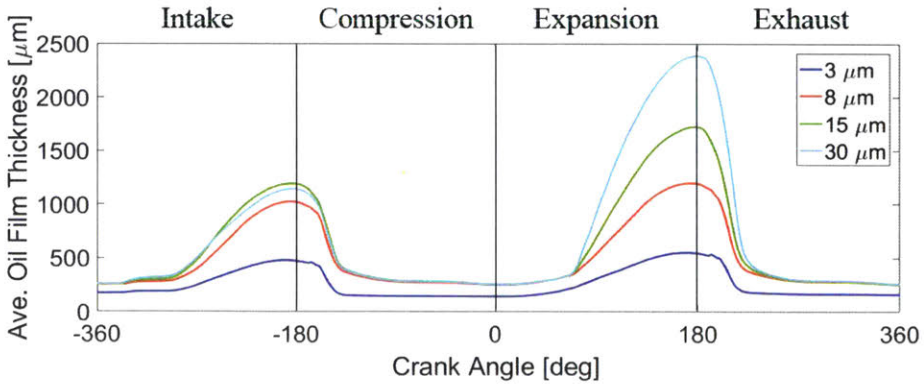

Figure 4-13 Average OFT in Chamfer on ATS of Cases with Different Oil Addition

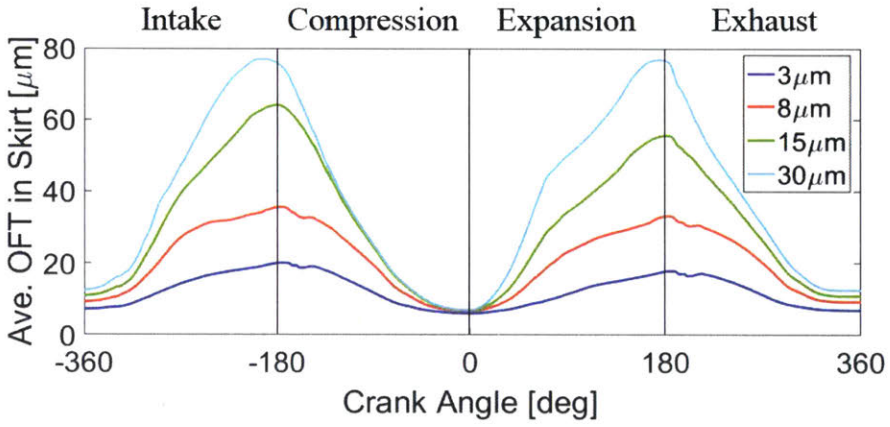

Figure 4-14 Average OFT in Skirt on ATS of Cases with Different Oil Addition

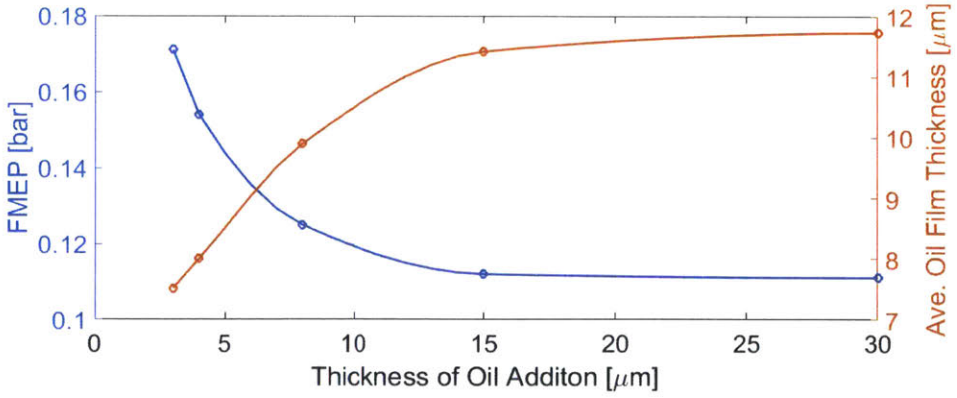

Figure 4-15 FMEP and Average OFT in Skirt on ATS near Compression TDC

4.1.3 Summary

By increasing the oil addition to the open liner, more oil can be available between skirt and liner in situations where side force is large and the piston is pushed to either thrust or anti-thrust side. Yet such advantage of more oil addition has limitation because of the quick release of oil in upstrokes.

4.2 Location of Oil Addition on the Open Liner

From table 3-1, the height of piston skirt is about 1/2.5 of the height of open liner. During a down stroke, the liner moves upwards as the piston is taken as the reference, dragging lubricant into skirt and then chamfer regions. However, in this situation where viscous drag drives oil between skirt and liner, oil does not move as much as the liner. Therefore, if an oil puddle is splashed onto the liner, the position where the puddle ends up in the skirt region when piston moves to bottom dead center will depend on its starting location on the liner. This section studies the results of three cases where oil is added to different axial locations of the liner.

There are four parts in figure 4-16, explaining the oil addition for these cases. In each part, the vertical grey bar on the left represents the liner on thrust side, and the yellow, red and green areas show the oil film in different regions. In the 'Upper 'case, the open liner is divided into three parts with equal axial heights, and additional lubricant (in blue) is added to the upper part. In the other two cases, oil is added respectively to the middle and lower parts of the open liner. Since the parts that receive oil have the same height for the three cases, the total volume of oil addition is also the same.

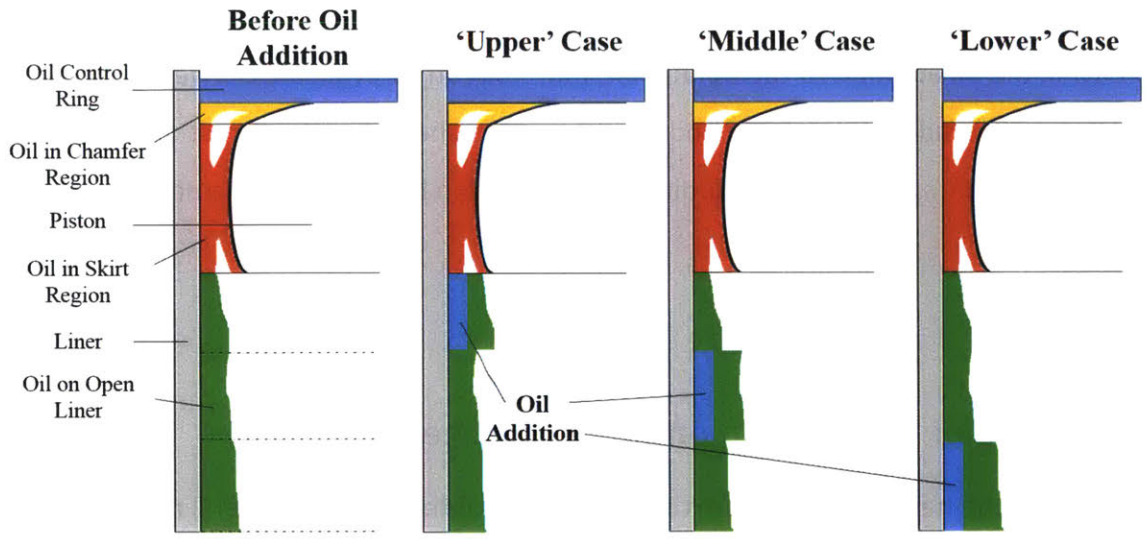

Figure 4-16 Different Locations of Oil Addition

Table 4-2 lists the FMEP values of different cases. In all the cases where only a part of the open liner receives additional lubricant, the total FMEPs are much higher than the baseline case contributed by the severely increased loss from boundary lubrication regime. On thrust side, the frictional loss from boundary lubrication increases when the position of oil addition is lower; on anti-thrust side, however, the 'Middle' case has the least friction among the last three cases.

Table 4-2 FMEP [bar] of Cases with Different Locations of Oil Addition

	Baseline	Upper	Middle	Lower
Total FMEP	0.112	0.180	0.216	0.306
From Hydro. Lubrication on TS	0.0438	0.0547	0.0526	0.0540
From Hydro. Lubrication on ATS	0.0175	0.0262	0.0196	0.0173
From Boundary Lubrication on TS	0.0296	0.0612	0.113	0.192
From Boundary Lubrication on ATS	0.0211	0.0371	0.0309	0.0410

To look into the cause of the different numbers above, the 'Upper' case will be compared with the baseline case in terms of secondary motion and oil transport in the first sub-section. In the next sub-section, results from the 'Upper', 'Middle', and 'Lower' cases will be discussed.

4.2.1 Comparison between the Baseline and 'Upper' Cases

The friction forces are shown in figure 4-17. The 'Upper' case has more friction both on anti-thrust side during compression stroke and on thrust-side on expansion stroke.

Figure 4-18 and 4-19 show the secondary motion of these cases. The lateral movement is similar during early intake stroke. This is because the piston is pulled to the anti-thrust side and touches the higher part of the liner, where both cases have the same amount of oil addition. At late intake stroke, where the piston is pushed to the thrust side. Because the 'Upper' case has less oil on the lower part of the open liner, the piston is able to move closer to the liner, thus has more lateral motion than the baseline case. Same situation happens during early compression and exhaust strokes when the piston moves up and towards anti-thrust side, where the baseline case accumulates more lubricant between piston and liner during the recent down stroke.

The tilt angle for the 'Upper' case also has larger magnitude in the similar periods of time. Also, it experiences some violent fluctuation especially in the early expansion stroke.

In general, the 'Upper' case has more friction force as well as larger and more unstable secondary motion than the baseline case. This can be again attributed to the oil supply and transport, which will be discussed next.

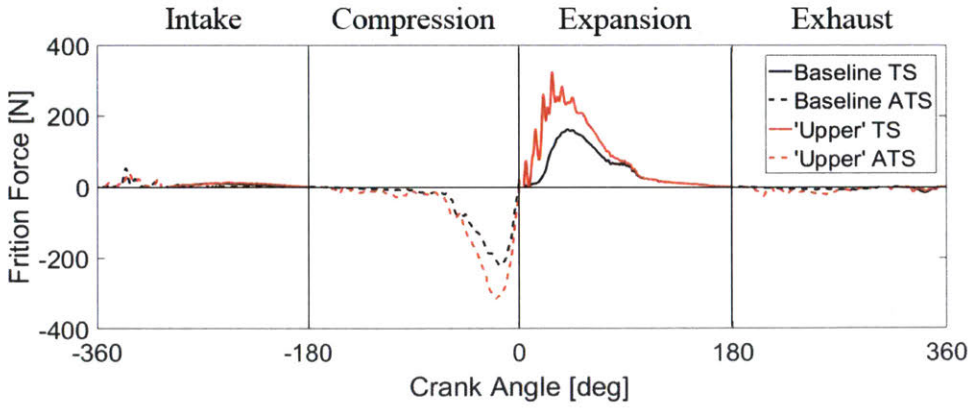

Figure 4-17 Friction Force of Baseline and 'Upper' Cases

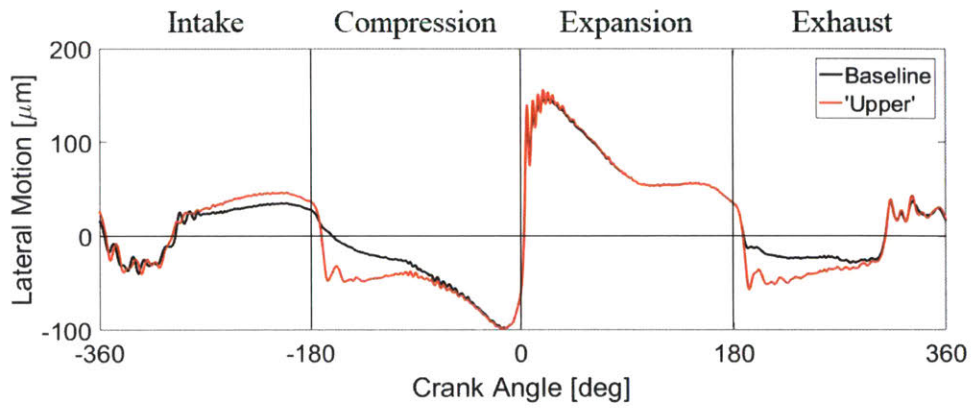

Figure 4-18 Lateral Motion of Baseline and 'Upper' Cases

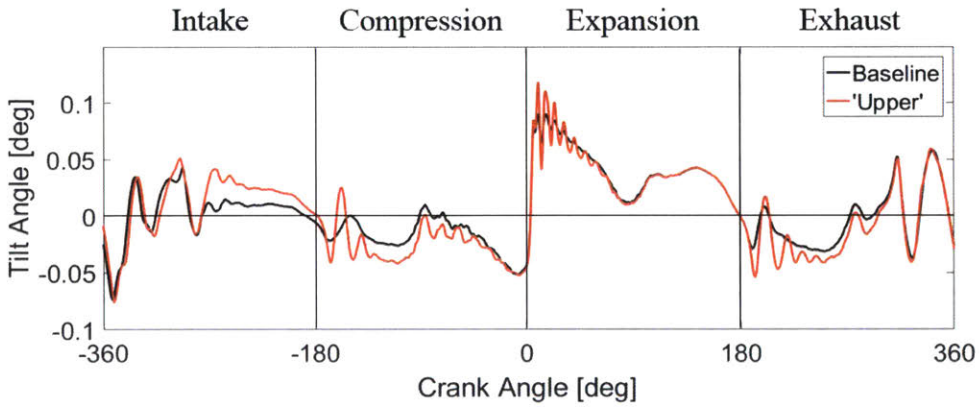

Figure 4-19 Tilt Angle of Baseline and 'Upper' Cases

The most direct effect of different oil addition is the oil flow rate from open liner to the skirt, and the total oil volumes stored in the chamfer and skirt regions. Figure 4-20 and 4-21 show the average flow rate along circumferential direction between skirt and liner on thrust and anti-thrust sides. Positive value means lubricant moves from liner to skirt. Figure 4-22 and 4-23 show the average oil film thickness in the chamfer on both sides. Figure 4-24 and 4-25 show the average oil film thickness in the skirt.

The curves in these figures gives a clearer picture of how friction can be affected by the oil supply.

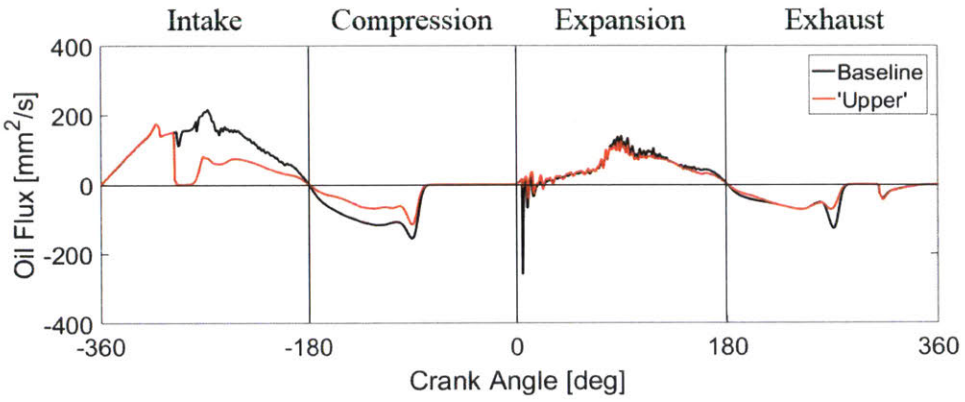

Figure 4-20 Oil Flow from Liner to Skirt on TS (1)

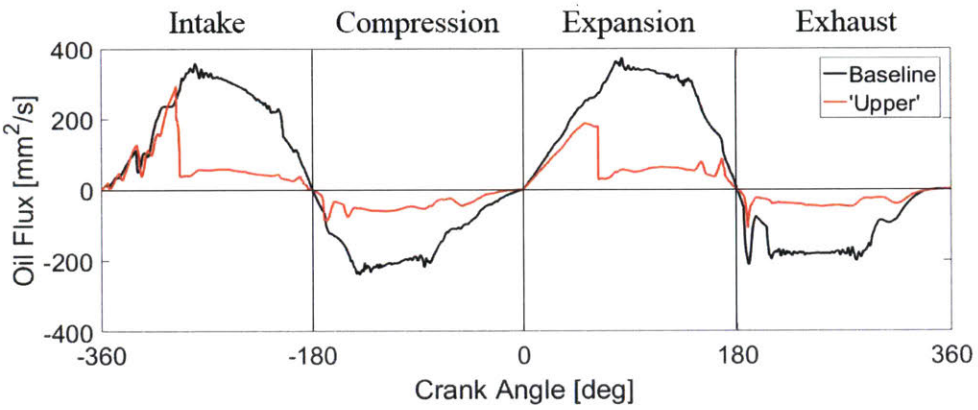

Figure 4-21 Oil Flow from Liner to Skirt on ATS (1)

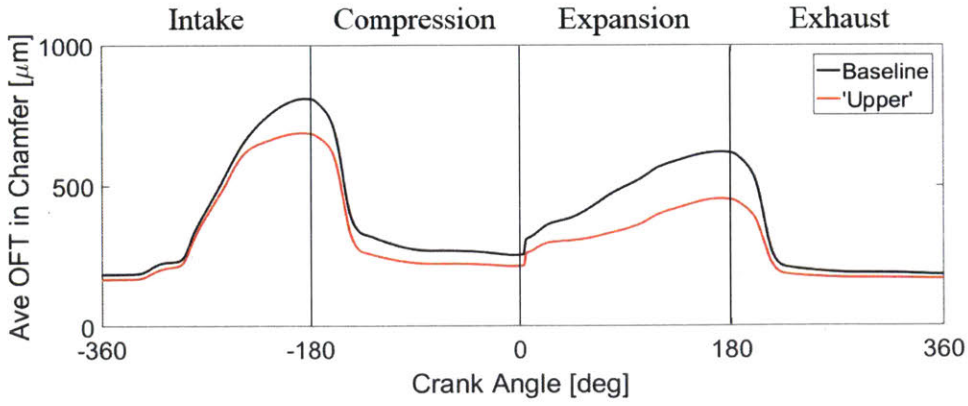

Figure 4-22 Average OFT in Chamfer on TS of Baseline and 'Upper' Cases

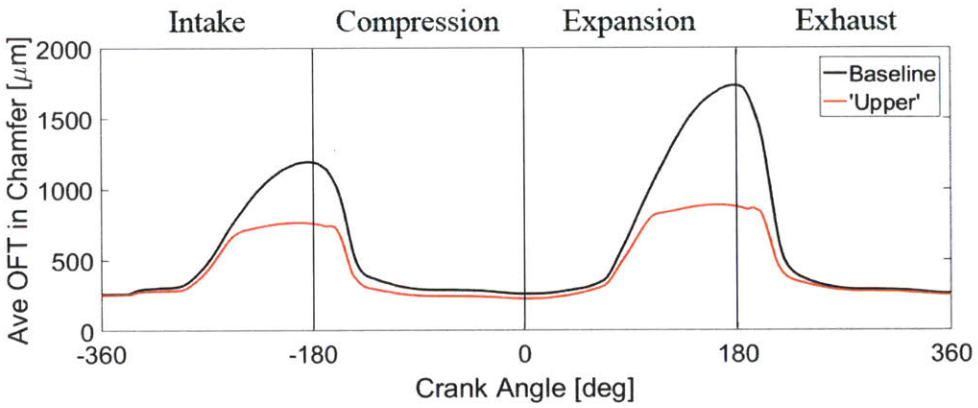

Figure 4-23 Average OFT in Chamfer on ATS of Baseline and 'Upper' Cases

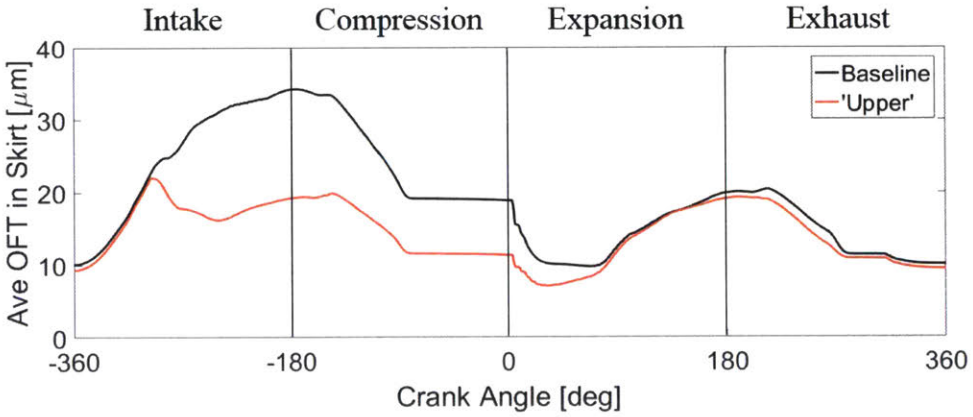

Figure 4-24 Average OFT in Skirt on TS of Baseline and 'Upper' Cases

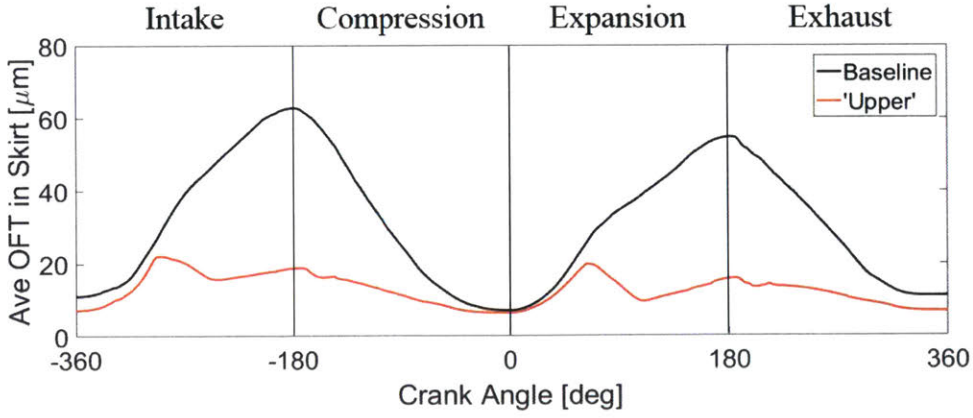

Figure 4-25 Average OFT in Skirt on ATS of Baseline and 'Upper' Cases

Starting with the intake stroke, many evident phenomena can be seen from the figures.

- At earlier intake stroke, the lubricant in the relatively higher area of the open liner is involved and collected by the skirt. As shown in figure 4-20 and 4-21, in this area, the amount of oil on the thrust side is almost the same for both cases, whereas the anti-thrust side has some slight differences. Figure 4-24 and 4-25 show that the increase in the oil amount in the skirt region is also similar. This is due to the release of lubricant during the exhaust stroke, which will be discussed later.
- After a certain time, the piston reaches the 'Middle' part of the open liner, and the skirt in the 'Upper' case stops receiving the additional oil splashed on the liner. On the other hand, it still gives oil to the chamfer. Therefore, the curves representing the average skirt oil film thickness in the 'Upper' case starts to drop and deviate from the baseline.
- At late intake stroke, piston moves towards the thrust side, so the flow rate and average skirt OFT on the anti-thrust side in the baseline case is higher than the thrust-side. Also during this period, the oil addition that comes originally from the open liner starts to enter the chamfer region.

As a result, after intake stroke, the baseline case accumulates more lubricant than the 'Upper' case on both sides in both skirt and chamfer regions.

- At the beginning of the compression stroke, the piston is pushed to the anti-thrust side, and the oil film will separate on the thrust side in both cases, as shown in figure 4-26. After that, there is still oil flow in figure 4-20 (from -180° to around -85° CA) mostly because the liner takes its oil out of the skirt region. On the other hand, the piston will keep its distribution of lubricant after separation, except for the influence of the inertia (figure 4-27, the extra oil on the bottom of the piston from -173° to 0° is the inertia-driven oil from the chamfer).
- On the anti-thrust side, both cases lose oil in skirt and chamfer region. Since the baseline case stores much more lubricant before this stroke, it manages to keep more of its accumulation during late compression stroke, where the lateral force from piston pin increases drastically.

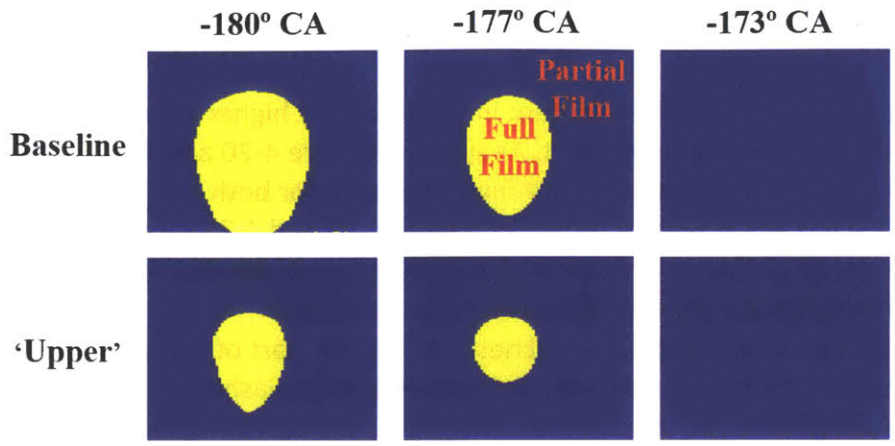

Figure 4-26 Full Film and Partial Film Areas on TS at Early Compression Stroke

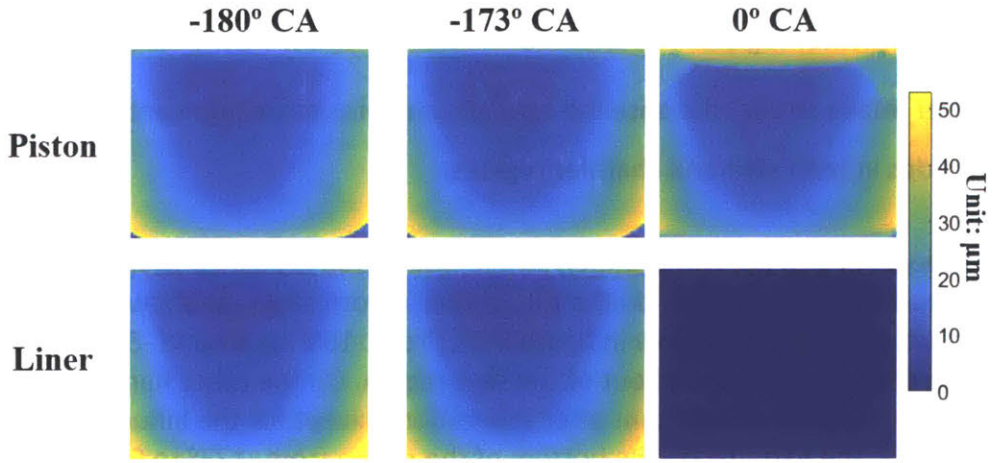

Figure 4-27 Distribution of Oil Film Thickness in Skirt Region on TS in Baseline Case

Figure 4-28 shows the distribution of hydrodynamic pressure and contact pressure for the two cases. The 'Upper' case has more severe contact on the lower part of the skirt since it is poorly lubricated. On the thrust side, it also has much less oil on the piston in the skirt region, which leads to serious frictional loss.

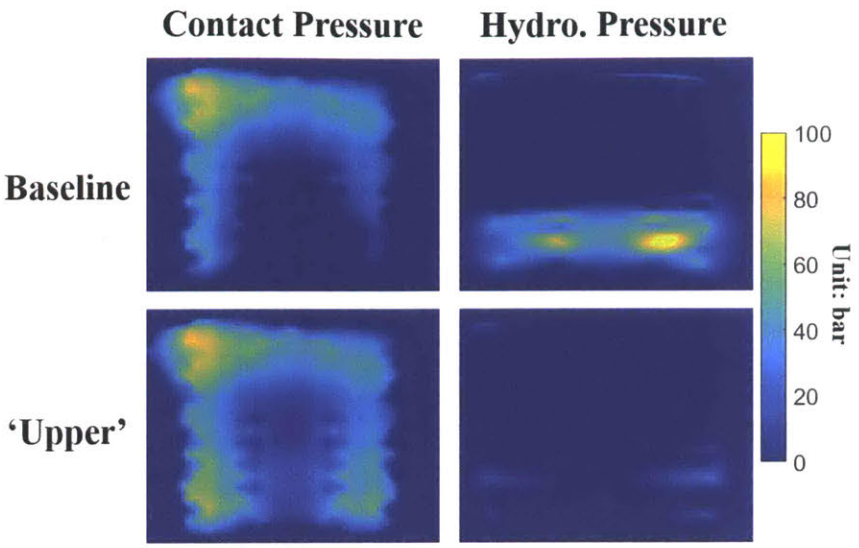

Figure 4-28 Pressure Distributions on ATS at -20° CA of Baseline and 'Upper' Cases

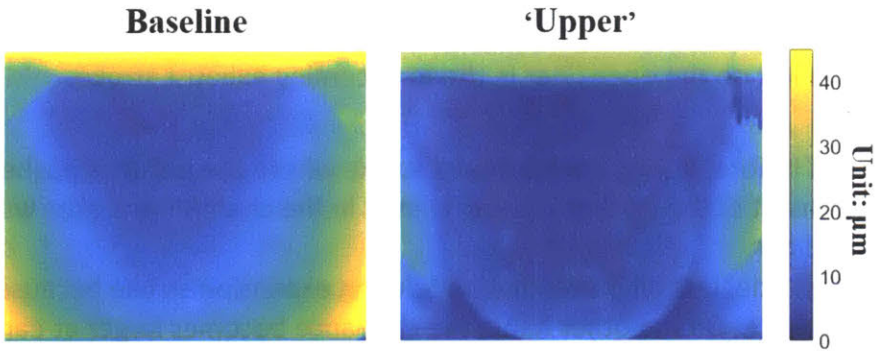

Figure 4-29 Distribution of Oil Film Thickness on Piston Skirt on TS at 0° CA

- At the beginning of the expansion stroke, the 'Upper' case has less oil attached to the piston skirt on thrust side, which is shown in figure 4-29. Since both cases do not have lubricant on the liner in the skirt region, the total oil film thickness for the 'Upper' case is also lower. This leads to the larger friction force around the piston slap at early expansion stroke.
- As for the oil transport, the anti-thrust side has a similar experience to the intake stroke, except for the larger magnitude because of larger clearance. On thrust side, at around 5° CA there is a sudden drop in figure 4-20 for the baseline case. This is because the lubricant in the piston is squeezed out of the skirt through all the boundaries. It is consistent with the sudden rise in the chamfer oil volume around the same time in figure 4-22, and the decline of the skirt oil volume in figure 4-24.

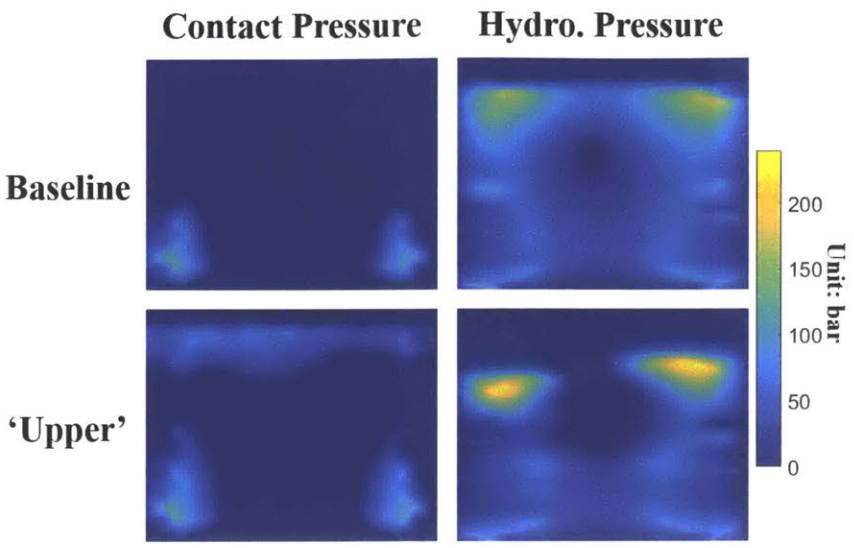

Figure 4-30 Pressure Distributions on TS at 30° CA of Baseline and 'Upper' Cases

At the end of the expansion stroke, the baseline case again has more oil accumulated on both sides. The oil will be left on the open liner in the forthcoming exhaust stroke.

- As discussed before, during early exhaust stroke where the piston is pushed to the anti-thrust side, most of the oil that is accumulated in the chamfer and skirt will be released to the open liner.
- On the thrust side, less oil is accumulated during expansion stroke because of the smaller clearance. On the other hand, the clearance becomes larger at early exhaust stroke as the piston moves away from this side. The quick loss of lubricant makes both cases too dry to leave much oil on the higher part of the open liner.

4.2.2 Comparison among the 'Upper', 'Middle', and 'Lower' Cases

The friction force, lateral motion, and tilt angle for these cases are shown respectively in figure 4-31, 4-32, and 4-33.

Compared with the 'Upper' case, the 'Middle' case has less friction during late compression stroke. During expansion stroke, however, the peak of friction force is closer to the mid-stroke where the piston has higher sliding velocity. Therefore, the 'Middle' case has less frictional loss in compression stroke, but much more in the expansion stroke, as shown in table 4-2. The

'Lower' case, which has similar situation as the 'Upper' case in compression stroke, suffers from a long-lasting and enormous friction force during expansion stroke.

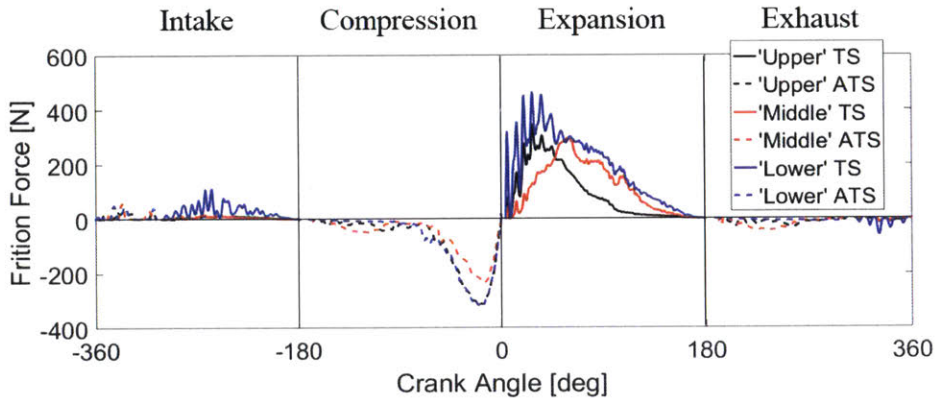

Figure 4-31 Friction Force of Cases with Different Locations of Oil Addition

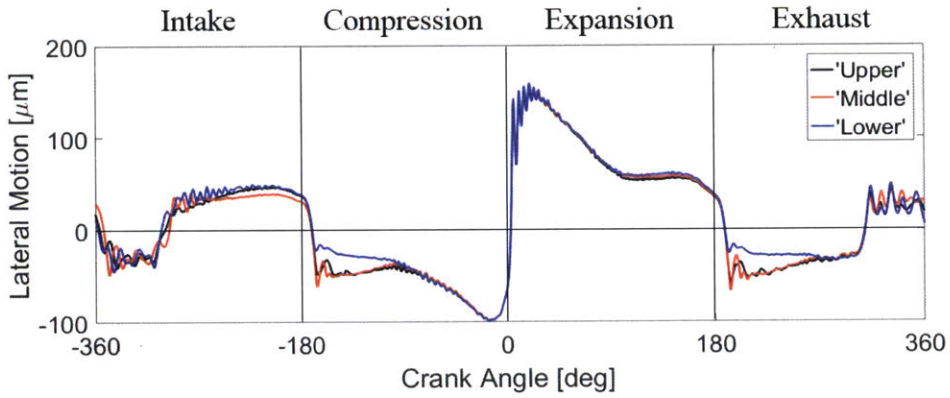

Figure 4-32 Lateral Motion of Cases with Different Locations of Oil Addition

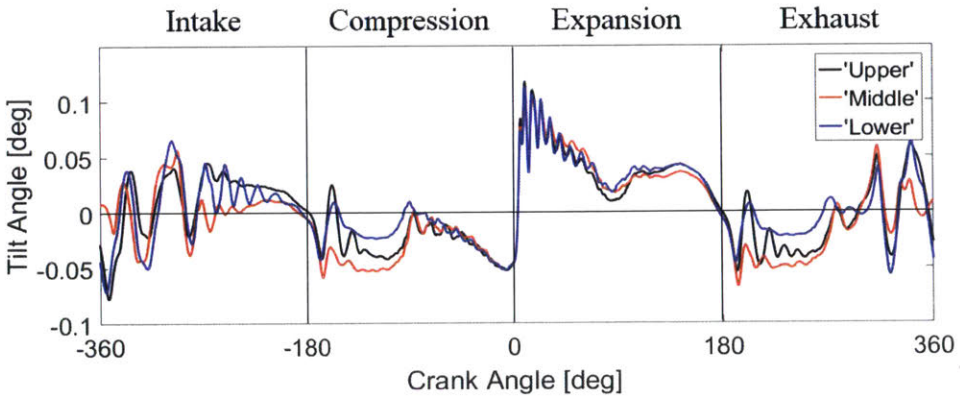

Figure 4-33 Tilt Angle of Cases with Different Locations of Oil Addition

For secondary motion, the 'Lower' case has the least lateral movement at early upstrokes because it has the most lubricant near the bottom of the liner to limit the lateral distance that the piston is able to travel. As for the tilt angle, there seems to be no clear pattern among these cases.

Figure 4-34 and 4-35 show the average flow rate along circumferential direction between skirt and liner. Figure 4-36 and 4-37 show the average oil film thickness in the chamfer on both sides. Figure 4-38 and 4-39 show the average oil film thickness in the skirt.

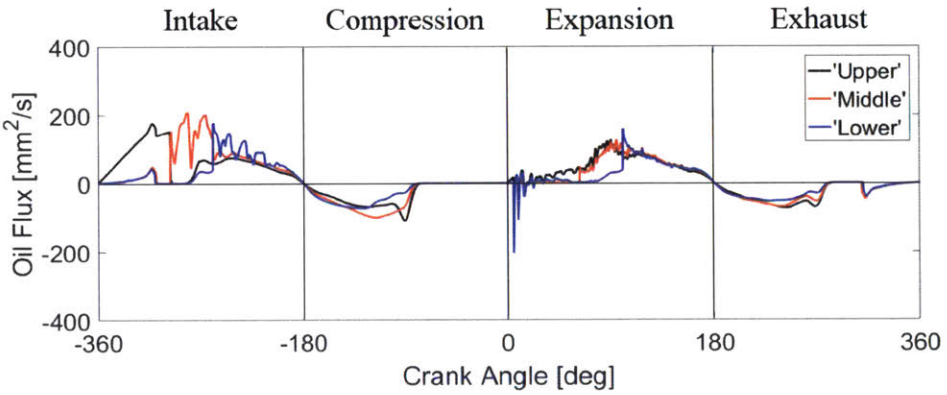

Figure 4-34 Oil Flow from Liner to Skirt on TS (2)

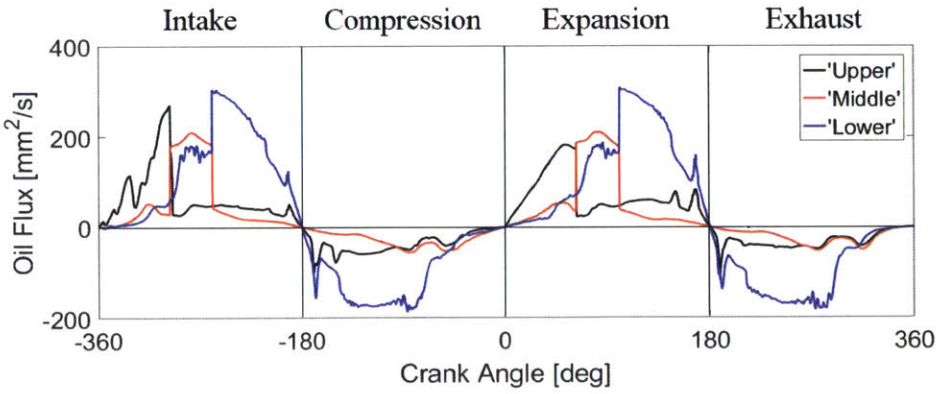

Figure 4-35 Oil Flow from Liner to Skirt on ATS (2)

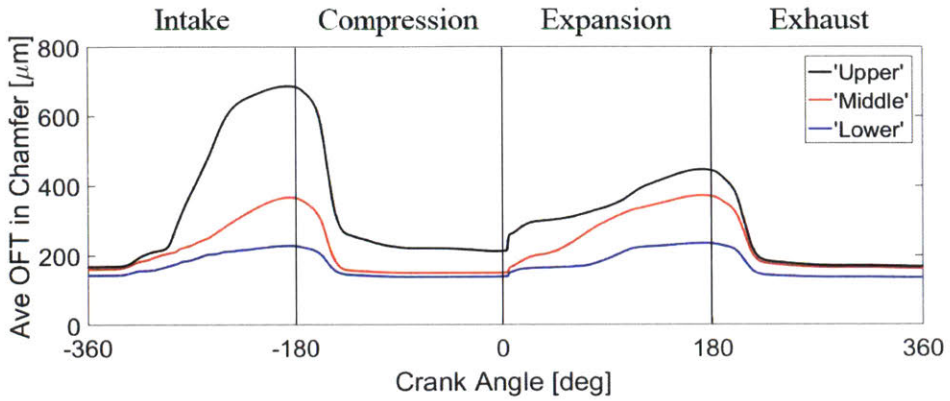

Figure 4-36 Average OFT in Chamfer on TS of 'Upper', 'Middle' and 'Lower' Cases

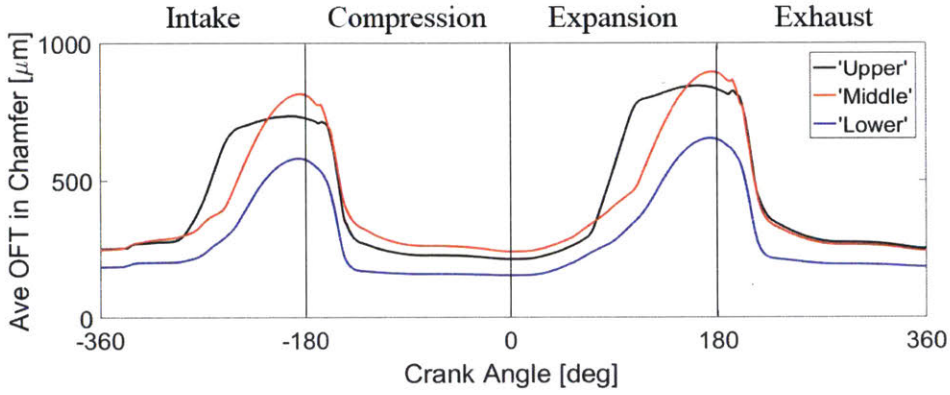

Figure 4-37 Average OFT in Chamfer on ATS of 'Upper', 'Middle' and 'Lower' Cases

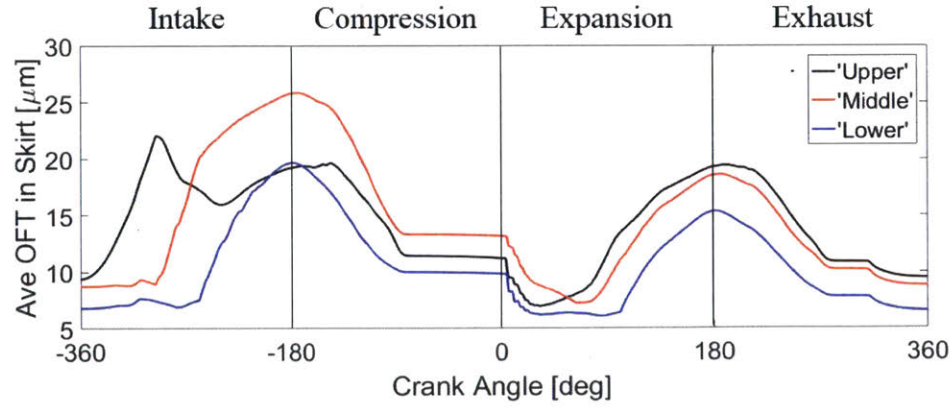

Figure 4-38 Average OFT in Skirt on TS of 'Upper', 'Middle' and 'Lower' Cases

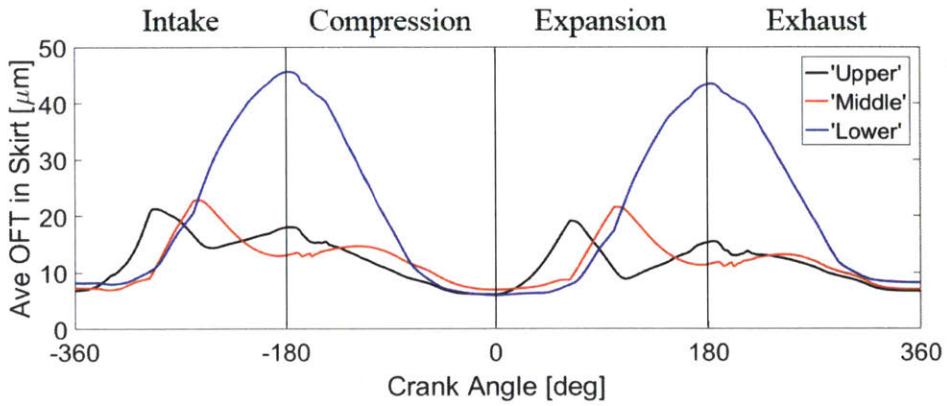

Figure 4-39 Average OFT in Skirt on ATS of 'Upper', 'Middle' and 'Lower' Cases

There are several notable phenomena and processes in the oil transport during the intake stroke.

- When piston reaches the top dead center and is about to start the intake stroke, the distributions of oil film thickness on the open liner are different in these cases. They are shown in figure 4-40 and 4-41.
- On thrust side, the distributions are similar. There is a narrow area of lubricant around the top of the open liner, resulting in the slight rise in the oil flow for 'Middle' and 'Lower' cases in figure 4-34. On the lower half of the open liner, more oil is located, which keeps the oil flow to be positive for 'Upper' and 'Middle' cases after the piston has passed their location of oil addition.
- On anti-thrust side, there is much more oil left on the liner in the 'Lower' case. Although a significant part of this oil can be collected by the skirt region at the end of intake stroke, as shown in figure 4-39, it does not benefit the 'Lower' case in terms of accumulating more lubricant in the chamfer region.
- Still on the anti-thrust side, the 'Middle' case is able to store more lubricant in the chamfer than the 'Upper' case when piston reaches bottom dead center, as is seen in figure 4-37. This is because when the 'Upper' case collects the additional oil, it is earlier in the stroke and the clearance is limiting the amount of oil that enters the skirt.

At the beginning of the compression stroke, the 'Upper' and the 'Middle' cases have the most volume of lubricant stored in the chamfer on thrust and anti-thrust sides, respectively. Although the 'Lower' case has much more oil in the skirt on anti-thrust side, it will quickly lose this oil instead of benefiting from it.

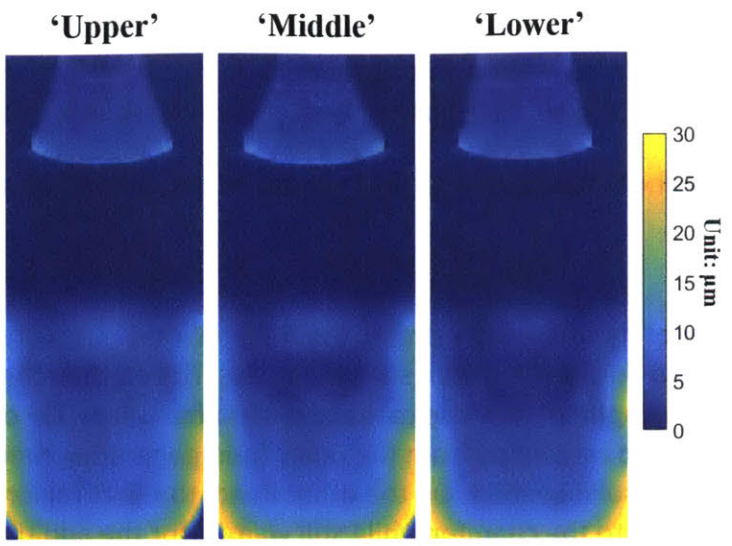

Figure 4-40 Distribution of OFT on the Open Liner on TS at -360° CA

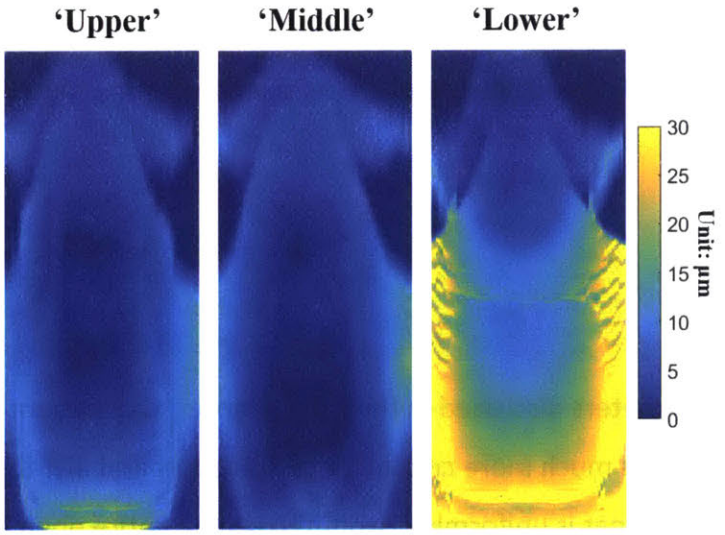

Figure 4-41 Distribution of OFT on the Open Liner on ATS at -360° CA

- On the thrust side, because the 'Middle' case has more oil in the skirt region to start the compression stroke, it also keeps more on the piston when the oil film separates. So at the end of this stroke, it still has more oil than the other cases in the skirt region. The same situation happens for the chamfer region of the 'Upper' case.
- On the anti-thrust side, the 'Middle' case has so much lubricant in the chamfer that some of the lubricant will be squeezed from chamfer to the skirt region when piston moves towards this side. Therefore, the curve for this case drops faster than the 'Upper'

case in figure 4-37, and the oil volume in its skirt region experiences an increase to surpass the 'Upper' case, as shown in figure 4-39.
- For this reason, the 'Middle' case has the least friction force at late compression stroke.

The oil transport during the previous two strokes set up for the interesting situation in the expansion stroke.

- At the beginning of the expansion stroke, the 'Middle' case has more oil on both sides of the skirt region. So during the piston slap, it has less friction than the 'Upper' case.
- However, the development of these cases reverses afterwards. On one hand, the 'Upper' case starts to receive oil from the open liner, generating more hydrodynamic pressure to replace solid contact. On the other hand, the skirt region in the 'Middle' case keeps losing oil to the chamfer while still waiting for the additional oil to come.
- The 'Lower' case has the least amount of lubricant in both skirt and chamfer regions on thrust side to start with the stroke, and is the last one to reach the oil addition. So it keeps having large friction force until the end of the stroke.

During the early exhaust stroke, the 'Lower' case has a lot of lubricant in the skirt region on anti-thrust side. This part of oil will be spread on the open liner for a much longer axial range, as is shown in figure 4-41.

4.3 Summary

Compared with the parameters discussed in the third chapter, the amount and location of oil addition to the open liner is much more critical for oil transport and distribution in the system. Firstly, for the oil addition that is uniformly distributed on the entire open liner, larger thickness helps the skirt and chamfer regions to collect more lubricant on both thrust and anti-thrust sides during down strokes. After intake stroke, cases with more oil supply will keep more lubricant in the skirt region when the side force is high so that more hydrodynamic pressure can be generated to reduce asperity contact. However, this trend stops when the amount of oil addition reaches some certain level. After such amount, the oil accumulation at bottom dead center still increases, but the extra oil will not be able to stay in the skirt or chamfer region during compression stroke, therefore will not help to further reduce friction.

As for the location of the oil addition, it has been found in this engine model that adding oil to the higher area of the open liner helps improve the lubricating performance on the thrust side during expansion stroke. Because the higher the oil is located, the more distance it can travel relative to the piston during intake stroke and the easier for it to enter the chamfer. Also, the clearance on the thrust side is larger during early intake stroke, which is favorable for the piston to collect lubricant.

On the anti-thrust side, adding more lubricant around the middle of the liner has more benefit to reduce friction during compression stroke. This is because if the oil is higher, it will be limited by the smaller clearance between piston and liner; and if the oil is lower, it will not go far enough to reach the chamfer, therefore will be left on the liner again in the early compression stroke.

Chapter 5

Conclusion

5.1 Development and Applications of the Model

At the beginning of this thesis work, the model was successfully improved to be able to handle the simulation of heavy duty diesel engines.

In every case studied in this project, where the same engine model is used, most of the frictional loss happens during late compression and early expansion strokes, from around -80° to 120° crank angle. The determining factor of the magnitude and duration of friction force is the amount of lubricant in the skirt region during this period of time, which is developed during the intake stroke and early compression stroke.

On the thrust side, since the oil film between piston and liner will separate at early compression stroke and the part of oil that is attached to the liner will be dragged out of the skirt region before piston reaches top dead center, most of the oil used for lubrication during early expansion stroke is the part that is attached to the piston (both skirt and chamfer) after separation. From the parametric study in section 3.3, it was found that stiffer liner is advantageous to getting more lubricant in the skirt region during intake stroke, therefore makes the piston keep more oil after separation. Also, according to section 4.2, it is more helpful to add more lubricant to the higher area of the open liner because it will be easier for the lubricant to reach the skirt and chamfer.

On the anti-thrust side, separation is unlikely to occur during compression stroke because the piston is pushed towards this side of the liner. Therefore, more oil will be available in the skirt region at late compression stroke if more oil can be stored in the chamfer during intake stroke. Section 3.2 shows that properly larger installation clearance can be helpful in this situation. In addition, from the study in section 4.2, to add oil to the middle part of the liner is the most

effective way to achieve this compared to adding oil to the other locations. This is because when piston reaches this location, the clearance starts to increase, and allows more oil to be dragged into the piston by the liner.

Since the distance traveled by the oil on the open liner during down strokes is not as much as the liner when there is full film in the skirt region, the sensitivity of the oil transport to the location of oil addition should also depend on the ratio of the stroke to the axial length of piston skirt. In the engine studied in this project, the ratio is about 2.5, and the FMEP varies a lot for different oil additions (for example, FMEP in the 'Upper' case is about 160% of that in the baseline case, and the 'Lower' case is almost three times as large as the baseline). For other engines with different stroke-skirt ratios, the influence of the location of oil addition may not have the same extent, but the determining factors will remain the same.

Finally, it can be seen from the results that it is crucial to keep the chamfer on both sides from losing oil too early in the compression stroke. In addition to a more appropriate distribution of oil supply, this might also be achieved by other approaches, which needs further study in the future.

5.2 Future Work

The potential future work falls into two major parts. The first part is to further improve the capability and accuracy of the model. First of all, currently the model still assumes the liner to be perfectly smooth, while the skirt is covered by triangular-shaped machine marks in the axial direction. In the future, the description of the surface needs to be more comprehensive, since the surface has influence on not only oil flow, but also the calculation of contact pressure. To assume the machine marks to be worn down to a new regular shape could be a reasonable start.

Then, the oil transport in the chamfer region could also use some modification. Since the clearance is much larger than skirt, lubricant in the chamfer is more likely to be driven by inertia force, and one of the most important results would be the bridging effect during late upstrokes. The current way to dealing with bridging effect is very rough and can be improved.

Pin lubrication is another potential topic connecting to the model, which still assumes there is no friction between pin and pin bore. On the other hand, the pin itself accounts for a significant proportion of engine frictional loss, and involves complicated physical and mechanical phenomena. These all make pin lubrication a valid candidate of future investigation.

The second part is the joint work with the experimental side. The research group where this thesis study is carried out has test cells equipped with floating liner engine and 2D LIF systems, which can provide measurement of frictional loss and observation of oil transport between skirt and liner. These experiments can to some extent validate the model, and the results from both sides can facilitate each other to help people understand the system better.

References

[1] Johnson, T., & Joshi, A. (2017). *Review of Vehicle Efficiency and Emissions* (No. 2017-01-0907). SAE Technical Paper.

[2] Richardson, D. E. (2000). Review of power cylinder friction for diesel engines. *Transactions of the ASME, Journal of Engineering for Gas Turbines and Power*, *122*(4), 506-519.

[3] Pogodaev, L. I., Tret'yakov, D. V., Valishin, A. G., & Matveevskii, O. O. (2008). Simulation of durability of cylinder liners of an internal combustion engine under vibration cavitation. *Journal of Machinery Manufacture and Reliability*, *37*(2), 143-151.

[4] Knoll, G. D., & Peeken, H. J. (1982). Hydrodynamic lubrication of piston skirts. *Journal of Lubrication Technology*, *104*(4), 504-508.

[5] Oh, K. P., Li, C. H., & Goenka, P. K. (1987). Elastohydrodynamic lubrication of piston skirts. *Transactions of the ASME, Journal of Tribology*, *109*, 356-362.

[6] Duyar, M., Bell, D., & Perchanok, M. (2005). *A comprehensive piston skirt lubrication model using a mass conserving EHL algorithm* (No. 2005-01-1640). SAE Technical Paper.

[7] Bai, D. (2012). *Modeling piston skirt lubrication in internal combustion engines* (Doctoral dissertation, Massachusetts Institute of Technology).

[8] Totaro, P. (2014). *Modeling piston secondary motion and skirt lubrication with applications* (Master's thesis, Massachusetts Institute of Technology).

[9] McClure, F. (2008). *Numerical modeling of piston secondary motion and skirt lubrication in internal combustion engines* (Doctoral dissertation, Massachusetts Institute of Technology).

[10] Li, Y. (2011). *Multiphase oil transport at complex micro geometry* (Doctoral dissertation, Massachusetts Institute of Technology).

[11] Przesmitzki, S. S. V. (2008). *Characterization of oil transport in the power cylinder of internal combustion engines during steady state and transient operation* (Doctoral dissertation, Massachusetts Institute of Technology).

[12] Zanghi, E. E. J. (2014). *Analysis of oil flow mechanisms in internal combustion engines via high speed Laser Induced Fluorescence (LIF) spectroscopy* (Master's thesis, Massachusetts Institute of Technology).

[13] Westerfield, Z. (2015). *A study of the friction of the power cylinder system in internal combustion engines using a floating liner engine* (Master's thesis, Massachusetts Institute of Technology).

[14] Lu, Y., Zhang, X., Xiang, P., & Dong, D. (2017). Analysis of thermal temperature fields and thermal stress under steady temperature field of diesel engine piston. *Applied Thermal Engineering*, *113*, 796-812.

[15] Soejima, M., Harigaya, Y., Hamatake, T., & Wakuri, Y. (2017). Study on Lubricating Oil Consumption from Evaporation of Oil-Film on Cylinder Wall for Diesel Engine. *SAE International Journal of Fuels and Lubricants*, *10*(2017-01-0883).

[16] Johnson, K. L. (1987). *Contact mechanics*. Cambridge university press.

[17] Elrod, H. G. (1981). A cavitation algorithm. *Transaction of the ASME, Journal of Lubrication Technology*, *103*(3), 350-354.

[18] Patir, N. & Cheng, H. S. (1978). An average flow model for determining effects of three-dimensional roughness on partial hydrodynamic lubrication. *Transaction of the ASME, Journal of Lubrication Technology*, *100*, 12-17.

[19] Taylor, R. I. (2012). Tribology and energy efficiency: from molecules to lubricated contacts to complete machines. *Faraday discussions*, *156*(1), 361-382.